Dissimilatory sulfur metabolism coupled to anaerobic oxidation of methane

Dissertation

zur Erlangung des Grades eines
Doktors der Naturwissenschaften – Dr. rer. nat. –

dem Fachbereich Biologie/Chemie der
Universität Bremen

vorgelegt von

Jana Milučká

Bremen 2011

Diese Arbeit wurde im Rahmen des Programms „The International Max Planck Research School of Marine Microbiology (MarMic)“ von September 2006 bis Februar 2011 in der Abteilung Mikrobiologie am Max-Planck-Institut für Marine Mikrobiologie in Bremen angefertigt.

1. Gutachter: Prof. Dr. Rudolf Amann
University of Bremen, Bremen
Max Planck Institute for Marine Microbiology, Bremen

2. Gutachter: Prof. Dr. Ir. Marc Strous
Radboud University, Nijmegen
University of Bielefeld, Bielefeld
Max Planck Institute for Marine Microbiology, Bremen

Tag des Promotionskolloquiums: 18. Februar 2011

TABLE of CONTENTS

ABSTRACT

"Something unknown is doing we don't know what."
Sir Arthur Stanley Eddington (1882–1944)

The seafloor and its microbial inhabitants play an important role in the biogeochemical cycling of elements. These environments are generally anoxic but contain high concentrations of sulfate penetrating from the overlying seawater. The main carbon mineralization processes – such as the anaerobic oxidation of methane (AOM; Eq. 1) – are therefore generally coupled to sulfate reduction.

$$CH_4 + SO_4^{2-} \rightarrow HCO_3^- + HS^- + H_2O \qquad \text{(Eq. 1)}$$

AOM plays a crucial role in both carbon and sulfur cycling. It oxidizes the majority of the methane – a potent greenhouse gas – diffusing from the seafloor and prevents its escape to the atmosphere. Methane oxidation also returns the carbon 'trapped' in the form of recalcitrant methane back to the carbon cycle as carbon dioxide. The AOM-coupled sulfate reduction consumes a large portion of the downwards sulfate flux and forms sulfide, which diffuses upwards towards the seafloor where it supports free-living sulfide- and sulfur-oxidizers but also gutless worms, clams and mussels that rely for their nutrition on the thiotrophic symbionts. Despite the pronounced effect of AOM on the sediment geochemistry little is known about its biology. The organisms responsible for AOM – a consortium of methanotrophic archaea and *Deltaproteobacteria* – have been identified *in situ* but their slow metabolism complicates growing them in pure cultures and renders the physiological investigations challenging. So far, AOM research has predominantly focused on the C1 metabolism of the methanotrophic archaea. The investigations presented in this thesis address the dissimilatory sulfur metabolism of the organisms involved in AOM and the mechanisms of its coupling to methane oxidation.

Chapters 2 and *3* describe the purification and characterization of the three known enzymes involved in dissimilatory sulfate reduction (SR enzymes; ATP sulfurylase, APS reductase, sulfite reductase). The enzymes were purified from a naturally enriched microbial mat using liquid chromatography. The identity of the SR

enzymes was confirmed by N-terminal amino acid sequencing and their activity – in total cell extracts as well as in individual chromatography fractions – was quantified by corresponding enzyme essays. Our aim was to assign these enzymes to a particular organism in the mat sample. For this purpose, polyclonal antibodies against the purified ATP sulfurylase and sulfite reductase were used – APS reductase could not be sufficiently purified for antibody generation – *in situ* in the original environmental sample as well as in our other enrichment cultures. This combination of "environmental proteomics" and immunolocalization allowed us to unambiguously assign the isolated SR enzymes exclusively to the bacterial partner. The archaea did not express detectable amounts of the identified SR enzymes themselves and therefore likely depend on their bacterial partners to perform the sulfate reduction. These results are presented as manuscripts *in revision* (Manuscript 1) and *in preparation* (Manuscript 2).

The following *Chapter 4* introduces experiments that were performed in order to elucidate sulfur transfer and speciation in AOM consortia. We used stable and radioactive sulfur isotopes to follow sulfur exchange between the medium and biomass and on a single cell level among individual cells. Based on our results and thermodynamic consideration we propose a model, in which DSS bacteria reduce sulfate to a zerovalent sulfur compound (probably polysulfide) that might be utilized by ANME as an electron acceptor for methane oxidation. Thus, unexpectedly, ANME participate in the dissimilatory sulfur metabolism coupled to AOM. Our combined data suggest that ANME obtain this compound from the associated bacteria. Such sulfur shuttling between two organisms not only represents a unique mechanism for a syntrophic relationship but also has significant implications for our understanding of sulfur transformations in the AOM zones in marine sediments. These results are presented as a manuscript *in preparation* (Manuscript 3).

ZUSAMMENFASSUNG

Der Meeresboden und dessen Bewohner spielen eine wichtige Rolle im biogeochemischen Kreislauf der Elemente. Diese Umgebungen sind im Generellen anoxisch jedoch enthalten sie hohe Konzentrationen von Sulfat welches aus dem Meerwasser in das Sediment diffundiert. Die hauptsächlichen Prozesse der Kohlenstoffmineralisierung, wie u.a die anaerobe Oxidation von Methan (anaerobic oxidation of methane, AOM), sind daher an die Reduktion von Sulfat gekoppelt.

AOM spielt eine entscheidende Rolle sowohl im Kohlenstoff- als auch im Schwefelstoffkreislauf. Dabei wird der größte Teil des aus dem Meeresboden aufsteigenden Methans, ein relevantes Treibhausgas, oxidiert und ein Entweichen in die Atmosphäre verhindert. Die Methanoxidation ist auch daher von Bedeutung, da der stabile Kohlenwasserstoff (Methan) zu Kohlendioxid umgewandelt und so erneut dem Kohlenstoffkreislauf zugeführt wird. Als Konsequenz der AOM-abhängigen Sulfatreduktion werden große Mengen Sulfid gebildet, welches in Richtung Sedimentoberfläche diffundiert und dort Substrat für freilebende und symbiotische Sulfid- und Schwefeloxidierer ist. Trotz der wichtigen Bedeutung der AOM als geochemischer Prozess ist wenig über dessen Biologie bekannt. Die für die AOM verantwortlichen Organismen – ein Konsortium aus methanotrophen Archaeen (ANME) und Deltaproteobakterien – wurden *in situ* identifiziert aber aufgrund ihres langsamen Wachstums nicht als Reinkultur gewonnen, welches physiologische Untersuchungen erschwert. Bisher haben sich Studien zur AOM überwiegend auf den C1-Metabolismus der beteiligten Archaeen fokussiert. Daher sollte in der vorliegenden Arbeit der Metabolismus der dissimilatorischen Sulfatreduktion, die daran beteiligten Organismen und der Mechanismus der Kopplung von Sulfatreduktion an die Methanoxidation untersucht werden.

Kapitel 2 und 3 dieser Arbeit beschreiben die Aufreinigung und Charakterisierung der für die dissimilatorische Sulfatreduktion verantwortlichen Enzyme (SR Enzyme; ATP-Sulfurylase, APS-Reduktase, Sulfitreduktase). Die Enzyme wurden aus einer natürlich angereicherten mikrobiellen Matte durch Verwendung chromatographischer Methoden aufgereinigt. Die Identität der Enzyme

wurde durch N-terminale Aminosäuresequenzierung bestätigt und deren Aktivität, sowohl im gesamten Zellextrakt als auch in individuellen chromatographisch getrennten Fraktionen wurde durch Enzymessays quantifiziert. Als nächstes sollten die Enzyme einzelnen Organismen der mikrobiellen Matte zugeordnet werden. Dazu wurden polyklonale Antikörper gegen die aufgereinigte ATP-Sulfurylase und Sulfitreduktase gewonnen und *in situ* in der mikrobiellen Matte und anderen AOM-Anreicherungen eingesetzt. Für die APS-Reduktase konnten keine Antikörper gewonnen werden, da sich das Enzym nicht genügend aufreinigen ließ. Die Kombination von „Umwelt-Proteomik“ und Immunolokalisation erlaubte die eindeutige Zuordnung der Enzyme ausschließlich zu dem bakteriellen Partner in den AOM-Konsortien. In den Archaeen konnten die identifizierten SR-Enzyme nicht nachgewiesen werden was darauf hindeutet, dass diese von ihren bakteriellen sulfatreduzierenden Partnern abhängig sind. Diese Ergebnisse sind in den Manuskripten *in Revision* (Manuskript 1) und *in Vorbereitung* (Manuskript 2) zusammengefasst.

Im Kapitel 4 werden Experimente vorgestellt, die den Schwefeltransport innerhalb der AOM-Konsortien aufklären sollten. Durch Verwendung von stabilen und radioaktiven Schwefelisotopen wurde der Austausch des Schwefels zwischen Medium und Biomasse, bis hin zu individuellen Zellen untersucht. Basierend an unseren Ergebnissen und thermodynamischen Betrachtungen schlagen wir ein Modell vor, wo die DSS Bakterien Sulfat zu Schwefel der Oxidationsstufe 0 (vermutlich Polysulfid) reduzieren, welcher von den ANME-Archaeen als Elektronen-Akzeptor für die Methanoxidation genutzt werden kann. Als ein unerwarteter Befund, scheinen die ANME an dem Prozess der dissimilatorischen Sulfatreduktion gekoppelt an AOM teilzuhaben. Unsere Daten lassen uns vermuten dass die Verbindungen von dem bakteriellen Partner bereitgestellt werden. Ein solcher Austausch von Schwefelverbindungen wurde hier das erste Mal für eine syntrophe Partnerschaft gezeigt und hat auch signifikante Auswirkung für das Verständnis der Umwandlung von Schwefelspezies in AOM aktiven marinen Sedimenten. Diese Ergebnisse sind im Manuskript *in Vorbereitung* (Manuskript 3) dargestellt.

ABBREVIATIONS

Acd	acyl-CoA dehydrogenase
Acs	acetyl-CoA-synthase
ANME	anaerobic methanotrophic Archaea
AOM	anaerobic oxidation of methane
APS	adenosine-5'-phosphosulfate
ATP (ADP, AMP)	adenosine-5'-tri(di, mono)phosphate
CoA	coenzyme A
CoB	coenzyme B (7-mercaptoheptanoylthreoninephosphate)
CODH	carbon monoxide dehydrogenase
CoM	coenzyme M (2-mercaptoethanesulfonate)
Cy (2,3,5)	cyanine fluorescent dyes
H_4MPT	tetrahydromethanopterin
Da	dalton
DIC	dissolved inorganic carbon
Dsr	dissimilatory sulfite reductase
E.coli	*Escherichia coli*
Eq.	equation
Fig.	figure
FITC	fluorescein isothiocyanate
Fmd	formyl-MFR dehydrogenase
Fpo	H_2F_{420}:phenazine oxidoreductase
Fqo	H_2F_{420}:quinone oxidoreductase
Fsr	coenzyme F_{420}-dependent sulfite reductase
Ftr	formyl-MFR:H_4MPT formyltransferase
GC-MS	gas chromatography mass spectrometry
Hdr	heterodisulfide reductase
HPLC	high performance liquid chromatography
IgG	immunoglobulin G
kJ	kilojoule

Mch	methenyl-H_4MPT cyclohydrolase
Mcr	methyl-CoM-reductase
Mer	methylene H_4MPT-reductase
MeSH	methylsulfide
MFR	methanofuran
Mtd	F_{420}-dependent methylene-H_4MPT dehydrogenase
Mtr	methyl-H_4MPT:CoM methyl-transferase
mV	millivolt
MV	mud volcano
OM	organic matter
PDB	Pee Dee Belemnite
pers. comm.	personal communication
(r)DNA	(ribosomal) deoxyribonucleic acid
(r)TCA	(reverse) tricarboxylic acid cycle
SIMS	secondary ion mass spectrometry
SMTZ	sulfate methane transition zone
SR	sulfate reduction (evtl. sulfate reducing)
Tg	teragram
TRITC	rhodamine isothiocyanate
XANES	X-ray absorption near-edge structure

CHAPTER 1
GENERAL INTRODUCTION

"Happy are they who are starting now."
Martinus Willem Beijerinck (1851-1931)

1. Microbial degradation of organic matter

The flux of organic matter (OM) in the ocean is mainly vertical; from the primary producers in the photic zone to the terminal consumers in the sediment. The (micro)organisms in the water column and in the sediment-overlying benthic boundary layer consume most of the OM formed in the sunlit surface waters and therefore only a part of the sinking OM reaches the seafloor and enters the (predominantly) anoxic world in it. The OM mineralization in these anoxic environments proceeds through several stages that involve fermenting, acetogenic, denitrifying, sulfate-reducing and methanogenic microorganisms. The 'left-over' sedimentary OM is thermogenically converted to petroleum and natural gas. The cycle of OM mineralization gets completed when these hydrocarbons seep back to the above-lying sediment and become oxidized to CO_2.

1.1 Syntrophic metabolism

The OM is subjected to many rounds of alteration and degradation during sedimentation and burial and might therefore be refractive to further mineralization. However, substrates that are not degradable by individual microorganisms can still be degraded through combined activity of metabolically different microorganisms. Such an unique lifestyle has been termed obligate syntrophy. Generally, the substrate is partially degraded by one organism to an intermediate which is scavenged by the second organism. The intermediates are small molecules capable of rapid diffusion like – in most instances – hydrogen. Occasionally, also formate and

acetate have been reported to serve as syntrophic intermediates; in methanogenic consortia (Bleicher and Winter, 1994) and syntrophic acetone and benzoate degradation, respectively (Platen & Schink, 1987; Warikoo *et al.*, 1996). Concentrations of these intermediates are kept low through their consumption by the second organism. Low intermediate concentrations prevent thermodynamic end-product inhibition and increase the energy gain of the first organism which allows syntrophs to perform reactions that are under standard conditions endergonic. The syntrophic cooperation requires that the free energy obtained from the substrate oxidation is shared among involved metabolic partners. Each of the two partners has to gain at least an equivalent of the biological energy quantum – the minimal metabolically conservable amount of energy (i.e. –20 kJ per mol ATP for *E. coli*; Thauer *et al.*, 1977). However, syntrophs can catalyze also reactions which provide less free energy than –40 kJ (i.e. 2 x –20 kJ) per mol substrate. This is due to the fact that the increment energy required for ATP synthesis for syntrophic organisms is probably much lower than for growing *E. coli*. For example methanogenic archaea require under physiological conditions a minimal free energy change of only –10 kJ (mol CH_4)$^{-1}$ (Hoehler *et al.*, 2001). Methanogens have a limited range of relatively simple substrates which makes them dependent on other anaerobic organisms and, consequently, very common syntrophic partners. Through methanogenic activity a large part of the energy locked in decaying biomass is stored as methane, forming vast reservoirs in the seafloor (10^7 Tg carbon; Dickens, 2003).

Of all the methane released from the reservoirs only around 10% successfully reaches oxic waters and, eventually, the atmosphere because most of the methane is efficiently oxidized to CO_2 in anoxic marine sediments.

2. Anaerobic oxidation of methane with sulfate (AOM)

$$CH_4 + SO_4^{2-} \rightarrow HCO_3^- + HS^- + H_2O \quad \text{(Eq.1)}$$

$\Delta G^{\circ\prime} = -16.6$ kJ.mol^{-1}

Anaerobic oxidation of methane stoichiometrically coupled to sulfate reduction (Eq. 1) was first observed in so-called sulfate-methane transition zones (SMTZ; Fig. 1) in the late seventies (Barnes & Goldberg, 1976; Martens & Berner, 1977; Reeburgh, 1976). Further knowledge on AOM has progressed slowly. It took more than two decades till the microorganisms – a consortium of anaerobic methanotrophic archaea and *Deltaproteobacteria* – were phylogenetically identified (Boetius *et al.*, 2000; Hinrichs *et al.*, 1999) and until now the biochemistry of the underlying biochemical mechanism remains unknown.

2.1 Habitats

AOM with sulfate as terminal oxidant is widespread in all oxygen-depleted marine environments where sulfate is the most abundant electron acceptor (marine methane seeps, vents and surface and deep sediments; Knittel & Boetius, 2009); but the most common AOM habitats are the SMTZ. The AOM rates in SMTZ are relatively low (0.001-50 nmol CH_4 oxidized cm^{-3} day^{-1}) but they are sufficient to consume up to 90 % of the upward methane flux (Hinrichs & Boetius, 2002; Reeburgh, 2007) demonstrating a crucial role of AOM for controlling methane efflux to the atmosphere. AOM with higher rates (10-

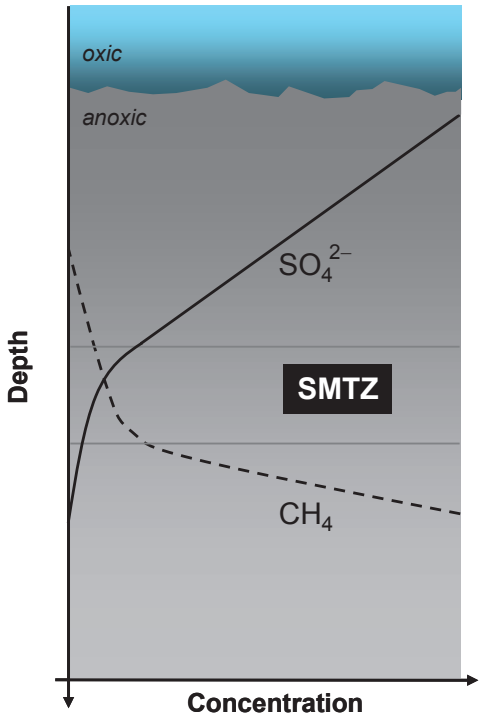

Figure 1. Schematic representation of SMTZ. In anoxic marine sediments sulfate diffusing from the seawater and methane diffusing from the subsurface are simultaneously consumed by AOM.

5,000 nmol CH_4 oxidized cm^{-3} day^{-1}) was observed in surface sediments overlying gas hydrates and underwater mud volcanos (MV) such as at Hydrate Ridge in the Pacific Ocean and Amon MV and Isis MV in the Mediterranean Sea, respectively. Highest AOM rates (1,000-10,000 nmol CH_4 oxidized cm^{-3} day^{-1}) have been reported from Black Sea microbial reefs, which are carbonaceous precipitates covered with methanotrophic microbial mats (Michaelis *et al.*, 2002; Fig. 2). The anatomy of these mats is stratified: the uppermost part which is in contact with seawater is black due to the presence of iron sulfide precipitates; under them lay pink mats which differ in microbial composition and cell-specific AOM activity.

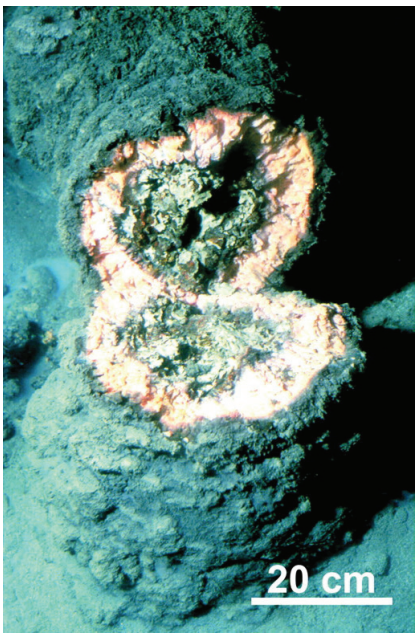

Figure 2. Carbonate chimney from Black Sea. Inner cavity of the chimney formed by porous carbonate is covered by microbial mats of pink and black colour. (from Michaelis et al., 2002)

2.2 Actors

Anaerobic methanotrophic archaea (ANME) and the associated *Deltaproteobacteria* form structured microbial consortia (Boetius *et al.*, 2000) Fig. 3). There are three phylogenetic ANME groups known to date – ANME-1, -2, and -3 (Knittel and Boetius, 2009 and references therein). They are related to methanogenic archaea of the *Methanosarcinales* or *Methanomicrobiales* order. Methanogens from these groups were shown to be capable of slow methane oxidation (Zehnder and Brock, 1979; Meulepas et al., 2010b) but it appears that ANME (based on lipid biomarkers, 16S rDNA and functional genes

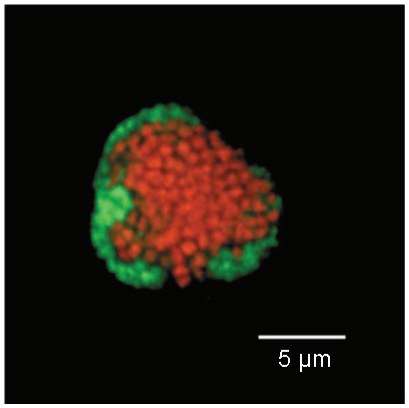

Figure 3. Fluorescent micrograph of an AOM consortium. ANME (red) and *Deltaproteobacteria* (green) are labeled with specific phylogenetic probes. (from Boetius et al., 2000)

phylogeny) form a lineage of specialized methanotrophs (Hinrichs et al., 1999; Kruger et al., 2003). Their bacterial partners are related to *Desulfosarcinales* and/or *Desulfobacterales* order of the sulfate-reducing *Deltaproteobacteria*. ANME-2 are mostly associated with *Desulfosarcina/Desulfococcus*, ANME-3 with *Desulfobulbus* and ANME-1 are regularly observed as monospecific archaeal aggregates or free living single cells (Knittel *et al.*, 2005; Niemann *et al.*, 2006; Orphan *et al.*, 2002; Schreiber *et al.*, 2010).

2.3 Mechanisms of ANME-SRB interaction

The co-occurrence of ANME with their bacterial partners hints at a syntrophic nature of their relationship but its mechanism is still poorly understood. To-date two syntrophic models have been proposed: (i) ANME produce an intermediate, which is an organic molecule, that is taken up by the bacteria and oxidized to CO_2 with concomitant reduction of sulfate (Fig. 4A) or (ii) only electrons – in form of e.g. hydrogen or via cytochromes or direct cell-to-cell contact – are transferred between the two organisms (Fig. 4B). Additionally, a principally different theory has been envisioned recently that suggests ANME might be sulfate reducers (Johnson

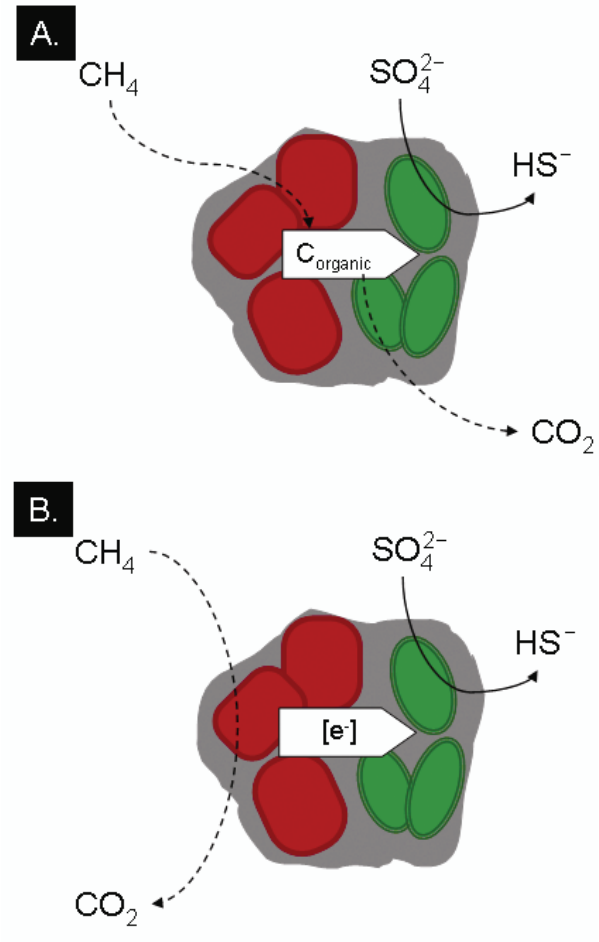

Figure 4. The proposed possible interactions between ANME and *Deltaproteobacteria*. *Deltaproteobacteria* (green) might obtain from the ANME (red) **(A)** an organic compound (such as acetate, formate or methanol, or **(B)** reducing equivalents in a form of e.g. H_2 or via cytochromes, or *(continued)*

& Mukhopadhyay, 2008; Thauer & Shima, 2008; Widdel *et al.*, 2007; Fig. 4C). Assuming that the ANME oxidize methane (Orphan *et al.*, 2001a) and the associated bacteria reduce sulfate, reducing equivalents have to be extracellularly shuttled from one organism to the other (Fig. 4B). Numerous possible intermediates have been tested on the premise that the addition of a given compound will inhibit AOM and stimulate sulfide production. Additions of classical syntrophic intermediates such as hydrogen, formate, acetate and methanol result in sulfate reduction rates identical (or lower) to the sulfate reduction rates with methane (Nauhaus *et al.*, 2002); moreover, these compounds fail to inhibit AOM (Meulepas *et al.*, 2010). Carbon monoxide and methanethiol (MeSH) are the only compounds which additions to AOM cultures were reported to result in partial or complete inhibition of methane oxidation (Moran *et al.*, 2008; Meulepas *et al.*, 2010). Both compounds, however, were described as toxic for (some) methanogens and/or sulfate reducing bacteria (Parshina *et al.*, 2010; Kiene *et al.*, 1986). Therefore, it needs to be shown that the inhibitory effect of CO or MeSH is AOM-specific. It is also not clear whether and how sulfide methylation would be coupled to energy conservation given that in other organisms (e. g. *Holophaga foetida*) a similar process is non-energetic (Kappler *et al.*, 1997). It has also been proposed that the bacterial partners feed on the polysaccharide matrix or on dead ANME biomass (Thauer & Shima,

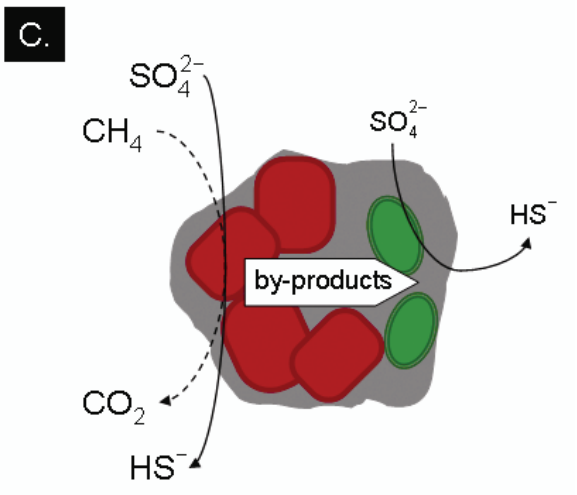

Figure 4. (*continued*) (C.) ANME perform the SR alone, and the *Delta-proteobacteria* only feed on the metabolic by-products and are not necessary for AOM.

2008) but a carbon transfer from ANME to the bacteria has been excluded based on ^{13}C labeling studies (Wegener *et al.*, 2008). ANME and the associated bacteria are not in a direct cell-to-cell contact (Reitner *et al.*, 2005a) and there is so far no evidence for a production of any inter-cellular connecting "nanowires" known from organisms growing with solid electron acceptors (such as iron minerals; Gorby *et al.*, 2006; Klimes *et al.*, 2010; Reguera *et al.*, 2005).

2.4 Cellular ultrastructure

Only Black Sea mats have so far been investigated on an ultrastructural level. ANME from these mats were shown to possess conspicuous intracellular membranes, probably originating from invaginations of the cytoplasmic membrane (Reitner *et al.*, 2005a). The function of these invaginations is still unknown. Some methanogens (*Methanosarcina*) form similar membranes during cell division and others (*Methanobacterium*) possess such membrane structures throughout their whole life cycle and they might be the site of methane and energy synthesis (Sprott & Beveridge, 1993 and references therein).

The bacteria appear to store polyhydroxyalkanoates (Reitner *et al.*, 2005a) and small electron-dense particles, of which some were shown to be enriched in iron sulfides. The function of these Fe-S-rich particles was proposed to be similar or identical to magnetosomes of magnetotactic bacteria (Reitner *et al.*, 2005a; Reitner *et al.*, 2005b).

2.5 Cellular physiology

Little to nothing is known about the biochemistry and physiology of the organisms involved in AOM. Due to their extremely slow growth (doubling times of up to 6 months) no pure cultures are available to-date. Our current knowledge on genetics, genomics and proteomics of ANME is derived from naturally- and/or man-enriched samples or inferred from our knowledge on the metabolism of their closest relatives – the methanogenic

archaea. Our knowledge on the physiology of the ANME-associated *Deltaproteobacteria* is also very scarce.

2.5.1 C1 metabolism

Stable isotope and lipid biomarker analyses have shown that both ANME and the associated bacteria have lipids depleted in ^{13}C (below −100‰ and below −60 ‰ versus PDB for ANME and SRB, respectively; Hinrichs *et al.*, 2000; Michaelis *et al.*, 2002; Pancost *et al.*, 2000). This is attributed to the fact that the two main carbon sources in SMTZ are isotopically light – the predominantly biogenic methane is depleted ≥60 ‰ versus PDB and the DIC has $\delta^{13}C$ values of less than –10‰ (Biddle *et al.*, 2006). The bacteria are solely autotrophic while ANME are expected to assimilate methane and CO_2 in nearly equimolar amounts (Eq. 2; Nauhaus *et al.*, 2007; Wegener *et al.*, 2008).

$$17CH_4 + 15CO_2 + 8NH_4^+ \rightarrow 8C_4H_8O_2N + 14H_2O + 8H^+ \qquad \text{(Eq. 2)}$$

Oxidation of CH_4 to CO_2 is only weekly exergonic and the involved reactions likely proceed close to equilibrium, which may result in heterogeneous $\delta^{13}C$ values of methane, CO_2 and ANME biomass that have been interpreted as evidence for concomitant methanogenesis and methanotrophy (Alperin & Hoehler, 2009a; Alperin & Hoehler, 2009b; House *et al.*, 2009). Methanogenic enzymes have been found in ANME genome but they probably work in reverse direction (Hallam *et al.*, 2004; Meyerdierks *et al.*, 2005; Meyerdierks *et al.*, 2010 and Meyerdierks pers. comm.). Correspondingly, methyl-coenzyme M (CoM) reductase (Mcr) likely activates methane to yield a methyl group bound to CoM. The activation of methane under anoxic conditions is challenging because of the high dissociation energy of its C–H bond (439 $kJ.mol^{-1}$) and because of the absence of any protein- or coenzyme-derived oxygen radicals that would facilitate its breakage. Instead, Mcr has adopted a unique mechanism that involves a nickel centre

of its prosthetic group, the coenzyme F_{430} (Scheller *et al.*, 2010). Mcr with modified F_{430} (951 Da instead of 905 Da) is expressed to large amounts (up to 7% total soluble protein) in Black Sea microbial mats (Krüger *et al.*, 2003). The methyl group bound to CoM is then transferred to the tetrahydromethanopterin cofactor

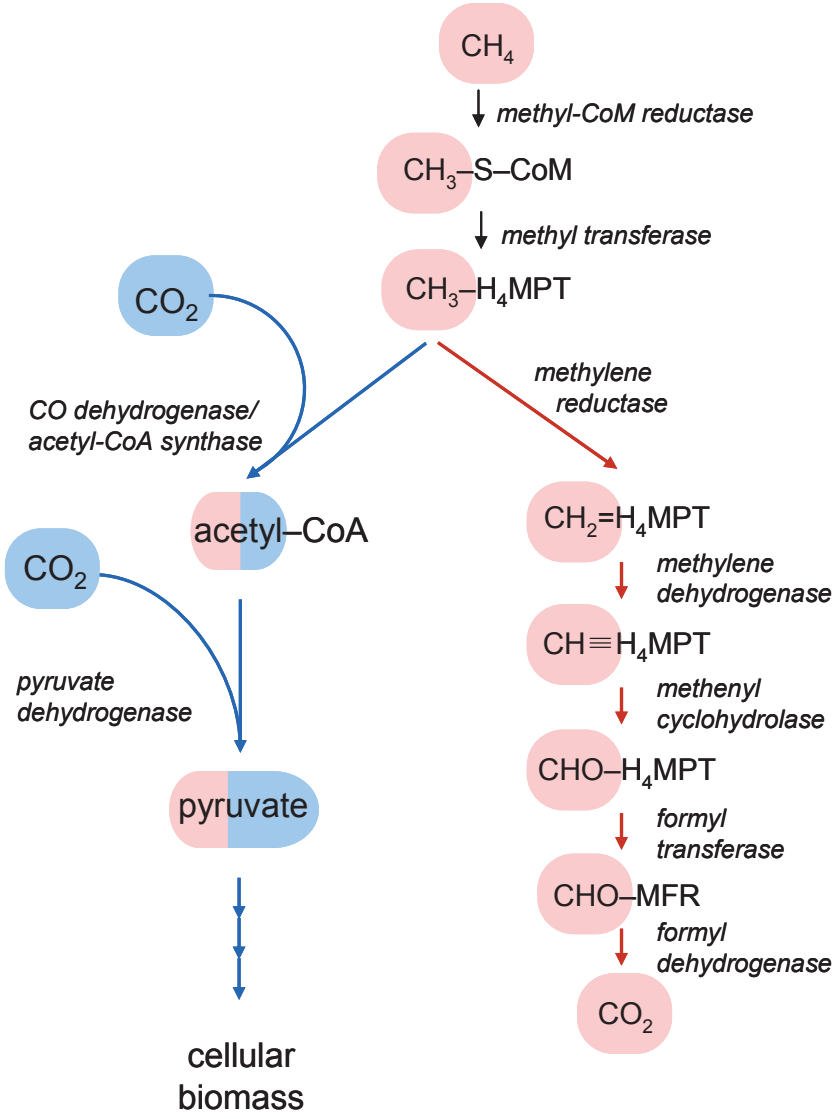

Figure 5. The proposed C1 metabolism in ANME. The majority of methane is oxidized to CO_2 via a reversed pathway of methanogenesis (red arrows). A small proportion of methane also enters the assimilative pathway (blue arrows) and is incorporated in ANME biomass.

(H_4MPT) and stepwise oxidized via methenyl-, methylene- and formyl- stage to CO_2. At the stage of methyl-H_4MPT some of the methyl groups are carboxylated by CO dehydrogenase to form acetyl-CoA and after further carboxylation pyruvate is formed that gets assimilated in the biomass (Meyerdierks *et al.*, 2010; Fig. 5). The bacteria probably use the same autotrophic pathway because

the observed isotopic offset between their biomass and ambient DIC (~30-40‰; House *et al.*, 2009) is in agreement with the isotope fractionation observed to be generated by the CODH/Acd pathway in other bacteria (House *et al.*, 2000; Sirevag *et al.*, 1977).

2.5.2 Sulfur metabolism

In the ANME genome, nearly all genes coding for enzymes involved in sulfate assimilation (assimilatory ATP sulfurylase, APS kinase and assimilatory sulfite reductase; Fig. 6) were found (Meyerdierks *et al.*, 2010); only PAPS reductase is missing. However, as a sulfur source, sulfide is likely preferred over sulfate as it is abundant in AOM habitats and energetically more favorable. Genes for enzymes involved in dissimilatory sulfur metabolism

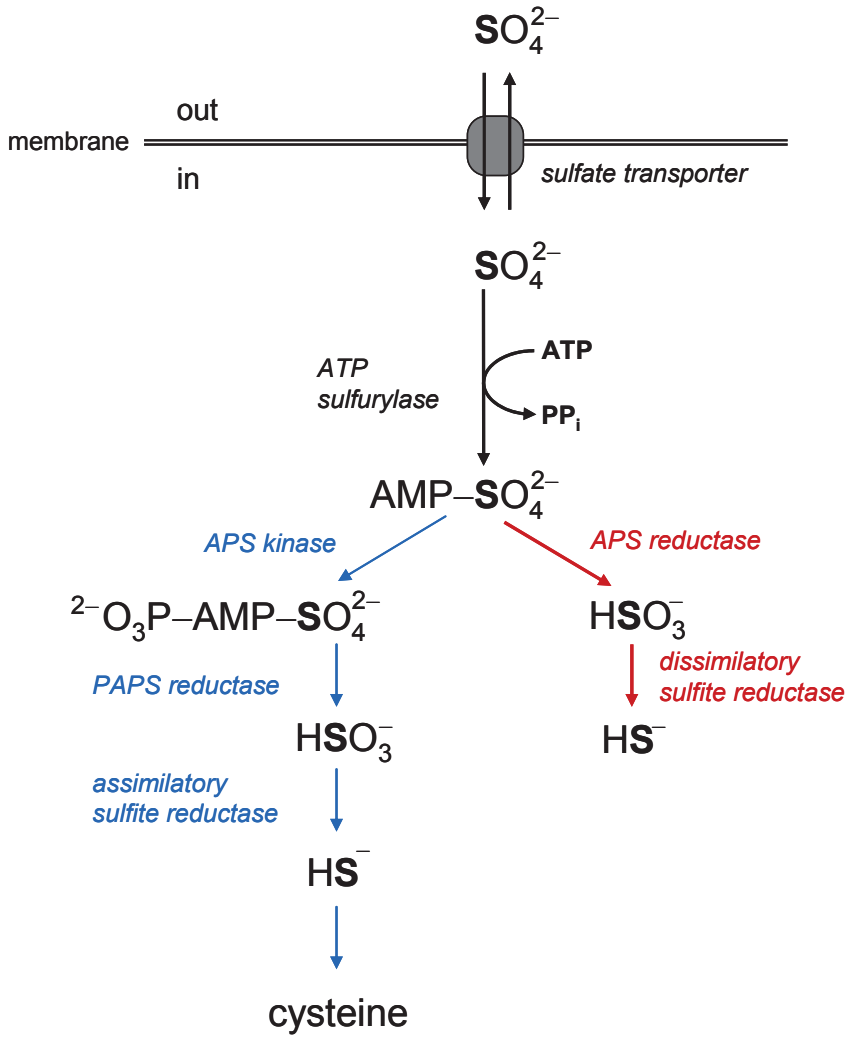

Figure 6. A general scheme of assimilatory and dissimilatory sulfur metabolism. Sulfate can serve either as a sulfur source for e.g. synthesis of S-containing amino acids (blue arrows) or as an electron acceptor for organisms capable of dissimilatory sulfate reduction (red arrows).

(dissimilatory ATP sulfurylase, APS reductase and dissimilatory sulfite reductase; Fig. 6) were not identified in ANME genomes (Meyerdierks *et al.*, 2010) and the capacity of ANME or the associated bacteria to reduce sulfate has not yet been confirmed either.

Interestingly, other genes with a putative role in dissimilatory sulfur metabolism have been identified in the ANME metagenome. There are two heterodisulfide reductases (Hdr) encoded in the ANME-1 metagenome (Meyerdierks *et al.*, 2010). The canonical (CoM-CoB-specific) Hdr is a disulfide reductase with a key function in the energy conservation in methanogenic Archaea. The other, non-canonical Hdr, is lacking CoM and CoB binding motifs and has thus an unknown function. Hdr-related genes have also been identified in the sulfate reducers *Desulfovibrio vulgaris* and *Archaeoglobus profundus* and sulfide oxidizers *Chlorobium tepidum* and *Allochromatium vinosum* (Dahl *et al.*, 1999; Eisen *et al.*, 2002; Mander *et al.*, 2004; Rossi *et al.*, 1993; Valente *et al.*, 2001). These Hdr share high similarities with Qmo and DsrJ, the likely physiological electron donors for APS reductase and sulfite reductase (Mander *et al.*, 2002; Rossi *et al.*, 1993). Presence of such non-canonical Hdr in ANME genome is surprising as dissimilatory sulfur metabolism in ANME has not been anticipated.

In the ANME-2 genome a homologue of the F_{420}-dependent sulfite reductase (Fsr) was found (Meyerdierks *et al.*, 2005). Fsr is a fusion between two enzymes: its N-terminus represents the $F_{420}H_2$ dehydrogenase (FpoF or FqoF), and the C-terminus is a homologue of a siroheme-containing dissimilatory sulfite reductase (DsrA or DsrB; Johnson & Mukhopadhyay, 2005). All investigated methanogens encode the Fsr subunit homologous to sulfite-reductase and its function was proposed to be detoxification of sulfite as this oxyanion inhibits Mcr. The methanogens

Methanocaldococcus jannaschii and *Methanococcus maripaludis* are nevertheless able to grow on sulfite as a sole sulfur source. In AOM cultures, added sulfite disappears without inhibiting AOM (Basen et al., unpublished data) but it remains to be resolved whether Fsr is involved in this process.

2.5.3. Nitrogen metabolism

The "AOM organisms" most likely use ammonium as a major nitrogen source but organic compounds such as glycine and leucine are taken up as well (Orphan *et al.*, 2009). In the ANME genome no genes for nitrite or nitrate reduction have been identified in accordance with the fact that both nitrate and nitrite are generally absent from sulfidic environments. Surprisingly, genes encoding group III nitrogenases were found (Meyerdierks *et al.*, 2010; Pernthaler *et al.*, 2008). SIMS studies suggest that ^{15}N-labeled N_2 gets incorporated in the ANME but so slowly that fixing molecular nitrogen cannot be a major nitrogen gaining process (Dekas *et al.*, 2009; Pernthaler *et al.*, 2008). It is, however, intriguing that these energy-limited organisms fix molecular nitrogen at all given the high energy requirements for nitrogen fixation (16 mol ATP per mol fixed N_2).

2.5.4. c-type cytochromes

In the ANME-1 metagenome, an operon containing genes coding for a molybdopterin oxidoreductase and multiple multi-heme *c*-type cytochromes was found (Meyerdierks *et al.*, 2010). Cytochromes *c* are small proteins with covalently bound hemes that mostly serve as electron transferring agents in aerobic respiratory chains as well as in ammonium and sulfur oxidation. Cytochromes *c* are generally uncommon for archaea although they are present in the closest relatives of ANME, *Methanosarcina* spp.. The function of the cytochromes in ANME has been speculated to be in extracellular electron transport by formation of nanowires (Meyerdierks *et al.*, 2010; see Chapter 2.3).

3. AOM with electron acceptors other than sulfate

Recently, also other, thermodynamicaly more favourable, oxidants than sulfate were described to serve as electron acceptors for anaerobic methane oxidation. In the following paragraphs AOM coupled to denitrification (Raghoebarsing *et al.*, 2006) and to reduction of iron and manganese oxides (Beal *et al.*, 2009) are briefly introduced.

3.1. AOM coupled to nitrate/nitrite reduction

$$5CH_4 + 8NO_3^- + 8H^+ \rightarrow 5CO_2 + 4N_2 + 14H_2O \quad \text{(Eq. 3)}$$

$\Delta G^{\circ\prime} =$ –765 kJ.mol^{-1}

$$3CH_4 + 8NO_2^- + 8H^+ \rightarrow 3CO_2 + 4N_2 + 10H_2O \quad \text{(Eq. 4)}$$

$\Delta G^{\circ\prime} =$ –928 kJ.mol^{-1}

Raghoebarsing and colleagues have obtained an AOM enrichment culture where methane oxidation was coupled to denitrification (Eq. 3 and Eq. 4) from a freshwater canal with agricultural run-off (Raghoebarsing *et al.*, 2006). The initial enrichment consisted of archaea belonging to the *Methanosarcinales* cluster (10%) and bacteria forming a novel phylum (90%; Raghoebarsing et al., 2006). During the course of incubation the archaea gradually disappeared from the enrichment culture and the bacterium, named NC-10, was identified as the sole organism responsible for AOM (Ettwig *et al.*, 2008).

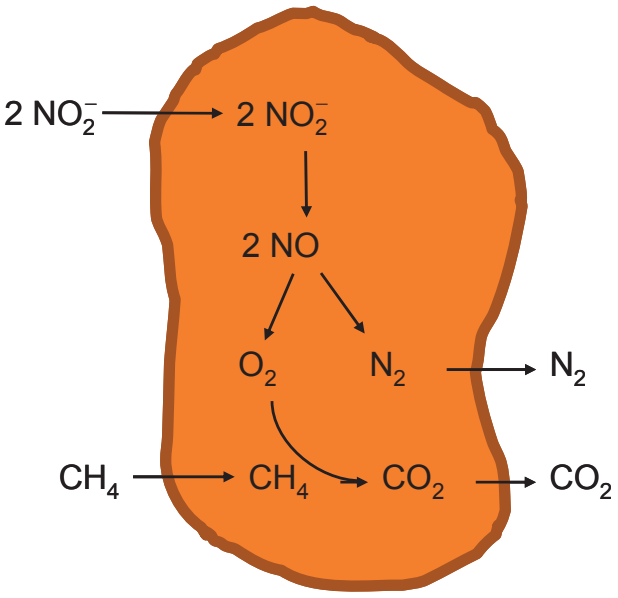

Figure 7. A scheme of the proposed pathway of methane oxidation with nitrite in Candidatus *Methylomirabilis oxyfera*. Under anaerobic conditions, '*M. oxyfera*' disproportionates NO and generates intracellularly oxygen, which is then used for methane oxidation.

Surprisingly, NC-10 (Candidatus *Methylomirabilis oxyfera*) did not possess any of the two types of enzymes known to be capable of C–H bond activation under anaerobic conditions (glycyl radical enzymes and nickel-containing methyl-CoM reductase). This enigma was solved by the discovery that this anaerobically-growing bacterium generates intracellularly oxygen, which is used for methane activation via aerobic methane monooxygenase (Ettwig *et al.*, 2010). The oxygen is produced from NO via a putative NO dismutase which represents a novel mechanism capable of generating molecular oxygen (Fig. 7)

The unique metabolism of '*M. oxyfera'* suggests that even before the oxygenation of the atmosphere organisms might have existed that had evolved aerobic enzymatic mechanisms for the utilization of the abundant atmospheric methane and possibly also of other substrates. The contribution of nitrite-coupled AOM to present-day methane cycling has not yet been quantified.

3.2. AOM coupled to iron (III) and manganese (IV) reduction

$$CH_4 + 4MnO_2 + 7H^+ \rightarrow HCO_3^- + 4Mn^{2+} + 5H_2O \quad \text{(Eq. 5)}$$

$\Delta G°' = -790$ kJ.mol^{-1}

$$CH_4 + 8Fe(OH)_3 + 15H^+ \rightarrow HCO_3^- + 8Fe^{2+} + 21H_2O \quad \text{(Eq. 6)}$$

$\Delta G°' = -572$ kJ.mol^{-1}

From an energetic point of view AOM coupled to manganese- or iron-reduction can provide up to 30 times more energy per mol methane (Eq. 5 and Eq. 6) than AOM with sulfate. Recently, Beal and colleagues reported that birnessite (a MnO_2 mineral) or ferrihydrite (a $Fe(OH)_3$ mineral) are used as electron acceptors for anaerobic methane oxidation in the anoxic marine sediments off California (Beal *et al.*, 2009). Methane oxidation was observed in incubations supplemented with birnessite or ferrihydrite as sole added electron acceptors but the rates (<0.3 µM/day) were

3 to 10 times lower than in the sulfate-supplemented controls. A direct link between the observed AOM and metal oxides reduction has not been shown. Based on the reported results it cannot be excluded that sulfide gets oxidized (a)biotically with the metal oxides to sulfate, which could then fuel “conventional” sulfate-coupled AOM through a cryptic S-cycle.

AIMS and OBJECTIVES

"The task is not to see what has never been seen before but to think what has never been thought before about what you see everyday. "

Erwin Schrödinger (1887-1961)

Given that AOM plays a crucial role in sulfur cycling it is intriguing how little is known about the dissimilatory sulfur metabolism coupled to it. From the beginning it has been accepted that the *Deltaproteobacteria* perform sulfate reduction although there was no experimental evidence to support this assumption apart from the phylogenetic affiliation of the bacteria to a clade of known sulfate reducing bacteria. It has been hypothesized later that ANME could perform sulfate reduction as well, which, if true, would dramatically change our understanding of the functioning of AOM. The possibility that methane oxidation and SR are intracellularly coupled in ANME would imply that AOM is not mediated in syntrophy and that the associated bacteria are merely commensals – if not parasites – of the methanotrophs. This study was initiated in order to clarify which enzymes are responsible for the dissimilatory sulfate reduction coupled to AOM, to which organism(s) these enzymes belong and how the process of sulfate reduction is linked to methane oxidation.

We used liquid chromatography, polyacrylamide gel electrophoresis and enzyme assays to search for the canonical SR enzymes and quantify their abundance and activity. We wanted to assign these proteins to a particular organism in the sample by using specific antibodies custom-generated against the purified proteins. Such immunolabeling approach for uncultivated microorganisms was not available at the time of the study and, correspondingly, a large part of my work was dedicated to antibody generation and methodological establishment of an immunolabeling protocol for environmental samples. The results of the immunolableling study indicated that the ANME-associated bacteria perform the AOM-coupled SR and, are therefore an active part of AOM consortia. Further investigations have focused on how these two organisms interact in their syntrophic relationship. We focused on analyzing whether any reduced sulfur compounds

derived from the dissimilatory sulfate metabolism could be involved in the electron transfer from ANME to bacterial partner. For this we used an integrated approach of bulk chemical extractions, HPLC and GC-MS analyses, single-cell secondary ion mass spectrometry, microRaman spectroscopy, and transmission electron microscopy coupled to energy-dispersive X-ray spectroscopy.

CHAPTER 2

Bacterial enzymes for dissimilatory sulfate reduction in a marine microbial mat (Black Sea) mediating anaerobic oxidation of methane

Mirko Basen, Martin Krüger, Jana Milucka, Jan Kuever, Jörg Kahnt, Olav Grundmann, Anke Meyerdierks, Friedrich Widdel, and Seigo Shima

Contributions to the manuscript:

M.B., J.M., F.W., and S.S. designed research and project outline, M.B. and J.M. performed FISH analysis, M.B., M.K., J.M., O.G. and S.S. performed protein purification, M.B., J.M, J.Ka performed enzyme analyses, M.B. performed enzyme activities measurements and apr *gene amplification,, M.B., J.Ku., and A.M performed phylogenetic analyses, M.B., J.M., F.W., S.S conceived, wrote and edited the manuscript.*

Chapter is *in revision* in Environmental Microbiology

Summary

Anaerobic oxidation of methane (AOM) with sulfate is catalyzed by microbial consortia of archaea and bacteria affiliating with methanogens and sulfate-reducing *Deltaproteobacteria*, respectively. There is evidence that methane oxidation is catalyzed by enzymes related to those in methanogenesis, but the enzymes for sulfate reduction coupled to AOM have not been examined. We collected microbial mats with high AOM activity from a methane seep in the Black Sea. The mats consisted mainly of archaea of the ANME-2 group and bacteria of the *Desulfosarcina-Desulfococcus* group. Cell-free mat extract contained activities of enzymes involved in sulfate reduction to sulfide: ATP sulfurylase (adenylyl:sulfate transferase; Sat), APS reductase (Apr), and dissimilatory sulfite reductase (Dsr). We partially purified the enzymes by anion-exchange chromatography. The amounts obtained indicated that the enzymes are abundant in the mat, with Sat accounting for 2% of the mat protein. N-terminal amino acid sequences of purified proteins suggested similarities to the corresponding enzymes of known species of sulfate-reducing bacteria. The deduced amino acid sequence of PCR-amplified genes of the Apr subunits is similar to that of Apr of the *Desulfosarcina*/*Desulfococcus* group. These results indicate that the major enzymes involved in sulfate reduction in the Back Sea microbial mats are of bacterial origin, most likely originating from the bacterial partner in the consortium.

Introduction

The anaerobic oxidation of methane (AOM) with sulfate according to

$$CH_4\ (g) + SO_4^{2-} \rightarrow HCO_3^- + HS^- + H_2O \qquad (1)$$

($\Delta G^{\circ\prime} = -16.6$ kJ mol^{-1}) is the major sink for methane produced in deep anoxic marine sediments and is thus of global importance (Reeburgh, 2007; Knittel & Boetius, 2009). The anaerobic oxidation of methane rather than the aerobic oxidation, which occurs in terrestrial habitats, is due to the much higher concentration of sulfate compared to that of oxygen in seawater (28 mM vs. approximately 0.3 mM); sulfate therefore penetrates deeper into sediments than oxygen.

AOM is often catalyzed by compact aggregates of archaea closely related to methanogens and bacteria clustering within the *Deltaproteobacteria*, most commonly within the *Desulfosarcina-Desulfococcus* clade (Boetius *et al.*, 2000; Orphan *et al.*, 2001a; Michaelis *et al.*, 2002; Knittel *et al.*, 2005, Schreiber *et al.*, 2010). Consortia with *Desulfobulbus*-related *Deltaproteobacteria* have recently been identified (Niemann *et al.*, 2006; Lösekann *et al.*, 2007; Pernthaler *et al*, 2008). A common view is that the archaea are anaerobic methanotrophs (ANME) that activate methane and process methane carbon to CO_2 via reverse reactions of methanogenesis, and that the bacterial partner scavenges reducing equivalents to reduce sulfate (Zehnder & Brock, 1979; Hoehler *et al.*, 1994;; Boetius *et al.*, 2000; Valentine *et al.*, 2000; Nauhaus *et al.*, 2002; Thauer & Shima, 2008;).

Consortia anaerobically oxidizing methane have been propagated *in vitro* (Nauhaus *et al.* 2007, Meulepas *et al.* 2009), but axenic cultures have not been isolated. Insights into the pathway of methane during AOM have come from metagenomic and protein analyses using natural samples, and from analogies to the well-established pathway of methanogenesis (Thauer 1998). The hypothesis of “reverse methanogenesis” was supported by the finding of orthologs of almost all genes of the methanogenic pathway in the metagenome of natural samples with AOM activity and of naturally enriched ANME groups (Hallam *et al.*, 2004; Meyerdierks *et al.*, 2005; Meyerdierks *et al.* 2010). The

putative methane-activating enzyme, a dominant nickel protein closely related to methyl-coenzyme M reductase (Mcr) of methanogens, was purified from microbial mats from the Black Sea (Krüger *et al.*, 2003). Furthermore, an Mcr-related protein was localized by immuno-labeling and electron microscopy of the archaeal cells of the mat community (Heller *et al.*, 2008). Recent NMR experiments have shown that purified MCR from methonogenic archaea can catalyze the endergonic back reaction (Scheller *et al.*, 2010).

Comparable insights into key genes and enzymes involved in sulfate reduction linked to AOM are lacking, and the assumption that the deltaproteobacterial cells associated with the archaea are genuine sulfate reducers has not been verified. Even at some marine sites with AOM activity, the archaeal cells detected were not associated with bacteria (Orphan *et al.*, 2002; Knittel *et al.*, 2005; Lösekann *et al.*, 2007; Treude *et al.*, 2007). Hence, it cannot be excluded that at least some archaea in AOM habitats are responsible for both methane oxidation and sulfate reduction. This is feasible since dissimilatory sulfate reduction is a well-established trait in *Euryarchaeota* (genus *Archaeoglobus*; Stetter, 1988; Dahl *et al.*, 1994). Genes for this pathway could have been acquired via lateral transfer from sulfate-reducing *Firmicutes* (Wagner *et al.*, 1998; Friedrich, 2002; Meyer & Kuever, 2007).

Here we show that Black Sea microbial mats with AOM activity contain substantial amounts of the three enzymes catalyzing sulfate reduction to sulfide: ATP sulfurylase (sulfate:adenylyl transferase; Sat), adenosine-5'-phosphosulfate (APS) reductase (Apr), and dissimilatory sulfite reductase (Dsr). We partially purified Sat, the small subunit of Apr (AprB), and the DsrAB directly from the natural mat biomass and showed that their N-terminal amino acid sequences were similar to those of deltaproteobacterial enzymes. Moreover, we show that the deduced products of the Apr-encoding genes (*aprBA*) are closely related to enzymes of known sulfate-reducing *Deltaproteobacteria* of the *Desulfosarcina-Desulfococcus* clade.

Results and discussion

Microbiological characterization of the intact microbial mat

Methane seepage in the northwestern Black Sea at 210–230 m depth sustains AOM, leading to deposition of chimney-like carbonate structures up to 4 m in height and 1 m in diameter (Pimenov *et al.*, 1997; Michaelis *et al.*, 2002). The *in situ* temperature is around 8 °C. The outside and interstitials of the chimneys are populated by soft, somewhat slimy microbial mats of up to 10 cm thickness (Fig. 1A). The exterior part of the mat directly exposed to the methane-rich fluid is black and harbors consortia of the ANME-2 and *Desulfosarcina-Desulfococcus* phylotypes (Blumenberg *et al.*, 2004; Reitner *et al.*, 2005; Krüger *et al.*, 2008). The interior part of the mat is pink and often dominated by ANME-1 cells with their characteristic cylindrical shape and also by *Desulfosarcina-Desulfococcus*-related cells. The latter do not form compact aggregates but are distributed within the mat matrix (Michaelis *et al.*, 2002).

→ **Fig. 1**

We collected mat samples in the Black Sea and selected a part of the mat with high AOM activity. The highest rates of methane-dependent sulfate reduction (Fig. 2) were measured in the black mat at approximately 16 °C; the rate per dry mass was 3.2 (± 0.55) nkat g_{dm}^{-1} (1 nkat = 6 × 10^{-2} µmol min^{-1} = 86.4 µmol d^{-1}). The presence of consortia in the selected sample was checked by microscopy. Almost all of the cells detected by general (DAPI) staining formed densely packed aggregates (Fig. 1B). Use of specific 16S-rRNA-targeting fluorescent oligonucleotide probes showed that consortia consisted either of an archaeal core surrounded by bacterial cells or of intermixed archaeal and bacterial cells (Fig. 1C–E). The selected black mat therefore appeared suitable for studying enzymes involved in sulfate reduction linked to AOM. We prepared a soluble cell-free extract of the mat.

→ **Fig. 2**

Activity of enzymes involved in sulfate reduction to sulfide

The pathway of dissimilatory sulfate reduction hitherto described in bacteria and archaea involves a canonical sequence of three enzymatic reactions (Thauer *et al.*, 1977; LeGall & Fauque, 1988;). ATP sulfurylase (adenylyl:sulfate transferase; Sat; EC 2.7.7.4)

activates sulfate with ATP to yield adenosine 5'-phosphosulfate (APS) and pyrophosphate. The latter is hydrolyzed to phosphate by pyrophosphatase. APS is reduced by APS reductase (Apr; EC 1.8.99.2), yielding inorganic sulfite (or bisulfite) and AMP. Dissimilatory sulfite reductase (Dsr; EC 1.8.99.1) finally reduces sulfite to sulfide.

Extract preparation was rendered difficult by carbonate grains and the matrix that formed voluminous bottom layers upon centrifugation of crude extract. Therefore, the obtained amount of soluble cell-free extract (supernatant) had to be used sparingly.

Activities of Sat and Apr were detected in mat extract (Table 1). The specific activity of Dsr was very low and variable in the different mat extracts. For comparison, we measured specific activities of the three enzymes in cell extracts of pure cultures of *Desulfococcus multivorans and Desulfosarcina variabilis;* the specific activities were in the range of those reported for sulfate-reducing prokaryotes (Krämer & Cypionka, 1989; Dahl *et al.*, 1994; Sperling *et al.*, 1998; Fritz *et al.*, 2000). The cell-type-related specific activities of Sat and Apr in mat extract did not differ much from activities in extracts of the pure cultures, especially when only one of two cell types in the consortium contained the enzymes.

→ **Table 1**

Fractionation of enzymes involved in sulfate reduction to sulfide

The soluble mat extract contained substances that interfered with chromatography. These substances were precipitated by 20% saturated ammonium sulfate. We then partially purified the enzymes in the desalted supernatant by anion-exchange chromatography, measured their activities, and analyzed them by denaturing SDS-PAGE.

Sat eluted as a single peak of activity at 0.25−0.32 M NaCl (fractions 16–18) that comprised 90% of the total activity eluted from the column. Fifty percent of the Sat activity was recovered in this purification step. SDS-PAGE of the fractions revealed a protein band of *ca*. 50 kDa (Fig. 3), similar to the monomer size of the known

homotrimeric Sat (Sperling *et al.*, 1998). The collected active fractions contained 2% of the total soluble mat protein. The N-terminal amino acid sequence of the 50-kDa protein band from the polyacrylamide gel was characteristic of Sat (Fig. 4). Attempts to clarify an ambiguous position by analyzing another mat sample in the same manner led to a similar sequence harboring another ambiguous position (Fig. 4).

→ **Fig. 3 and 4**

Total Apr activity was significantly decreased by ammonium sulfate precipitation, leaving 20% of the initial activity in the supernatant. Since there was no detectable Apr activity in the precipitate and no measurable protein loss by ammonium sulfate treatment, the observed loss must have been caused by the salt addition and desalting. Subsequent anion-exchange chromatography eluted more than 80% of the Apr activity applied to the column at 0.33−0.38 M NaCl (fractions 19–23). These fractions contained a *ca*. 20-kDa protein (Fig. 3). Native Apr from sulfate-reducing bacteria and *Archaeoglobus* is a heterodimer composed of two subunits, AprA (*ca*. 70 kDa) and AprB (*ca*. 20 kDa) (Fritz *et al.*, 2000; Fritz *et al.*, 2002). However, in our denaturing gels, only the small subunit was visible because the large AprA subunit probably overlapped with the highly abundant subunit of “reverse” methyl-coenzyme M reductase (Mcr) from archaea. The N-terminal amino acid sequence of the small protein had a high similarity to that of bacterial AprB (Fig. 4).

Dsr activity eluted at 0.35−0.44 M NaCl (fractions 24–26) and thus overlapped partly with the peak containing Mcr and Apr activity. SDS-PAGE of fractions harboring Dsr activity showed protein bands of *ca*. 43 and 47 kDa; these masses are similar to those of the two subunits of the described Dsr (Arendsen *et al.*, 1993). The intensity of these bands indicated that Dsr is a relatively abundant protein. A third small subunit corresponding to DsrC (~11 kDa) (Arendsen *et al*., 1993; Oliveira *et al*., 2008) was negligible in our Dsr fraction. SDS-PAGE of higher polyacrylamide concentrations revealed that the Dsr fraction containes several minor proteins at 10~15 kDa but the intensity of these bands was too weak to analyze the N-terminal sequence. N-terminal sequence analysis of the DsrA and DsrB candidate proteins yielded only relatively short

sequences. Nonetheless, they exhibited similarity to Dsr from sulfate-reducing bacteria (Fig. 4). The N-terminal sequences included some ambiguous positions, which indicated that Dsr preparations from mat extract were probably not homogenous and might have originated from related sulfate-reducing bacteria. The Dsr-containing fraction was greenish. Its UV-VIS absorption spectrum showed a distinct maximum at 410 nm, a weak maximum at 540 nm, and a weak shoulder at 580 nm (Fig. S1). This indicates that the absorption spectrum represented the combined spectra of the siroheme-containing dissimilatory sulfite reductase (Arendsen *et al.*, 1993) and the co-eluted Mcr harboring a nickel cofactor (Krüger *et al.*, 2003).

Full-length sequence of APS reductase from the microbial mat

We used the obtained N-terminal amino acid sequences to design degenerate primers to retrieve full-length sequences of the corresponding genes. Only clones of genes encoding AprA and AprB were obtained. Their N-terminal sequences were identical with that of five Apr proteins. The full-length sequences were most closely related to those of AprBA from the *Desulfosarcina-Desulfococcus* cluster and constituted a sixth lineage distinct from the hitherto known lineages from *Desulfosarcina* spp., *Desulfonema magnum*/*Olavius* symbiont Delta-1, *Desulfobacterium indolicum*, *Desulfonema limicola*/*Desulfococcus* spp., and *Desulfatibacillum* spp. (Fig. 5; Friedrich, 2002; Meyer & Kuever, 2007). The AprBA sequence tree mirrors that of 16S rRNA, including sequences from bacteria associated with ANME from seep areas (Orphan *et al.*, 2001b; Knittel *et al.*, 2003), which suggests that the Apr partially purified from the mat originates from a member of the *Desulfosarcina*/*Desulfococcus* group.

→ **Fig. 5**

Conclusions

If the analyzed enzymes are involved in AOM with sulfate, their activities should in principle be sufficient to account for the in vivo AOM rate (see above). The measured protein-to-dry-mass ratio of 0.28 yields a protein-related AOM activity in the intact mat of

11 nkat g_{pr}^{-1}. This activity was measured at 16 °C, which is similar to the temperature optimum of the viable mat. Enzyme activities in optical assays were generally measured at 28 °C, which is the growth temperature of the pure cultures used for comparison and the appropriate temperature for the auxiliary enzymes in the coupled Sat assay. Assuming that enzyme activity increases two- to fourfold per temperature increase of ΔT = 10 K, activities of Sat and Apr (Table 1) are still more than sufficient to account for sulfate reduction to sulfide with methane as electron donor. In contrast, the measured Dsr activity would be barely sufficient to explain the observed in vivo rate, even though the abundance of the enzyme was relevant according to the band intensity in the gel (Fig. 3). It is possible that Dsr is a particularly sensitive enzyme that easily loses activity upon cell disruption or that our assay, which used an artificial electron donor, may be insufficient to reveal its *in vivo* function. Structural studies of the enzyme from *Desulfovibrio vulgaris* (Oliveira *et al.*, 2008) indicate that DsrC is highly important for the catalytic function of Dsr and may be involved in sulfite reduction. The very low Dsr activity in the mat extract and the anion-exchange column fractions might be attributed to the instability of the DsrC in the samples.

The similarity of the deduced Apr sequence to Apr sequences from the *Desulfosarcina-Desulfococcus* group indicates that the retrieved enzyme is from the bacterial partner in the methane-oxidizing consortium, which is a member of this group (Fig. 5). The N-terminal amino acid sequence of Sat and Dsr from the mat showed the highest similarity to that of the respective proteins of sulfate-reducing *Deltaproteobacteria*. Thus, Sat, Dsr, and Apr likely arise from the bacterial partner in the mat.

Our study supports the assumption that enzymes of the canonical sulfate reduction pathway are important in AOM in Black Sea microbial mats and arise from the associated bacterial partner. The study is one of the few examples of the direct characterization of an enzyme from a natural microbial habitat. Other examples include the study of Mcr (most likely involved in AOM) in the same habitat (Krüger *et al.*, 2003) and of Sat in aerobic sulfur bacteria in the trophosome of a tube worm from a

hydrothermal vent (Renosto *et al.*, 1991). Such combined enzyme and gene analyses are a promising approach towards understanding the *in situ* role of particular microorganisms, if these microorganisms are highly enriched in their habitats, such as in microbial mats.

Experimental procedures

Origin of microbial mats and cultivation of strains

Microbial mats were collected by means of a submersible in methane seep areas in the northwestern Black Sea at 220 m water depth during RV Meteor cruise M72/2 in February/March 2007 (Project MUMM, Max Planck Institute for Marine Microbiology, Bremen) at 44° 46' N, 31° 59' E. A mat sample maintained from RV Poseidon cruise POS 317-2 in August 2004 (Project GHOSTDABS, University of Hamburg) at 44° 46' N, 31° 60' E was used for the preliminary experiments; in principle, the same results were obtained. Collected samples were maintained active in artificial sea water medium (Widdel & Bak, 1992) in anoxic 1-l bottles under a headspace (*ca*. one-third of the bottle volume) of CH_4 and CO_2 (5:1) at 8 °C. If more than *ca*. 10 mM sulfide accumulated, the supernatant was replaced with fresh anoxic seawater. Strains of sulfate-reducing bacteria were obtained from the German Collection of Microorganisms and Cell Cultures (DSMZ, Braunschweig). *Desulfococcus multivorans* (DSM 2059) and *Desulfosarcina variabilis* (DSM 2060) were grown at 28 °C in synthetic brackish medium and seawater medium (Widdel & Bak, 1992), respectively, with 5 mM benzoate. All subsequent manipulations were done in anoxic glove boxes with an N_2-CO_2 (9/1, v/v) atmosphere for manipuration of the mat and with an N_2-H_2 (95/5, v/v) atmosphere for the enzyme purification.

Incubation experiments with intact mats

Microbial mats were gently homogenized using a tissue grinder and suspended in anoxic artificial seawater medium at a dry mass content of 2.9 mg ml^{-1}. Suspensions of 10 ml were incubated in 20-ml glass tubes with a headspace of CH_4 or N_2 (controls) and CO_2.

Tubes were sealed with butyl rubber stoppers and during the experiment horizontally shaken (40 rpm) to facilitate gas transport. Aliquots were withdrawn with syringes flushed with N_2.

Chemical and other analyses

Sulfide production was determined colorimetrically as brown colloidal CuS (Cord-Ruwisch, 1985) and via the methylene blue formation reaction (Cline, 1969) in a miniaturized assay (4 ml). Methane was quantified using a GC14B gas chromatograph (Shimadzu, Kyoto, Japan) equipped with a Supel-Q Plot column (30 m × 0.53 mm; Supelco) and a flame ionization detector. The carrier gas was N_2 at a flow rate of 3 ml min^{-1}. The column temperature was 110 °C. Dry mass was measured after drying at 80 °C for 48 h. Protein content was determined according to Bradford (1976).

Fluorescence in situ hybridization

Homogenized mat samples (see above) were fixed with 2% formaldehyde in phosphate-buffered saline (PBS; 7 mM Na_2HPO_4, 3 mM NaH_2PO_4, 130 mM NaCl; pH 7.2) for 12 h, washed with 1× PBS and stored in PBS/ethanol (1:1) at −20 °C. Small proportions were collected on GTTP polycarbonate filters of 0.2 µm pore size (Millipore, Eschborn, Germany). Staining with 4′,6′-diamidino-2-phenylindole (DAPI), hybridization, and microscopy were carried out as described (Amann *et al.*, 1995). Fluorescent oligonucleotide probes and formamide concentrations (v/v) were as follows: negative control, NON338, 10% (Wallner *et al.*, 1993); archaea, Arch915, 35% (Amann *et al.*, 1990); bacteria, EUBI-III, 35% (Daims *et al.*, 1999); *Desulfosarcina-Desulfococcus* group, DSS658, 50% (Manz *et al.*, 1998); ANME-1, ANME-1 350, 40% (Boetius *et al.*, 2000); and ANME-2, ANME-2 538, 50% (Treude *et al.*, 2005). Probes labeled with Cy3 or carboxyfluorescein (FLUOS) were purchased from ThermoHybaid (Ulm, Germany).

Preparation of extract and protein fractionation

Pieces of the microbial mats (15 g) were cut into smaller (2 mm) pieces and suspended in 30 ml of 50 mM MOPS-KOH pH 7.0. The cells were disrupted by ultrasonication three times for 8 min at 160 W (sonication tip MS 72; pulse duration 0.5 s). The resulting crude extract was centrifuged at 150,000 × *g* for 1 h. The membrane-free supernatant was fractionated by ammonium sulfate precipitation (20% saturation), followed by centrifugation at 18,000 × *g* for 20 min. The supernatant (40 ml) was concentrated by ultrafiltration to 5 ml (10-kDa cut off). The concentrate was diluted 50-fold with 50 mM MOPS-KOH, pH 7.0. From this, 125 ml were applied to a 5-ml Q-Sepharose anion-exchange chromatography column (HiTrap Q HP; GE Healthcare) equilibrated with 50 mM MOPS-KOH, pH 7.0. Proteins were eluted with a linear NaCl gradient from 0 to 0.6 M. Enzyme activity in the eluted fractions was measured (see below), and proteins were analyzed by 4-15% gradient SDS-PAGE (mini-format), followed by staining with Coomassie Blue G-250. For N-terminal amino acid sequence analysis, protein bands were blotted onto a PVDF membrane using a wet blot device (BioRad) according to the manufacturer's instructions. Protein bands were excised and analyzed by Protein Analytics (Giessen, Germany).

Enzyme assays

ATP sulfurylase activity was determined in the reverse direction by coupling the following reactions and photometric (340 nm) determination of NADPH (Dahl and Trüper, 1994) in 50 mM Tris-HCl buffer, pH 7.5, supplemented with 20 mM $MgCl_2$: $APS^{2-} + PP_i^{3-} \rightarrow ATP^{4-} + SO_4^{2-} + H^+$; ATP^{4-} + glucose $\rightarrow ADP^{3-} + G\text{-}6\text{-}P^{2-} + H^+$; $G\text{-}6\text{-}P^{2-} + NADP^+ + H_2O \rightarrow$ 6-phosphogluconate^{3-} + NADPH + 2 H^+ (APS, adenyl-5'-phosphosulfate; PP_i, pyrophosphate; G-6-P, glucose 6-phosphate). APS reductase activity was determined in the reverse direction according to $SO_3^{2-} + AMP^{2-} + 2\,[Fe(CN)_6]^{3-} \rightarrow APS^{2-} + 2\,[Fe(CN)_6]^{4-}$ with photometric (420 nm) determination of $[Fe(CN)_6]^{3-}$ (Kobayashi *et al.*, 1975) in 50 mM Tris-HCl buffer, pH 7.5. The rate of abiotic $[Fe(CN)_6]^{3-}$ reduction was subtracted. Dissimilatory sulfite reductase activity was determined with reduced

methylviologen (MV^+) according to $SO_3^{2-} + 6\ MV^+ + 7\ H^+ \rightarrow HS^- + 6\ MV^{2+} + 3\ H_2O$ with photometric (578 nm) determination of MV^+ consumption (Dahl and Trüper, 2001**)** in anoxic 50 mM Tris-HCl buffer in cuvettes under N_2. Directly before the assay, MV^{2+} was reduced with 0.2 mM titanium (III) citrate. We also performed the assay with sodium dithionite as reducing agent. Enzyme activities (1 nkat = 10^{-9} mol s^{-1} = $6 \cdot 10^{-2}$ µmol min^{-1}) refer to ATP, APS, or SO_3^{2-}.

DNA manipulation and analysis

Genomic DNA of Black Sea microbial mats and of pure cultures of sulfate-reducing bacteria was extracted according to the genomic tip protocol (Genomic DNA Handbook, Qiagen, Hilden, Germany). The degenerated primer BS-AprB-1-F (5'-ATG CCD AGT TAT GTH ATH AC-3') was newly designed based on the N-terminal amino acid sequence of the purified AprB protein. *aprBA* was amplified using primer combinations BS-AprB-1-F/AprA-5-RV and AprA-1-FW/AprA-10RV (Meyer & Kuever, 2007), as well as BS-AprB-1-FW/AprA-10-RV; the latter yielded almost full-length *aprBA* sequences. Primer annealing was optimal at 53 °C. PCR products were purified using the Qiaquick PCR purification kit (Qiagen). Clone libraries were constructed using the TOPO pCR4 vector (TOPO TA cloning kit, Invitrogen, Karlsruhe, Germany) following the manufacturer's instructions. PCR products were sequenced using the ABI BigDye terminator cycle sequencing kit (Applied Biosystems). Sequences were analyzed with the Lasergene software package (DNAstar, GATC Biotech, Konstanz, Germany) or the Bioedit sequence alignment editor version 7.0.9.0 (Hall, 1999).

Sequences used for comparison of N-terminal amino acids (Fig. 4) were from the following microorganisms. Sat: *Desulfatibacillum alkenivorans* strain AK-01 (ZP_02131628.1); *Desulfococcus oleovorans* strain Hxd3 (ABW66812.1); *Desulfobacterium autotrophicum* strain HRM2 (YP_002604365); *Desulfovibrio desulfuricans* strain G20 (YP_388757.1); *Desulfotomaculum reducens* strain MI-1 (ABO49175.1); *Desulfotomaculum acetoxidans* strain 1ac2 (YP_003192914.1); and *Archaeoglobus fulgidus* strain VC-16 (AAB89581.1). AprB: *Desulfatibacillum*

alkenivorans (YP_002430736); *Desulfococcus oleovorans* (YP_001528884); *Desulfobacterium autotrophicum* (YP_002601731), *Desulfovibrio desulfuricans* .(YP_387605); *Desulfotomaculum reducens* .(YP_001112001); *Desulfotomaculum acetoxidans* (YP_003192913.1); and *A. fulgidus* (NP_070497). DsrA: *Desulfatibacillum alkenivorans* (YP_002433449.1); *Desulfococcus oleovorans* (ABW68472.1); *Desulfobacterium autotrophicum* (YP_002605460.1); *Desulfovibrio desulfuricans* (ABB37327.1); *Desulfotomaculum reducens* (YP_001114514.1); *Desulfotomaculum acetoxidans* (YP_003189665.1); *A. fulgidus* (NP_069259.1). DsrB: *Desulfatibacillum alkenivorans* (YP_002433448.1); *Desulfococcus oleovorans* (YP_001530550.1); *Desulfobacterium autotrophicum* (ACN17295.1); *Desulfovibrio desulfuricans* (ABB37328.1); *Desulfotomaculum reducens* (YP_001114513.1); *Desulfotomaculum acetoxidans* (YP_003189666.1); and *A. fulgidus* (NP_069260.1).

Contigs of sequences of AprB and AprA were analyzed using ClustalW alignment and tree construction with the PhyML program (maximum-likelihood method, http://atgc.lirmm.fr/phyml, 100 bootstraps) as described (Meyer & Kuever, 2007).

Nucleotide sequence accession numbers

The *aprBA* nucleotide sequence data are deposited in the EMBL, GenBank, and DDBJ sequence databases under the accession numbers HQ188925 to HQ188929 for AprBA 1−5 from Black Sea microbial mats, HQ188924 for AprBA *Desulfosarcina ovata* strain oxyS1, and HQ188930 for AprBA *Desulfosarcina cetonica*.

Acknowledgements

We are indebted to Rolf Thauer for continuous advice and support, and to Walter Michaelis, Richard Seifert, and Antje Boetius for access to samples. We thank the crews of RV Poseidon with JAGO, and RV Meteor with ROV QUEST (MARUM) for help during field work, Thomas Holler for sample collection, and Daniela Lange and Alexander Galushko for providing strains. We also thank Chris Hopkins, Jens Harder, and Rudolf Amann for helpful discussions and critical reading of the manuscript. This work was

supported by the Max Planck Society, the Fonds der Chemischen Industrie, the Marie Curie Early Stage Training Site in Marine Microbiology (MEST-CT-2004-007776), and the projects MUMM, GHOSTDABS (program GEOTECHNOLOGIEN of the BMBF and DFG), and BEBOP (University of Hamburg). Seigo Shima received support from an emeritus grant (Max Planck Society) given to Rolf Thauer. This is publication number xxxx *(will be provided)* in the framework of MUMM II (program GEOTECHNOLOGIEN).

Figure legends

Fig. 1. Images of microbial mats from the methane seepage area in the northwestern Black Sea.

A) Piece of a chimney-like structure showing the outer black and inner pink microbial layers (courtesy of Walter Michaelis, Hamburg). B) "Super" consortium of archaeal-bacterial consortia from a black mat exhibiting fluorescence after DAPI staining. C) The same consortium as in B exhibiting fluorescence of labeled oligonucleotide probes targeting 16S rRNA. The probes were specific for ANME-2 (Cy3, red signal) and the *Desulfosarcina-Desulfococcus* group (FITC, green signal). D) Consortium with an archaeal core and surrounding bacteria stained as in C. E) Consortium with intermixed archaeal and bacterial cells stained as in C.

Fig. 2. Methane-dependent sulfate reduction in the black microbial mat used for enzymatic analysis.

Fig. 3. Upper panel: Elution profile of Sat Apr activities in anion- exchange chromatography fractions. Shown are: activity of Sat (grey bars) and Apr (black bars), relative absorption at 280 nm (solid line with crosses) and NaCl concentration (dashed line). One unit (U) of activity refers to one µmol substrate turnover per minute. Inset: Elution profile of Dsr in a separate run of anion-exchange chromatography.

Lower panel: Denaturing gel electrophoresis (SDS-PAGE) of fractions from anion-exchange chromatography of supernatants from the microbial mat. Fractions (loaded on two gels) eluting from 0.23 M (fraction 15) to 0.43 M (fraction 27) NaCl are shown. The protein bands were assigned to ATP sulfurylase (Sat, *ca*. 50 kDa), APS reductase (small subunit, AprB, *ca*. 20 kDa), and (dissimilatory) sulfite reductase (Dsr, *ca*. 47 and 43 kDa bands of DsrA and DsrB) based on N-terminal sequences (Fig. 4); sizes were in accordance with those of orthologous enzymes from sulfate-reducing bacteria. Assignment of AprB was further corroborated by cloning and sequencing of the encoding

gene (see text; Fig. 5). The large subunit, AprA (*ca*. 70 kDa), is probably masked by a subunit of one of the methyl-coenzyme M reductases (Mcr). N-terminal sequencing of the Mcr subunits in the fractions did not reveal the Apr-like sequence, probably because Mcr was in excess. Mcr is highly abundant in the mat (Krüger *et al.*, 2003) and is assumed to catalyze methane activation. The spreading of Mcr from fractions 19 to 27 indicates variant forms of Mcr (see also Krüger *et al.*, 2003) consisting of three subunits (*ca*. 66, 48, and 30−37 kDa according to published sizes). The α-subunit (66 kDa) of one Mcr protein (fractions 19–23) is partly present as a second, somewhat lighter protein, as revealed by an additional band.

Fig. 4. Analyzed N-terminal sequences of ATP sulfurylase (Sat), the small APS reductase subunit (AprB), and both subunits of (dissimilatory) sulfite reductase (DsrA and DsrB) from the Black Sea mat and alignment with orthologs from known sulfate-reducing microorganisms. Species: *Desulfatibacillum alkenivorans* strain AK-01, *Desulfococcus oleovorans* strain Hxd3, *Desulfobacterium autotrophicum* strain HRM2, *Desulfovibrio desulfuricans* strain G20, *Desulfotomaculum reducens* strain MI-1, *Archaeoglobus fulgidus* strain VC-16.

Fig. 5. Phylogenetic tree of AprBA sequences, including five clones from the Black Sea mat (bold). The tree is based on maximum likelihood. Numbers represent bootstrap values (100 trials). Bar, 10% estimated sequence divergence.

Table 1. Specific activity of key enzymes for dissimilatory sulfate reduction in the cell-free extract of microbial mats (Black Sea) and pure cultures of sulfate-reducing bacteria.

	Specific activity[a] (nkat g_{pr}^{-1})	
	ATP sulfurylase	APS reductase
Mat extract	1 300	4 500
Desulfococcus multivorans	6 300	6 300
Desulfosarcina variabilis	8 200	15 000

[a] Determined at 28°C. 1 nkat = 0.06 µmol min^{-1}.

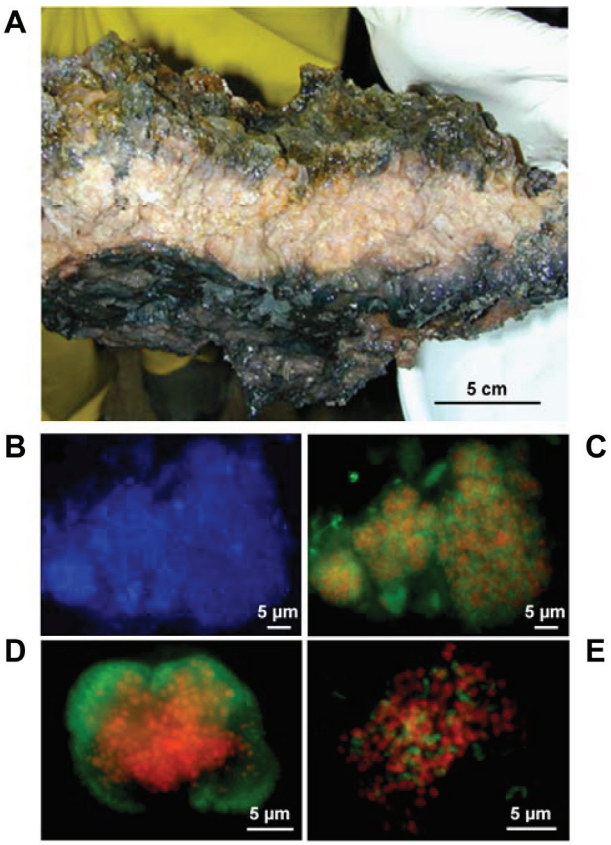

Figure 1

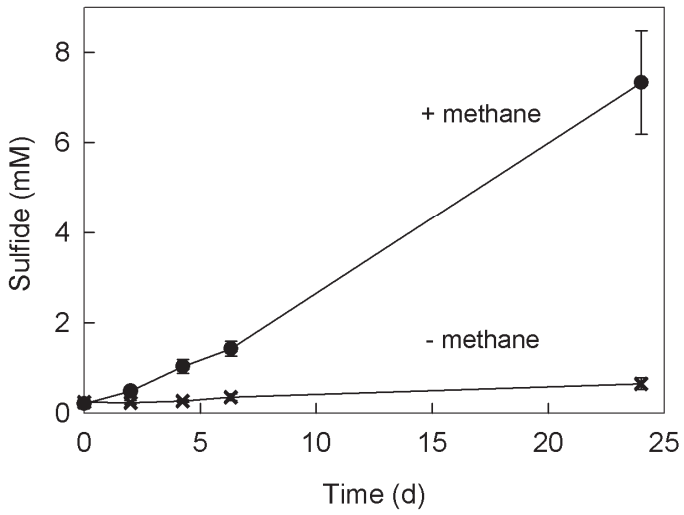

Figure 2

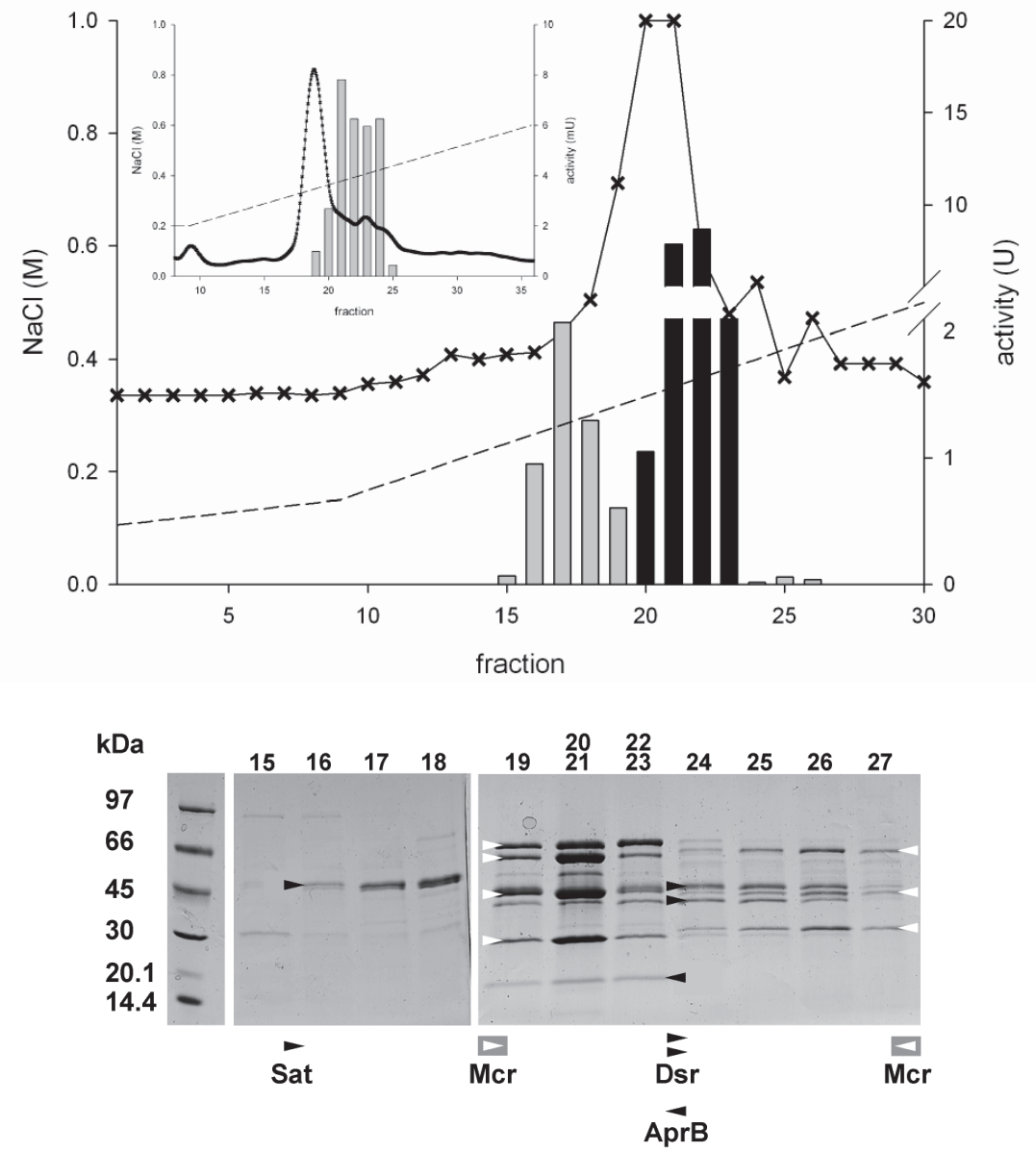
NaCl (M)
activity (U)
fraction
kDa
97
66
45
30
20.1
14.4
15 16 17 18 19 20 21 22 23 24 25 26 27
Sat
Mcr
Dsr
AprB
Mcr

Figure 3

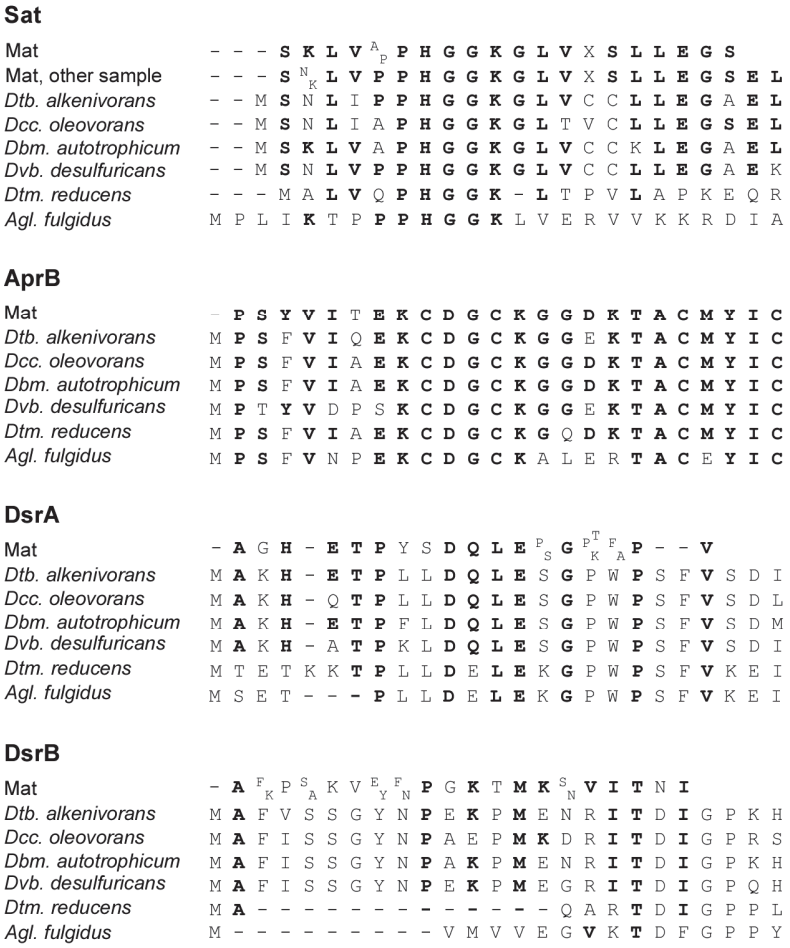
Sat
Mat
Mat, other sample
Dtb. alkenivorans
Dcc. oleovorans
Dbm. autotrophicum
Dvb. desulfuricans
Dtm. reducens
Agl. fulgidus
AprB
Mat
Dtb. alkenivorans
Dcc. oleovorans
Dbm. autotrophicum
Dvb. desulfuricans
Dtm. reducens
Agl. fulgidus
DsrA
Mat
Dtb. alkenivorans
Dcc. oleovorans
Dbm. autotrophicum
Dvb. desulfuricans
Dtm. reducens
Agl. fulgidus
DsrB
Mat
Dtb. alkenivorans
Dcc. oleovorans
Dbm. autotrophicum
Dvb. desulfuricans
Dtm. reducens
Agl. fulgidus

Figure 4

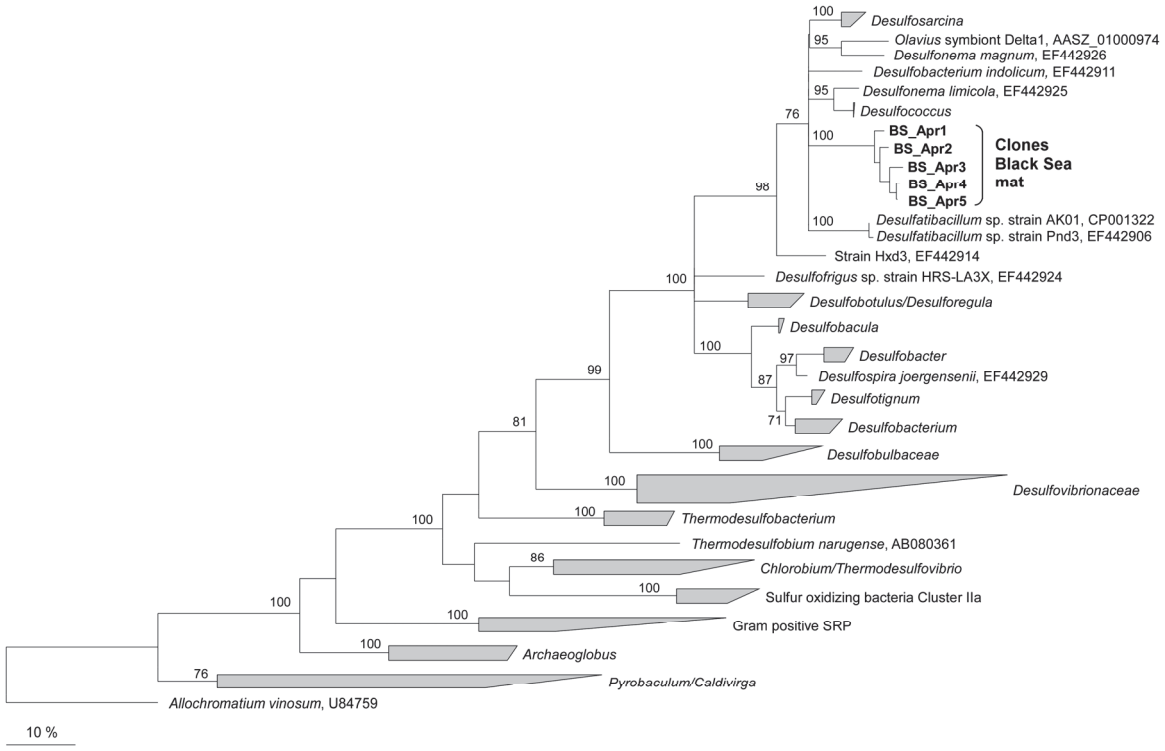
100
Desulfosarcina
95
Olavius symbiont Delta1, AASZ_01000974
Desulfonema magnum, EF442926
Desulfobacterium indolicum, EF442911
95
Desulfonema limicola, EF442925
Desulfococcus
76
100
BS_Apr1
BS_Apr2
BS_Apr3
BS_Apr4
BS_Apr5
Clones
Black Sea
mat
98
100
Desulfatibacillum sp. strain AK01, CP001322
Desulfatibacillum sp. strain Pnd3, EF442906
Strain Hxd3, EF442914
100
Desulfofrigus sp. strain HRS-LA3X, EF442924
Desulfobotulus/Desulforegula
Desulfobacula
100
97
Desulfobacter
99
87
Desulfospira joergensenii, EF442929
Desulfotignum
81
71
Desulfobacterium
100
Desulfobulbaceae
100
Desulfovibrionaceae
100
100
Thermodesulfobacterium
Thermodesulfobium narugense, AB080361
86
Chlorobium/Thermodesulfovibrio
100
Sulfur oxidizing bacteria Cluster IIa
100
100
Gram positive SRP
100
Archaeoglobus
76
Pyrobaculum/Caldivirga
Allochromatium vinosum, U84759
10 %

Figure 5

Supporting information

Basen *et al*.

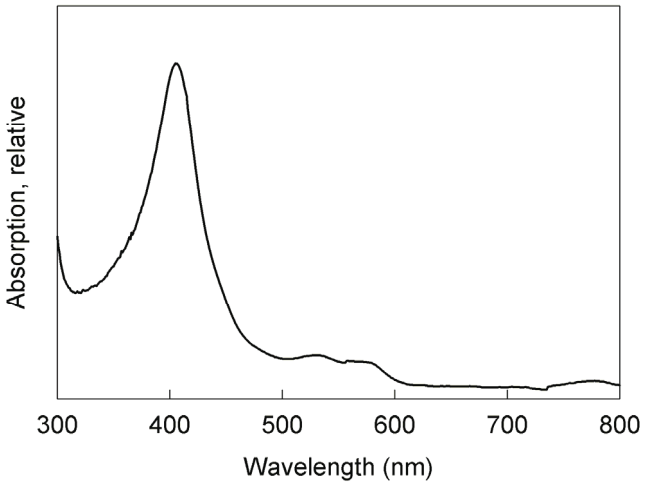

Figure S1. UV-visible spectrum of the Q-Sepharose fraction containing dissimilatory sulfite reductase (Dsr) and methyl-coenzyme M reductase (Mcr). The sulfite reductase exhibits the peak at 545 nm, which is the desulforubidin fingerprint, and a peak and a shoulder at 398 and 582 nm (Arendsen *et al.* 1993). Mcr exhibits a peak at ~410 nm, which is the absorption peak of F_{430}.

CHAPTER 3

Immunological detection of enzymes for sulfate reduction in bacterial cells of anaerobic methane-oxidizing microbial consortia

Jana Milucka, Friedrich Widdel and Seigo Shima

Contributions to the manuscript:

J.M. and F.W. designed research and project outline, J.M. and S.S. performed protein purification, J.M. tested the antibodies and established the immunolabeling protocol, J.M., F.W. and S.S conceived, wrote and edited the manuscript.

Chapter is *in preparation* for ISME Journal

Summary

Microbial consortia mediating anaerobic oxidation of methane coupled to sulfate reduction (AOM) are formed by methane-oxidizing archaea (ANME) and bacteria belonging mostly to the *Desulfosarcina/ Desulfococcus* (DSS) clade of *Deltaproteobacteria*. Whereas it is generally accepted that methane oxidation is catalyzed by ANME it has not yet been resolved which organism(s) perform the AOM-coupled sulfate reduction. Here we demonstrate distribution of enzymes of the methane oxidation pathway and dissimilatory sulfate-reducing pathway *in situ* in the ANME-DSS consortia from Black Sea microbial mats. Using antibodies raised against ATP sulfurylase and dissimilatory sulfite reductase purified directly from the active mats we show that these sulfate reducing enzymes were detected exclusively in one abundant microbial morphotype (~ 50% of all cells) reminiscent of the DSS bacteria. In contrast, none of the cells labeled with antibodies against methyl-coenzyme M reductase, an archaeal enzyme catalyzing methane oxidation, contained the sulfate-reducing enzymes. Our findings show that the abundant enzymes for methane oxidation and sulfate reduction belong to two dominant but different microbial morphotypes and suggest that the (major) sulfate-reducing activity associated with AOM is catalyzed by bacteria.

Introduction

The anaerobic oxidation of methane (AOM) with sulfate is an environmentally relevant process controlling both carbon and sulfur cycling in anoxic marine environments (Valentine & Reeburgh, 2000; Knittel & Boetius, 2009). AOM is presumed to be catalyzed in a syntrophic manner by a consortium of anaerobic methane-oxidizing archaea (ANME) and *Deltaproteobacteria* (Boetius *et al.*, 2000). There are three groups of ANME described to date – ANME-1, -2, -3. Their bacterial partners mostly belong to the clades of *Desulfosarcina/Desulfococcus* (ANME-1 and -2; Boetius *et al.*, 2000; Orphan *et al.*, 2002a; Knittel *et al.*, 2005; Schreiber *et al.*, 2010) and *Desulfobulbus* (ANME-3; Niemann *et al.*, 2006). Mechanism of the ANME-*Deltaproteobacteria* interaction remains, despite their common co-occurrence at AOM sites, enigmatic. It is generally accepted that ANME catalyze the anaerobic methane oxidation. The enzyme likely responsible for the activation of methane is a 'reverse' methyl-CoM-reductase (Mcr) known from methanogenic archaea (Krüger *et al.*, 2003; Scheller *et al.*, 2010). Further oxidation of the bound methyl moiety probably follows a reversed pathway of methanogenesis because corresponding genes have been found in the ANME (meta)genome (Krüger *et al.*, 2003; Hallam *et al.*, 2004; Chistoserdova *et al.*, 2005; Meyerdierks *et al.*, 2010; A. Meyerdierks, pers. comm.). A presumed function of the ANME-associated bacteria is utilization of reducing equivalents originating from methane oxidation for the reduction of sulfate. This would imply that the reducing equivalents are extracellularly shuttled from ANME to the DSS bacteria but the chemical nature of the shuttled compound is not yet elucidated. In nature ANME-2 also occur as single cells and/or monospecies aggregates (Orphan *et al.*, 2002b; Chistoserdova *et al.*, 2005; Orphan *et al.*, 2009) which provided support for a recent alternative AOM theory suggesting that (at least some) ANME archaea perform both methane oxidation and sulfate reduction alone (Widdel *et al.*, 2007; Thauer & Shima, 2008). So far, no genes encoding for enzymes of the pathway of dissimilatory sulfate reduction could be retrieved from ANME metagenomes (Hallam *et al.*, 2004; Meyerdierks *et al.*, 2005; Meyerdierks *et al.*, 2010). Interestingly, the sulfate reducing capability of the bacterial

partners has never been directly shown either and is merely based on their 16S rDNA phylogenetic affiliation to a clade of known sulfate reducers.

The biochemical pathway for dissimilatory sulfate reduction is identical in all currently known sulfate-reducing microorganisms and produces activated sulfate (APS; adenosine-5'-phosphosulfate) and sulfite as intermediates (Rabus *et al.*, 2006). The responsible enzymes – adenosine triphosphate (ATP) sulfurylase (Sat), APS reductase (Apr), and dissimilatory sulfite reductase (Dsr) – have only recently been identified in the Black Sea mats (Basen *et al.*, in revision). Analysis of the corresponding full-length gene sequence for APS reductase suggested a bacterial origin of this protein (Basen *et al.*, in revision). However, a clear assignment of the sulfate reducing enzymes to the DSS bacteria based on gene or short N-terminal protein sequences might be ambiguous due to the fact that the genes coding for SR enzymes have been often subjected to horizontal gene transfer (Klein *et al.*, 2001; Stahl *et al.*, 2002).

In this work we investigate which organism(s) possess the enzymes for sulfate reduction that are found in large quantities in the cell extracts from AOM samples and thus which organism(s) are capable of performing AOM-associated sulfate reduction. We raised specific antibodies against partially purified Sat and Dsr from the Black Sea microbial mat. The same mat sample was then used for preparing semi-thin (300 – 400 nm) cryosections, on which immunolabeling was performed. This new immunolabeling approach allowed us for the first time to localize the abundant sulfate-reducing enzymes from the Black Sea mats and assign them to specific cells in the AOM consortia.

Materials and methods

Microbial cultures

Strains of methanogenic archaea and sulfate-reducing bacteria were obtained from the German Collection of Microorganisms and Cell Cultures (DSMZ, Braunschweig). *Methanosarcina barkeri* strain Fusaro (DSM 804) was grown anaerobically at 37°C in freshwater medium supplemented with 2 mM acetate under an H_2:CO_2 (80:20) atmosphere (Widdel & Bak, 1992). *Desulfococcus multivorans* (DSM 2059) and

Desulfosarcina variabilis (DSM 2060) were grown at 28°C in synthetic brackish or seawater medium, (Widdel & Bak, 1992), respectively, supplemented with 4 mM benzoate. The sulfate-reducing archaeon *Archaeoglobus fulgidus* (DSM 4304) was grown in DSM 399 medium with an H_2:CO_2 (80:20) headspace at 85°C.

Samples of microbial mats were obtained during the cruise of RV Meteor M72-2 to the northwestern Black Sea in February-March 2007 (GHOSTDABS station no. 328; water depth 220 m; 44° 46' 31'' N, 31° 59' 25''E). The mat pieces were incubated anoxically in artificial seawater medium (Widdel & Bak, 1992) with pure methane headspace at 12°C in dark. Maintenance and handling of the samples was performed in an anoxic glove box (Mecaplex) under N_2:CO_2 (90:10) atmosphere. At the time of experiment, the AOM rates were 230 µmol gram (dry weight)$^{-1}$ day^{-1}.

Fluorescence in situ *hybridization*

Slurry of homogenized Black Sea mats (black part) was fixed for 12 h in 2% formaldehyde in phosphate-buffered saline (PBS; 7 mM Na_2HPO_4, 3 mM NaH_2PO_4, 130 mM NaCl; pH 7.2), washed with 1× PBS and an aliquot was filtered onto 0.2 µm GTTP polycarbonate filters (Millipore). *In situ* hybridizations were performed at 46°C for 120 min in a hybridization buffer containing 0.9 M NaCl, 50% formamide, 20 mM Tris-HCl, pH 7.4, and 0.01% SDS (sodium dodecyl sulfate). Probe concentrations were 5 ng/ml. Hybridization mixtures were removed by washing filters for 15 min in a buffer containing 20 mM Tris-HCl, pH 7.4, 35 mM NaCl, and 0.01% SDS at 48°C. The washing buffer was removed by washing with distilled water and the filters were air dried and mounted onto glass slides. Oligonucleotide probes were purchased from Biomers (Germany) or ThermoHybaid (Germany). For double hybridization experiments ANME2-538 (Treude *et al.*, 2005) labeled with Cy3 and DSS-658 (Manz *et al.*, 1998) labeled with carboxyfluorescein were used.

Purification of enzymes

The cell fractionation and protein purification steps were performed in an anaerobic chamber under an N_2:H_2 (95:5) atmosphere on ice or at 18ºC. Methyl-coenzyme M reductase (Mcr) was isolated from cells of *Methanosarcina barkeri* according to Grabarse *et al.* (2000), omitting the hydroxyapatite column purification step. Sat and Dsr were isolated from the black microbial mats as described by Basen *et al.* (in revision). The mats were cut in pieces and suspended in 50 mM MOPS-KOH buffer (pH 7.0). The cells were disrupted by ultrasonication for 3 times of 8 min at 120 W (puls duration 0.5 s). The resulting crude extract was subjected to ultracentrifugation at 150,000 × g for 1 h. The membrane-free supernatant was fractionated by ammonium sulfate precipitation (20% saturation) followed by centrifugation at 18,000 × g for 20 min. After desalting by ultrafiltration, the supernatant was applied on a Q-Sepharose column (HiTrap Q HP; 5 ml; GE Healthcare), which was equilibrated with 50 mM MOPS/KOH buffer (pH 7.0). The proteins were eluted with a linear-increasing gradient of NaCl from 0 to 0.6 M. The eluted fractions (5 ml) were analyzed by small gradient (4-15%) SDS-PAGE (mini-format) and by Sat-, Apr- and Dsr-specific activity assays. The fractions containing an Sat-specific activity peak and an abundant *ca.* 50 kDa protein (0.25 – 0.32 M NaCl) were pooled and stored at 4°C until immunization. Fractions containing a double band of ca. 43 and 47 kDa (0.35 – 0.44 M NaCl) exhibited a peak of Dsr activity. These fractions were pooled and applied on a gel filtration column (Superdex 200; 1 x 30 cm; GE Healthcare) for further purification. Fractions (5 ml in Tris buffer, pH 8) eluting from the gel filtration column were analyzed by SDS-PAGE and the ones containing the 43 and 47 kDa double bands were pooled and stored at 4°C until immunization. Identity of the immunizing proteins was ultimately confirmed by N-terminal amino acid sequencing of the peptides blotted on polyvinylidene difluoride (PVDF) membrane (for details see Basen *et al.*, in revision).

Antibody production and validation

All primary antibodies used in this study were polyclonal, raised against purified proteins in rabbits (Mcr) or guinea pigs (Sat, Dsr). Immunizations (*ca.* 500 µg protein for rabbit

and *ca.* 100 µg protein for guinea pig), animal maintenance and antisera preparations were done by Eurogentec S.A., Seraing, Belgium. IgG concentrations of final bleeds of anti-Mcr, anti-Sat and anti-Dsr antisera were 25.7, 23.6, and 20.5 mg/ml, respectively; the working dilutions are listed in the text. The following commercially available secondary antibodies were used: goat anti-rabbit IgG FITC conjugate (Invitrogen; cat. nb. 81-6111), goat anti-guinea pig IgG TRITC conjugate (Santa Cruz Biotechnology; cat. nb. sc-2442), goat anti-rabbit IgG peroxidase conjugate (Pierce Biotechnology; cat. nb. 31460), pig anti-guinea pig IgG peroxidase conjugate (Sigma; A5545). The concentrations of secondary antibodies were adjusted according to manufacturers' instructions.

SDS PAGE and Western Blotting

Lysates of Black Sea mats and three control strains - *Methanosarcina barkeri* as methanogenic archaeon, *Desulfosarcina variabilis* (or *Desulfococcus multivorans*) as sufate-reducing bacterium, and *Archeoglobus fulgidus* as sulfate-reducing archaeon - were used for testing the antibody specificity. Protein concentrations were determined using bicinchoninic acid (BCA) Protein Assay (Pierce Biotechnology). Proteins were resolved on 10% or 12% denaturing polyacrylamide gels (mini-format), according to Laemmli (1970). The separated peptides were blotted on a nitrocellulose membrane using wet blot (BioRad) according to manufacturer's instructions. The membranes were blocked overnight with non-fat 5% milk in PBS. After immunolabeling (60 min, room temperature), the membranes were developed (exposition time $<$ 1 min) using SuperSignal Chemiluminescent Substrate (West Pico; Pierce Biotechnology) and the signal was recorded on CL-Xposure Films (Pierce Biotechnology).

Preparation of cryosections

Small pieces of the mats were fixed in an anoxic chamber by addition of 8% formaldehyde in 100 mM phosphate buffer (PB; pH 7.4) in a 1:1 ratio to the sample. The fixation was performed for 30 minutes at 12ºC. The sample was briefly washed with cold

PB and fixed again with fresh 4% formaldehyde in 100 mM PB. The samples were stored in 2% formaldehyde in 100 mM PB at 4ºC until processed further. Pieces of mats were embedded in 10% gelatine (in water) or 2% low melting point agarose (in water) and cut to cubes of a volume of ~1 mm^3. Afterwards, the sample was infiltrated overnight at 4°C with 2.3 M sucrose (in PB) on a rotational shaker. Semi-thin cryosections (300-400 nm) were prepared with an ultramicrotome according to Tokuyasu (1973, 1980), transferred on poly-L-lysine-coated coverslips in a 1:1 mixture of 2.3 M sucrose:methylcellulose and dried.

Immunofluorescent labeling on cryosections

All washing and incubation steps were performed "section-side down" on drops of 300 μl, and 30 μl, respectively. The coverslips with attached sections were washed in PBS to dissolve the sucrose:methylcellulose support. After washing, the sections were incubated with primary and secondary antibodies and each incubation was followed by three washing steps in PBS with 0.01% Tween. Ultimately, the coverslips were counterstained and mounted in Mowiol/DABCO (1,4-diazobicyclo-[2,2,2]-octane; Sigma; 2% w/v)/DAPI (4',6'-diamidino-2-phenylindole; Sigma; final concentration, 1μg ml^{-1}) mixture. Double labeling, e.g. anti-Mcr + anti-Sat, anti-Mcr + anti-Dsr, and anti-Sat + anti-Dsr, was performed in a single step. Negative controls without primary antibodies or with pre-immune sera instead of primary antibodies did not yield any detectable signals. Blocking step with 5% non-fat milk did not affect the specificity of the signal and was routinely omitted from the immunolabeling procedure.

Image acquisition and processing

The sections were examined with a Zeiss AxioCam MRc attached to a Zeiss Axioplan Microscope (Zeiss, Jena, Germany) equipped with oil immersion planapochromat lens (100x1.3NA; Zeiss, Jena, Germany).

The obtained images were processed with Adobe Photoshop CS4 (version 11.0.2). The fluorescent signals of TRITC and FITC were changed to green and red color,

respectively, to facilitate comparison of the immunolabeling images with the FISH images where the archaea are probed with red fluorescent probes.

Results

Characterization of antisera

Purified Mcr, Sat and Dsr were used for polyclonal antibody generation. Pre-immune sera from each immunization were checked for unspecific binding. Final antisera were analyzed by Western blotting for their ability (i) to discriminate their target proteins among others in the soluble extract from Black Sea mats and (ii) to cross-react with homologous proteins from related species.

The anti-Mcr antibody raised against Mcr purified from *Methanosarcina barkeri* bound to three proteins in the extract from Black Sea mats. Their sizes corresponded to the sizes of α, β, and γ subunits of Mcr (Ni-protein II; Figure 1A) isolated from Black Sea mats as reported by Krüger *et al.* (2003). The methanogenic and methanotrophic Mcr proteins thus appear to share enough structural similarities to be reciprocally recognized by our antibody. This is in agreement with the high sequence similarity (64%) between Mcr-encoding genes from methanogenic archaea and ANME (Hallam *et al.*, 2003; Krüger *et al.*, 2003).

The anti-Sat and anti-Dsr antisera were raised against proteins that were purified from the mats and identified via N-terminal amino acid sequencing, activity assays and polyacrylamide gel electrophoresis. These proteins were the only Sat and Dsr enzymes recovered from the cell extracts. The antibodies selectively bound peptides with sizes of their immunizing proteins (ca. 50 kDa Sat and ca. 43 kDa and 47 kDa Dsr; Figure 1B, C) in the soluble extract from the mat. The antisera were also tested against crude extracts from *Desulfosarcina variabilis* where they bound to a ca. 50 kDa (anti-Sat; Figure 1B) and ca. 43 and 50 kDa (anti-Dsr; Figure 1C) proteins. These sizes agree with previous reports of known dissimilatory Sat (Baliga *et al.*, 1961; Akagi & Campbell, 1962; Skyring *et al.*, 1972; Sperling *et al.*, 1998) and Dsr (Arendsen *et al.*, 1993). However, it appears

that the Dsr subunits of the mat protein are closer in size to the Dsr from *Desulfococcus multivorans*, a different relative from the DSS clade (Supplementary Figure 1).

→ **Figure 1**

Our anti-Sat and anti-Dsr antisera did not bind to their respective target proteins in the extracts of *A. fulgidus* (Figure 1B, C), even though the sulfate reducing archaeon harbors dissimilatory Sat and Dsr (Sperling *et al.*, 1998; Dahl & Trüper, 2001). This suggests that the archaeal proteins and the proteins isolated from the mats (immunizing proteins) do not share enough structural or sequence similarities to cause the antibodies to cross-react. Importantly, neither of the two antisera against SR enzymes bound to any proteins in the extracts from methanogenic archaea (Figures 1B, C).

In situ localization of Mcr

Our immunofluorescent labeling shows that the cells labeled with the anti-Mcr antibody constitute a dominant morphotype in the sample. The cells are large and irregularly shaped (Figure 2) and form small aggregates or are mixed as single cells among other, mostly rod-shaped, cells in the sample.

→ **Figure 2**

The fluorescent signal within the cells appears diffuse suggesting cytoplasmic localization of the enzyme. A similar “diffuse” labeling pattern of Mcr was observed in (presumable) ANME cells with immunogold labeling for TEM (Heller *et al.*, 2008). The Mcr from methanogenic archaea is also localized in the cytoplasm (Ossmer *et al.*, 1986; Aldrich *et al.*, 1987; Hoppert & Mayer, 1999).

In situ localization of Sat and Dsr

Both sulfate reducing enzymes (Sat and Dsr) co-occur in one cell morphotype, which is rod-shaped and constitutes a large fraction of cells in the sample (~ 50% of all cells; Figure 3).

→ **Figure 3**

The diffuse fluorescent signal suggests cytoplasmic distribution of the proteins as reported earlier for Sat and Dsr from *Desulfovibrio* (Odom & Peck, 1981). The labeled

cells are rod- or vibrio-shaped and clearly morphologically different from the Mcr-labeled cells. Indeed, simultaneous double labeling of Mcr and Dsr confirmed that the cells targeted with these two antibodies form two different cell populations (Figure 2). Importantly, none of the investigated cells labeled with anti-Mcr antibody contained detectable amounts of Dsr. Simultaneous labeling of Mcr and Sat showed that the anti-Mcr labeled cells did not contain detectable amounts of Sat either (data not shown).

Discussion

The view of AOM as an obligately syntrophic process has been challenged by the recent hypothesis, which proposed that the methane oxidizing archaea might also be capable of performing AOM-coupled sulfate reduction (Widdel *et al.*, 2007; Thauer & Shima, 2008). To answer this question we located two of the sulfate reducing enzymes *in situ* in single cells of the AOM consortia with specific antibodies. The immunolabeling was performed on thin cryosections of the microbial mat sample. Compared to whole-cell labeling the sectioning approach allowed full accessibility of both cell types for antibody binding without any permeabilization steps because the cells were 'open' on the surface of each section. Low thickness of the sections reduced the depth of focus of the objectives and allowed clear single-cell resolution in these tight microbial aggregates also with epifluorescence microscopy. The cryosectioning is (currently) incompatible with FISH and we therefore did not have a direct way of correlating the protein expression of a given cell with its 16S rDNA-based identity. We used Mcr, the enzyme responsible for methane activation, as a 'marker enzyme' for ANME. In the mat, our anti-Mcr antibodies bound to cells, which were abundant (Figure 2) and which had size and shape characteristic of ANME-2 visualized by FISH (Knittel *et al.*, 2003) and with transmission electron microscopy in AOM consortia (TEM; Reitner *et al.*, 2005; Heller *et al.*, 2008). The antibody was raised against Mcr purified from a methanogen and it could therefore also target methanogenic archaea in the mat. However, all genes coding for Mcr in AOM samples have been so far attributed to ANME (Hallam *et al.*, 2004; Meyerdierks *et al.*, 2005) and the abundant Ni protein ('reverse' Mcr) purified from the Black Sea mats has

been shown to belong to ANME too (Krüger *et al.*, 2003). Upon addition of methanogenic substrates to the mat sample only negligible methanogenic activity was measured (Basen *et al.*, in revision, and unpublished data) suggesting that the number of methanogenic archaea in the sample is very low. Therefore, we defined cells labeled with the anti-Mcr antibody as ANME.

None of these archaeal cells expressing Mcr was targeted by the antibodies raised against the sulfate reducing enzymes. One could argue that we did not detect the archaeal sulfate reducing enzymes because archaeal proteins as e.g. in the extracts of *A. fulgidus* could not be recognized by our anti-Sat and anti-Dsr antisera. However, considering that the antibodies only bind to proteins with sufficient similarity to the immunizing proteins this would suggest that the archaeal proteins (e.g. from *A. fulgidus*) share only little homology with the Black Sea mat proteins used for immunization. Indeed, the N-terminal sequences of the purified mat proteins show higher similarities to bacterial proteins than to the ones from *A. fulgidus* providing additional evidence for bacterial origin of the mat proteins (Basen *et al.*, in revision).

Simultaneous anti-Sat and anti-Dsr labeling showed only one cell morphotype contained both enzymes for sulfate reduction (Figure 3). The high abundance of labeled cells agrees well with the high AOM-coupled sulfate reduction rates in the Black Sea mats and with the conspicuous amount of the isolated enzymes in the cell extracts (ca. 2% of total soluble proteins; Basen *et al.*, in revision). The purified Sat and Dsr used for antibody generation were the only canonical SR enzymes in the mat extract detectable with polyacrylamide gels and the enzyme activity assays (Basen *et al.*, in revision). Fluorescence in situ hybridization data show that the second most abundant cell type in the mats (apart from ANME) are the bacteria of *Desulfosarcina/Desulfococcus* cluster (Figure 2; see also Basen *et al.*, in revision). These bacteria have the same vibroid to rod-like shape and a similar size as the cells labeled with the anti-Sat and anti-Dsr antibodies (ca. 1 µm length; Figure 2 and 3). Based on these similarities we consider the cells visualized with the antibodies against sulfate reducing enzymes as bacteria of the deltaproteobacterial DSS cluster.

Implications for the ANME-SRB syntrophy

Our data suggest that in the Black Sea mats ANME-2 themselves do not express detectable amounts of 'classical' SR enzymes and instead all these enzymes are found in the abundant cells reminiscent of the partner DSS bacteria. Our observations thus render unlikely those mechanisms of AOM which assume presence of major canonical sulfate-reducing enzymes in the ANME-2 or by which the ANME-2 manage to catalyze AOM at observed rates in the absence of their bacterial partners.

A modeling study predicted that if the observed rates of AOM involve shuttling of classical intermediates (H_2, acetate, formate) then methane oxidation and sulfate reduction must be performed in a single organism or in two organisms that are tightly associated (Sørensen *et al.*, 2001). If the SR enzymes that we detected in the mat sample are the only ones employed in AOM the site of methane oxidation (i.e. ANME) and sulfate reduction (i.e. partner bacteria) in the investigated aggregates are separated by several micrometers (Figure 3). In agreement with previous studies (Nauhaus *et al.*, 2002; Wegener *et al.*, 2008) we thus conclude that a simple shuttling of "classical" syntrophic intermediates, as investigated by Sørensen *et al.*, is unlikely to occur between ANME-2 and the associated bacteria. Although we cannot exclude that ANME-2 produce minor amounts of canonical sulfate-reducing enzymes and/or other enzymes of either unconventional structure or with unique reaction intermediates (other than APS and/or sulfite) our results support the syntrophic theory of organisms involved in AOM and further encourage the search for mechanisms of their metabolic coupling.

Acknowledgements

We are indebted to Antje Boetius for access to samples, Thomas Holler for collecting the samples and Mirko Basen for assistance with FISH. We thank Marc Strous, Marcel Kuypers, Rudolf Amann and Jens Harder for critically reading and correcting the manuscript. This work was supported by the Max Planck Society and Marie Curie Early Stage Training Site in Marine Microbiology (MEST-CT-2004-007776). Seigo Shima was financed by the emeritus grant (Max Planck Society) given to Rudolph K. Thauer.

Figure legends

Figure 1. Western blots probed with anti-Mcr antibody (A), anti-Sat antibody (B), and anti-Dsr antibody (C). Values on the left indicate molecular mass (in kilodaltons). The subunits of respective detected proteins are marked by arrows. Asterisk indicates the cleaved α subunit (α') of Mcr (Ellermann *et al.*, 1989). The different intensities of the bands result from differences in different protein amounts and chemiluminiscent substrate development conditions.

Individual lanes contain crude extracts from Methanosarcina barkeri (Ms), Desulfosarcina variabilis (Ds), black microbial mats from the Black Sea (BS), and Archaeoglobus fulgidus (Af).

The antibodies were used at following dilutions: anti-Mcr 1:2000, anti-Sat 1:5000, anti-Dsr 1:5000.

Figure 2. Representative images of AOM consortia stained with DAPI and FISH (upper panel) and DAPI and IFL (lower panel). Upper panel: cells of ANME-2 archaea (red) and DSS bacteria (green) form intermixed consortia in the Black Sea sample. Lower panel: in the same sample, Mcr is localized in the larger, irregularly shaped cells whereas Dsr is found in the rod-shaped bacteria on the periphery of the aggregate. An overlay of the anti-Mcr (red) and anti-Dsr (green) antibody signal clearly shows that the respective enzymes are localized in two different organisms. Note the morphological similarities between the Mcr-labeled cells (IFL) and ANME (FISH) and Dsr-labeled cells (IFL) and DSS (FISH).

The antibodies were used at following dilutions: anti-Mcr 1:200, anti-Dsr 1:200. Scale bar = 5µm

Figure 3. AOM consortium visualized with DAPI staining and with anti-Dsr and anti-Sat antibodies. An overlay of the fluorescent signal from anti-Sat (green) and anti-Dsr (red) antibodies shows that both enzymes co-occur in the same cells.
The antibodies were used at following dilutions: anti-Sat 1:200, anti-Dsr 1:200. Scale bar = 5µm

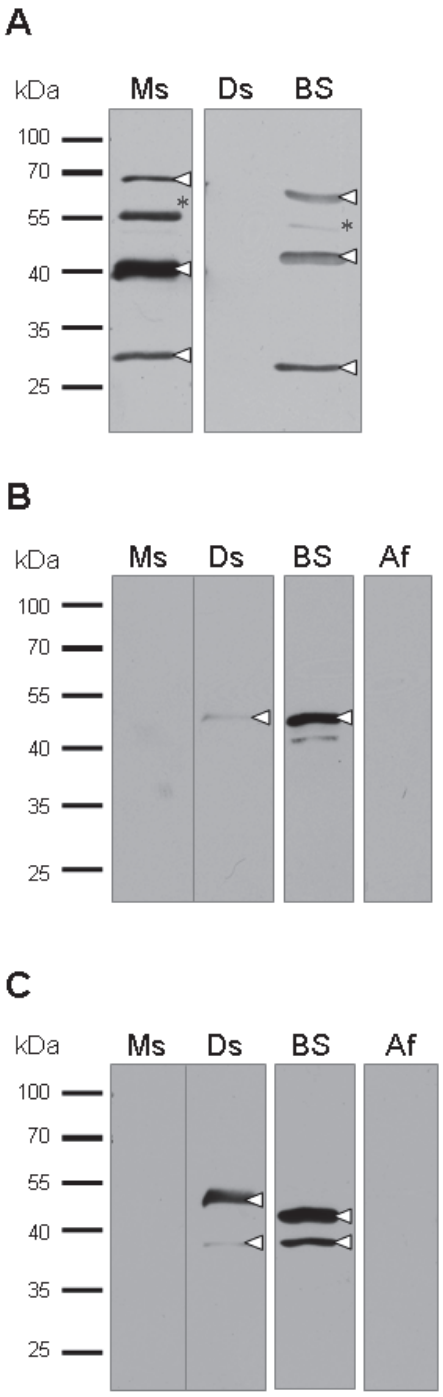
A
kDa
Ms
Ds
BS
100
70
55
40
35
25
B
kDa
Ms
Ds
BS
Af
100
70
55
40
35
25
C
kDa
Ms
Ds
BS
Af
100
70
55
40
35
25

Figure 1

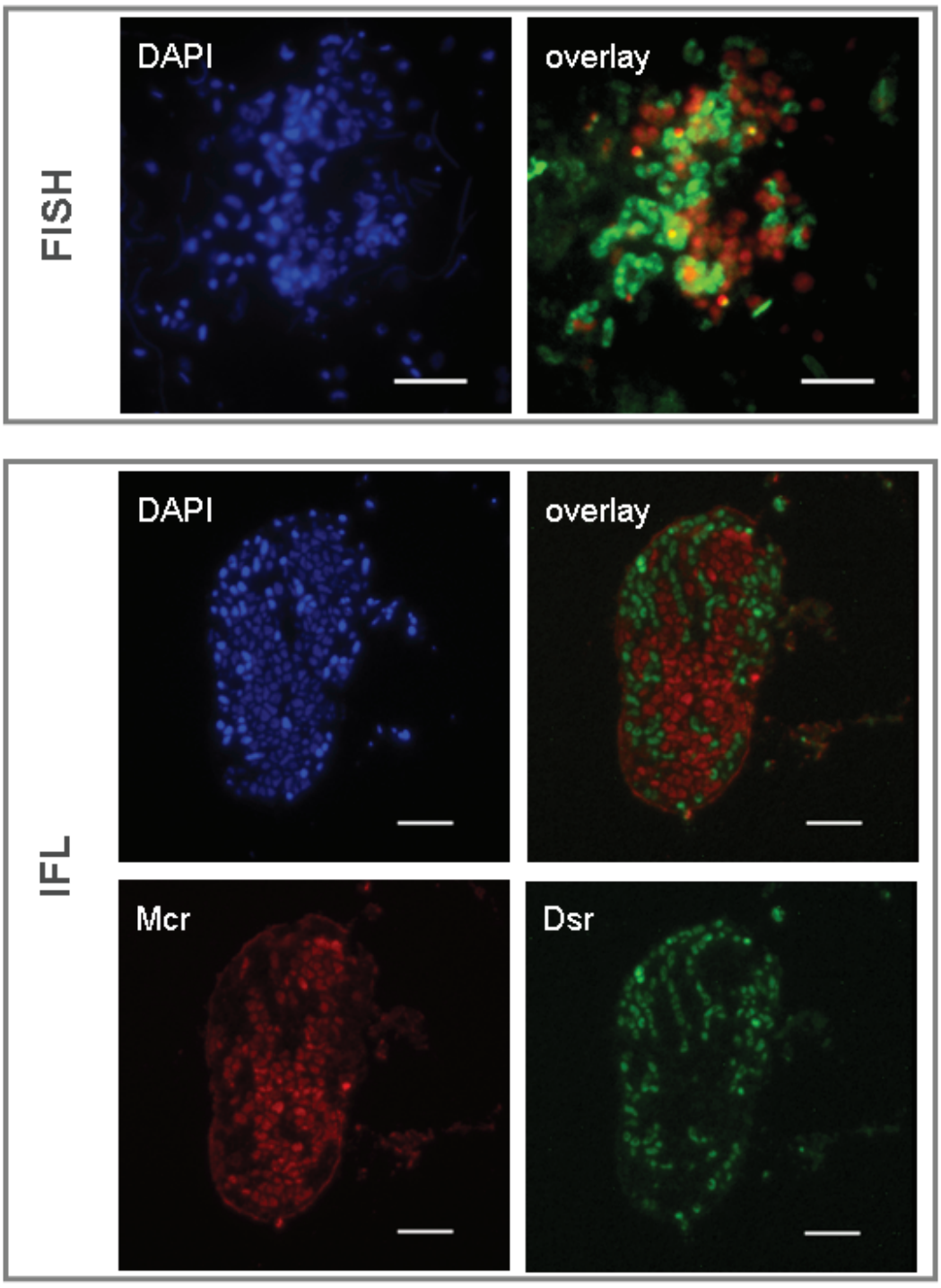

Figure 2

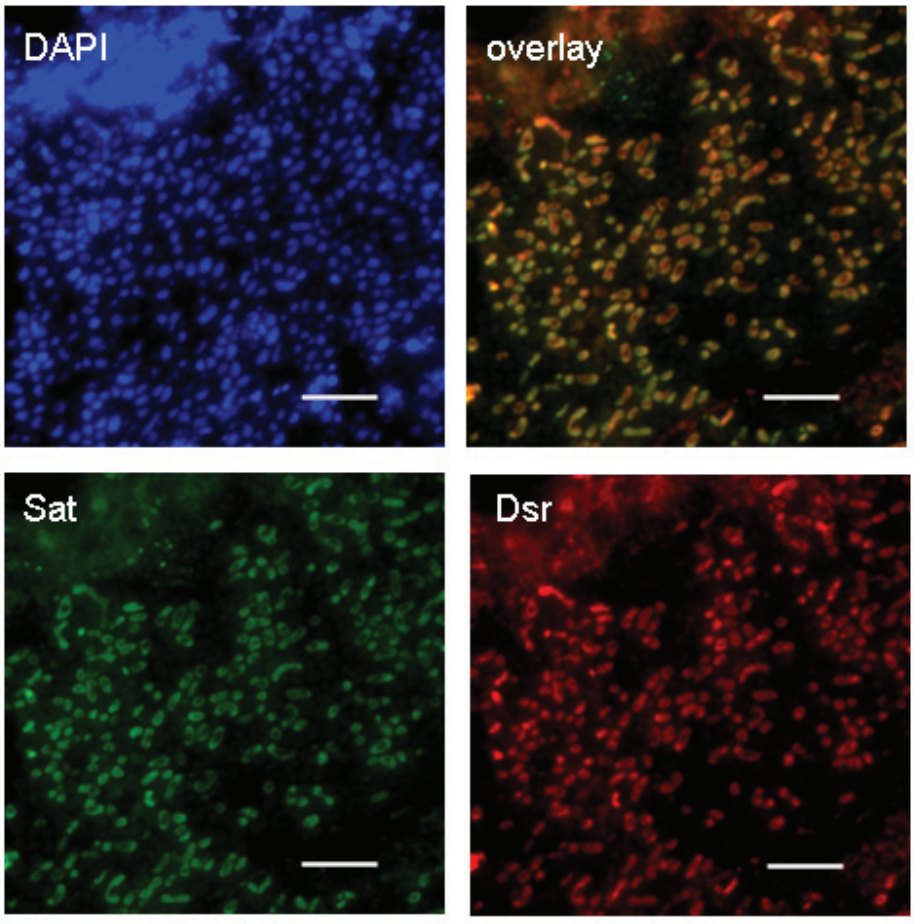

Figure 3

Supporting information

Milucka *et al*.

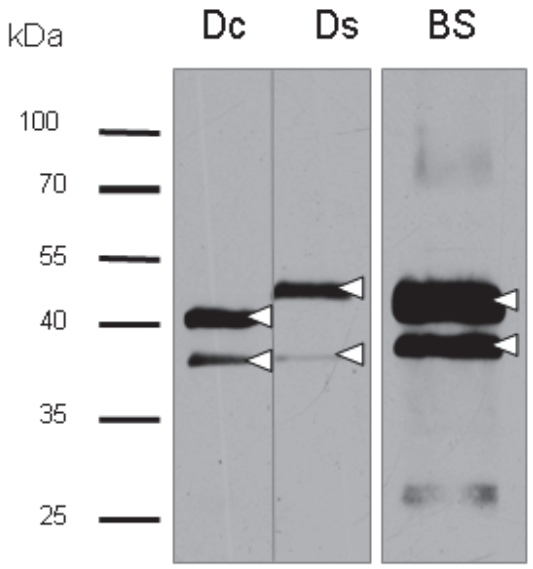

Figure S1. Western blot probed with anti-Dsr antibody at a 1:5000 dilution. Values on the left indicate molecular mass (in kilodaltons). The subunits of DSR are marked by arrows. Individual lanes contain crude extracts from *Desulfococcus multivorans* (*Dc*), *Desulfosarcina variabilis* (*Ds*), black microbial mats from the Black Sea (BS).

CHAPTER 4

Sulfur cycling between archaea and bacteria is involved in anaerobic oxidation of methane

Jana Milucka, Timothy G. Ferdelman, Marcel M. M. Kuypers

Contributors and potential co-authors: Gabriele Klockgether, Lubos Polerecky, Tomas Vagner, Michael Formolo, Ingo Lieberwirth, Gunter Wegener, Friedrich Widdel, Markus Schmid, Michael Wagner

Contributions to the manuscript:

J.M., F.W., T.G.F. and M.M.M.K. designed research and project outline, J.M. provided enrichment cultures and performed isotope labeling experiments, J.M. performed FISH, IFL and IGL analysis, J.M. and I.L. performed TEM/EDX analysis, J.M., M.M.M.K., M.S. and M.W. performed Raman spectroscopy and data analysis, J.M., T.V., L.P. and M.M.M.K. performed nanoSIMS analysis and data evaluation, G.K. and T.F. performed analysis of sulfur compounds, M.F. performed sulfur extractions, G.W. and T.F. contributed new analytical technique, T.F. performed thermodynamic calculations, J.M., T.F. and M.M.M.K. conceived, wrote and edited the manuscript.

Chapter is *in preparation*

Summary

The anaerobic oxidation of methane (AOM) coupled to sulfate reduction plays a crucial role in biogeochemical carbon and sulfur cycling in marine sediments. AOM is most likely mediated by a consortium of methanotrophic Archaea (ANME) and sulfate-reducing *Deltaproteobacteria* via a so far unknown mechanism. Here we propose that this mechanism might involve a transfer of zerovalent sulfur (S^0) between the bacteria and the ANME. We show that ANME intracellularly accumulate large amounts of S^0, which is at least partly derived from sulfate. We provide evidence for sulfur turnover in ANME being directly linked to methane oxidation. We cannot unambiguously conclude the directionality of sulfur transport between the ANME and the DSS but based on our observations and thermodynamic considerations a following model for sulfur cycling between ANME and SRB involved in AOM can be envisioned. The SRB reduce sulfate with sulfide to polysulfide, which is released from the cells. The disulfides will likely react with reduced sulfur outside the cells to form longer-chain polysulfides. This S^0 is taken up by the ANME and used to oxidize methane to CO_2. During this process sulfide is released, which is partly re-used by the SRB to reduce sulfate. Such cooperation maintained through extracellular sulfur cycling not only represents a unique syntrophic mechanism but also has significant implications for our understanding of biogeochemical sulfur cycling and its transformations in marine sediments.

Introduction

Anaerobic oxidation of methane coupled to sulfate reduction (AOM; Eq. 1) is widespread in all oxygen-depleted marine environments where sulfate is the most abundant electron acceptor (methane seeps, vents, and surface and deep sediments (Knittel & Boetius, 2009 and references therein).

$$CH_4 + SO_4^{2-} \rightarrow HS^- + HCO_3^- + H_2O \qquad \text{(Eq. 1)}$$

AOM plays a crucial role in biogeochemical carbon and sulfur cycling. It oxidizes the majority of methane – a potent greenhouse gas – diffusing from the seafloor and prevents it from escaping to the atmosphere (Hinrichs & Boetius, 2002; Reeburgh, 2007). The AOM-coupled sulfate reduction consumes a large portion of the downwards sulfate flux (Devol & Ahmet, 1981) and forms sulfide, which diffuses upwards towards the seafloor and supports free-living and symbiotic sulfide- and sulfur-oxidizers.

Despite the pronounced effect of AOM on sediment biogeochemistry the biological basis for AOM has persistently eluded clarification and remains a geomicrobiological puzzle to this day (Alperin & Hoehler, 2010). The process has been proposed to be syntrophically mediated by a consortium of methanotrophic Archaea (ANME) and *Deltaproteobacteria* (Boetius *et al.*, 2000; Orphan *et al.*, 2001a) because of their co-occurrence at all so far investigated AOM sites and in all enrichment cultures. However, the syntrophic nature of their relationship is still a matter of debate because the necessary intermediate that would shuttle reducing equivalents originating from methane oxidation in the ANME to the associated bacteria has never been conclusively identified. Moreover, in case of a syntrophy, the extremely low energy yield of the net reaction (*ca*. 20 kJ mol^{-1} CH_4) would have to be shared between two partners. Therefore, it has been suggested (Widdel *et al.*, 2007; Thauer & Shima, 2008; Johnson & Mukhopadhyay, 2008) that (at least some) ANME might perform sulfate reduction on their own. Currently, there is no direct evidence for this hypothesis, in fact, recent biochemical studies, which show the only detectable enzymes for sulfate reduction are expressed by the associated bacteria provide evidence for an active involvement of both organisms in AOM (Milucka *et al.,* in preparation).

Several alternative hypotheses have been put forward, all of which involve a flow of electrons, or intermediates, from the ANME to the bacteria, to explain the syntrophic mechanism. None of the plausible syntrophic intermediates (i.e. hydrogen, formate, acetate, or methanol) was conclusively shown to be involved in AOM (Nauhaus *et al.*, 2002; Meulepas et al., 2010) and a shuttling of a carbon-containing intermediate in general has been excluded (Wegener *et al.*, 2008). Furthermore, there is no experimental evidence for pure electron transfer via extracellular nanowires (Shima & Thauer, 2005; Meyerdierks *et al.*, 2010) or a direct cell-to-cell contact.

Alternatively, it is feasible that reduced sulfur compounds e.g. formed during SR may serve as intermediates in AOM. Based on energetic and thermodynamic considerations, zerovalent sulfur (S^0) might be used as an electron acceptor for methane oxidation (Shima & Thauer, 2005) because its redox potential is sufficiently low to be compatible with the enzyme likely responsible for methane activation in AOM, 'reverse' methyl Co-M reductase (Mcr; Krüger *et al.*, 2003; Scheller *et al.*, 2010). Zerovalent sulfur in the form of elemental sulfur and dissolved polysulfides (up to 200 µM; Kamyshny & Ferdelman, unpubl. res.) have been observed in the AOM active zone of Black Sea sediments. Here we investigate the potential role of zerovalent sulfur in AOM using a combination of microbiological, imaging and biogeochemical techniques. The analyses were performed on microbial cultures highly enriched in AOM biomass (>95% of all cells).

Results and Discussion

Microbial biomass of enriched AOM cultures contains conspicuous amounts of zerovalent sulfur

Wet biomass from AOM enrichment cultures was anaerobically extracted with methanol and subsequently analyzed by HPLC UV spectrometry to examine the potential presence of S^0. The analysis revealed high abundance of elemental sulfur of up to ~ 2 mmol S^0 per gram dry biomass (~6 weight %). Other organisms that are known to store high amounts of sulfur (up to 40% cell dry weight) are chemoheterotrophic and chemophototrophic sulfur and sulfide oxidizers. These organisms store S^0 as cyclic S_8

sulfur (e.g. *Beggiatoa sp.*), polythionates (e.g. *Acidithiobacillus ferrooxidans*) or linear sulfur chains of polysulfides with or without hydrocarbon groups at the ends (e.g. *Allochromatium vinosum*; Prange *et al.*, 2002). Polysulfides and even organic polysulfanes, are prone to interconversion reactions and are readily converted into elemental sulfur during methanol extractions (Steudel, 2002). Therefore, wet AOM biomass was extracted with methanol in the presence of triflate, a strong methylating agent that converts labile polysulfides into more stable dimethylpolysulfides, which are HPLC and GC amendable (Kamyshny *et al.*, 2006). HPLC analysis of the triflate-treated methanol extracts showed that the sample contained besides elemental sulfur substantial amounts of inorganic polysulfides with chain lengths of 3 to 6 S atoms. The abundance of polysulfides in the AOM biomass was confirmed by GC-MS (data not shown). In contrast, biomass-free medium from the same active culture contained little to no detectable S^0.

Bulk extractions cannot distinguish between intracellular and extracellular sulfur, present either in between the cells or adsorbed to the organic intercellular matrix. Therefore, in order to locate the S^0 at a cellular resolution (~ 1µm) micro-Raman spectroscopy was performed. Two morphologically distinct cell types were identified in our sample – small rods and large irregular cells – and for both Raman spectra were obtained (Fig. 1). FISH (Schreiber *et al.*, 2010) and antibody staining (Fig. 2) that was performed in parallel on the same sample identified the larger irregular cells as ANME and the rod-shaped cells as *Deltaproteobacteria*. Characteristic Raman peaks for elemental sulfur (149, 214 and 480 cm^{-1}; Pasteris *et al.*, 2001, Trofimov *et al.*, 2009) were recorded for both cell types but were most prominent in fresh ANME cells indicating that they contain more S^0 than the bacteria (Fig. 1A-C). Although SR bacteria and ANME are present in equal abundance, most of the AOM biomass is composed of ANME (~75%) due to their substantially larger biovolume (ANME:SRB = 3:1). Therefore, the bulk of S^0 found in the AOM biomass appears to be present as intracellular sulfur in the ANME. While the SR bacteria do not exhibit strong Raman peaks for sulfur, they show strong peaks at 549, 569, 960 and 1061 cm^{-1} that were tentatively attributed to iron (II) phosphates (Fig. 1C).

The presence of amorphous particles enriched in Fe and P in rod-shaped gram-negative (i.e. contaning the characteristic double membrane) bacteria was confirmed by transmission electron microscopy/energy-dispersive X-ray spectroscopy analysis (Figs. 1D-E). Although the function of these particles remains currently unknown, their exclusive occurrence in one cell type served as a biomarker for the ANME-associated SR bacteria for the single-cell activity measurements using nanoscale secondary ion mass spectrometry (nanoSIMS; see below).

The abundance of S^0 in ANME is surprising because they lack known SR enzymes (Milucka *et al.*, in preparation), and in fact a dissimilatory sulfur metabolism was only anticipated for the associated bacteria (e.g. Hoehler et al., 1994; Valentine & Reeburgh, 2000). To determine the origin of this S^0, the enrichment culture was incubated for up to 24h with $^{35}SO_4^{2-}$. The accumulation of reduced sulfate in medium and biomass was followed over time by determining the $^{35}SO_4^{2-}$ turnover in these pools. In incubations with $^{35}SO_4^{2-}$ and a small (< 50 µM) added non-labeled sulfide pool, ^{35}S-label accumulation in AOM biomass was detectable within 1 hour and preceded the release of detectable $H^{35}S^-$ into the medium indicating that the reduced S present in the AOM biomass is, at least partly, derived from sulfate (Fig. 3A). It is unlikely that the accumulation of sulfate-derived biomass S is a result of assimilatory metabolism because, based on genomic data, the ANME utilize sulfide, and not sulfate, as a sulfur source (Meyerdierks *et al.*, 2010). Additionally, the rate of sulfur accumulation (µM to mM per day) in the AOM biomass by far exceeds the sulfur requirements of such ultra-slow growing organisms for anabolic purposes (nM per day). The rates of sulfur turnover, however, are comparable to the cell-specific rates of methane oxidation (see below).

Incubation experiments with $^{35}SO_4^{2-}$ and a large non-labeled sulfide pool (3.5 mM) showed that most of the reduced $^{35}SO_4^{2-}$ ended up in the medium but again a substantial fraction of the reduced radio-labeled sulfate accumulated in the AOM biomass (Fig. 3B).

Combined results from these experiments with $^{35}SO_4^{2-}$ indicate that the S^0 compound, apparently mainly present in ANME, is at least partly derived from sulfate. This produced $^{35}S^0$ and HS^- can rapidly equilibrate with the external polysulfide pool in solution through

abiotic isotope exchange (Fossing & Jørgensen, 1990) and the ANME might incorporate some ^{35}S from the already equilibrated $H^{35}S^-/^{35}S^0$ pool in solution. This would give rise to the strong linear correlation of radiolabeled sulfur accumulating in the AOM biomass with the radiolabel accumulating in the medium (Fig. 4).

The biomass sulfur is turned-over in proportional amounts to the oxidized methane

We incubated the AOM culture after the addition of either $^{13}CH_4$ or $^{13}CO_2$ to see whether the abundant S^0 present in ANME biomass is involved in AOM. NanoSIMS was used to determine cell-specific methane incorporation rates and cellular S concentrations. Individual cells in the AOM biomass (Fig. 5A) were identified based on the presence of phosphorus-rich particles that exclusively occur in the SRB (Fig. 5B), and by gold-labeled antibodies targeting the enzyme likely responsible for methane activation in ANME (Mcr; Fig. 5C). These results showed that the rate of methane carbon assimilation (Fig. 5D) strongly correlates with the cellular S content (Fig. 5E).

Parallel $^{14}CH_4$ incubations show that bulk methane carbon assimilation strongly correlates (r^2 = 0.9) with AOM rates, with assimilation accounting for ~0.2% of the total methane turnover. This is at the lower end of previously reported methane carbon assimilation efficiencies by ANME determined from stable isotope incorporation in lipid biomarkers (0.3-1%; Nauhaus *et al.*, 2007; Wegener *et al.*, 2008). These compound-specific stable-isotope based studies showed that most of the carbon in the biomass derives from CO_2 assimilation. Our nanoSIMS results confirm these findings and show that both ANME and associated bacteria primarily (~90% of total C fixation) derive their biomass carbon from CO_2 assimilation. The average doubling times determined from cellular CO_2 assimilation show that both ANME and SRB have the same doubling time of ~180 days, which is in good agreement with doubling times determined from bulk dry weight and activity measurements (Nauhaus *et al.*, 2007; Holler T., Milucka J., unpubl. res.). More importantly, the identical doubling times also indicate coordinated ANME and SRB metabolisms, which is crucial for a syntrophic coexistence.

We performed isotope labeling experiments with simultaneous additions of $H^{13}CO_3^-$, $^{14}CH_4$, $^{34}SO_4^{2-}$ and $^{35}SO_4^{2-}$, to directly determine whether turnover of sulfate-derived biomass S correlates with the rate of methane oxidation. The incubation experiments with added $^{35}SO_4^{2-}$ and $^{14}CH_4$ and a small pool of unlabeled sulfide show that most (~80%) of the sulfate-derived reduced sulfur goes into the biomass at a rate proportional to the methane oxidation rate (Fig. 6A). These results provide additional evidence for S^0 turnover in ANME being directly linked to methane oxidation. Moreover, the total amount of sulfate reduced and methane oxidized follows a 1:1 ratio, with one mol of methane being oxidized for every mol of sulfate reduced. This is in good agreement with the predicted overall stoichiometry of the AOM reaction and confirms previous experiments that obtained a 1:1 ratio for methane oxidized to sulfate reduced (e.g. Nauhaus et al., 2002).

Zerovalent sulfur might serve as electron acceptor for AOM

Isotope labeling experiments with additions of $^{34}SO_4^{2-}$ show that both ANME and bacteria become enriched in ^{34}S-label with time (Fig. 6B), which suggests that the complete sulfate reduction to sulfide proceeds via S^0 formation and involves both organisms. The question is whether the S^0 is formed by the ANME and then shuttled to the bacteria or vice versa. Based on the shown data it is feasible to imagine three possible scenarios about the sulfur cycling between ANME and DSS: either (i) DSS or (ii) the ANME reduce sulfate to sulfur, which is then shuttled to the partner organism, which reduce this sulfur to sulfide. Or, (iii) the ANME might perform the complete reduction of sulfate to sulfide (over sulfur) alone and the DSS might be involved in a secondary sulfur metabolism. Although at this point we cannot make definite conclusions about the directionality of the transport, the compound might be shuttled from SRB to ANME based on the following considerations: (i) there is only metagenomic and protein-derived evidence for sulfate reduction in SRB, (ii) the transfer of ^{34}S-label pulse follows the gradient of SO_4^{2-} pool > SRB > ANME > HS^- (more labeled to less labeled; see also Fig. 6B). If so, the S^0 that is stored in the ANME biomass might be the actual electron

acceptor used for anaerobic methane oxidation. From a thermodynamic point of view, AOM coupled to sulfur reduction is a feasible process (Table 1). Furthermore, the sulfur/sulfide pair has a low redox potential and is thus compatible with the involvement of Mcr in methane oxidation.

Although the actual (enzymatic) mechanism of such a sulfur reduction in the ANME is thus far unknown, the published ANME (-1) metagenome contains a number of genes that might be involved in the dissimilatory sulfur metabolism. First, the ANME-1 genome encodes a unique, molybdopterin-containing oxidoreductase from a family of dimethylsulfoxide reductases (Meyerdierks *et al.*, 2010) that is reminiscent of the polysulfide reductase from *Wolinella succinogenes* (Jankielewicz *et al.*, 1994). Second, in the same operon, multiheme c-type cytochromes are encoded that might catalyze S^0 reduction such as the c-type cytochromes in some strains of sulfate reducing bacteria (e.g. *Desulfovibrio desulfuricans*; Fauque *et al.*, 1979). Third, non-canonical heterodisulfide reductases, as the one found in the ANME-1 genome, might serve as a physiological donor for sulfate reduction (Mander *et al.*, 2002; Rossi *et al.*, 1993).

A model for sulfur cycling between ANME and SRB involved in AOM

The oxidation of one mol of methane requires four moles of S^0 based on stoichiometry (Eq. 2).

$$CH_4 + 4S^0 + 2H_2O \rightarrow 4HS^- + CO_2 + 4H^+ \qquad \text{(Eq. 2)}$$

Hence the observed overall stoichiometry of one mol sulfate being reduced per mol methane oxidized (Fig. 6A) can only be explained if the sulfur directly derived from sulfate is not the only source of S^0 in the ANME. Concentrations of reduced sulfur species in the medium such as sulfite, thiosulfate, methyl-sulfide, dimethylsulfide and dimethyldisulfide were below or close to detection limit. The only reduced sulfur species present in the medium in high enough concentrations to explain the high rates of S^0 turnover is sulfide.

Although the reduction of sulfate with sulfide to S^0 – a so-called comproportionation

$$H^+ + SO_4^{2-} + 7HS^- \rightarrow 4S_2^{2-} + 4H_2O \quad \text{(Eq. 3)}$$

(for instance the formation of disulfide, Eq. 3) – has so far never been observed in natural aquatic environments, it becomes thermodynamically feasible when disulfide concentrations are kept low (Table 1) and could in principle be the source of S^0 in the ANME.

Based on these results and thermodynamic considerations the following model for sulfur cycling between ANME and SRB involved in AOM could be envisioned (Fig. 7). The SRB reduce sulfate with sulfide to polysulfide (for example disulfide see Table 1), which is released from the cells. The disulfide will likely react with reduced sulfur outside the cells to form longer-chain polysulfide. This S^0 is taken up by the ANME and used to oxidize methane to CO_2. During this process sulfide is released, which is partly re-used by the SRB to reduce sulfate.

To provide unambiguous support for this model, a labeling experiment with ^{35}S-labeled sulfide should be performed in order to confirm that the ^{35}S-label accumulation in the biomass is then faster, as expected from Eq.3.

Material and Methods

Enrichment cultures

The enrichment culture 'Isis' was obtained through a continuous (~ 7 years) incubation from a sediment sample collected on a cruise of RV Atalante in September 2003 in Eastern Mediterranean Sea. The culture was incubated at room temperature in artificial seawater medium (Widdel and Bak, 1992) in closed culture vials with CH_4/CO_2 headspace. During incubation, the vials were continuously shaken (40 rpm) to facilitate gas transport. AOM activity was followed by quantification of methane-dependent sulfide formation using colorimetry (Cord-Ruwisch; 1985). As soon as the sulfide concentrations in the medium reached ~ 10 mM the 'used' medium was replaced by fresh medium.

Maintenance and handling of the sample was performed in an anoxic glove box (Mecaplex) under N_2:CO_2 (90:10) atmosphere. At the time of the experiment, the AOM

rates were 1 mmol gram (dry weight)$^{-1}$ day^{-1} but the culture were diluted into smaller aliquots for individual experiments.

Fluorescence in situ *hybridization*

An aliquot of the Isis enrichment culture was fixed at room temperature for 2 h with 4% formaldehyde in phosphate buffer (PB; pH 7.4), washed with 1x phosphate buffered saline (PBS; 130 mM NaCl, 10 mM sodium phosphate; pH 7.4), and filtered onto 0.2 µm GTTP polycarbonate filters (Millipore). *In situ* hybridizations were performed at 46°C for 120 min in a hybridization buffer containing 0.9 M NaCl, 50% formamide (ANME2-538) 20 mM Tris-HCl (pH 7.4), and 0.01% SDS (sodium dodecyl sulfate). Probe concentrations were 5ng/ml. Hybridization mixtures were removed by washing filters for 15 min in a buffer containing 20 mM Tris-HCl (pH 7.4), 35 mM NaCl (ANME2-538) and 0.01% SDS at 48°C. The washing buffer was removed by washing with distilled water and the filters were air dried and mounted onto glass slides. Oligonucleotide probes were purchased from Biomers (Germany) or ThermoHybaid (Germany). For double hybridization experiments ANME2-538 (Treude et al., 2005) labeled with Cy3 and DSS-658 (Manz et al., 1998) labeled with carboxyfluorescein were used.

Image acquisition and processing

The sections were examined with a Zeiss AxioCam MRc attached to a Zeiss Axioplan Microscope (Zeiss, Jena, Germany) equipped with oil immersion planapochromat lens (100x1.3NA; Zeiss, Jena, Germany). Following filter sets were used: DAPI (365/10 nm excitation, 420 LP emission, FT 395 Beam Splitter), FITC/fluorescein (472/30 excitation, 520/35 emission, 495 Beam Splitter) and Cy3 (562/40 excitation, 624/40 emission, 593 Beam Splitter). The exposure times were < 50ms for DAPI and < 300 ms for FITC and Cy3, respectively. The obtained images were processed with Adobe Photoshop CS4 (version 11.0.2).

Incubation experiments with isotope labelled substrates

Three different sets of incubation experiments were performed with the Isis enrichment culture. First, the enrichment culture was incubated with $^{35}SO_4^{2-}$ tracer (~ 2.5 MBq; 18 GBq mol^{-1}; Amersham) and either 50 µM or 3.5 mM sulfide in Hungate tubes at room temperature for up to 24 hours. Subsamples (1 ml) were taken after 1, 3, 6, 11, and 24 hours and directly filtered through a 0.22 µm GTTP filter into zinc acetate solution (0.9 M) to stop the reaction and fix sulfide. The filter containing biomass flocks was subsequently washed with artificial seawater and 20 ml of 1 M HCL solution to dissolve precipitated iron sulfides and subsequently analyzed by scintillation counting. At 0 and 24 hours subsamples (0.3 ml) were taken for total sulfide measurements using Cline (Cline, 1969). Additionally, at 24 hours a subsample (0.5 ml) was filtered for beta-imaging.

Second, the Isis enrichment culture was incubated with either ^{13}C-labeled methane (50 atom percent ^{13}C) or ^{13}C-labeled bicarbonate (6 atom percent ^{13}C) in Hungate tubes at room temperature for 28 and 44 days. For both experiments the sulfide concentrations were regularly monitored and the medium was exchanged as soon as 2 mM sulfide was produced to prevent accumulation of dissolved ^{13}C-intermediates and products (e.g. $^{13}CO_2$ in the $^{13}CH_4$ incubations). Subsamples were taken for bulk measurements of carbon and for nanoSIMS analysis of single cells for both incubation time points. Biomass samples for bulk carbon measurements were filtered on 0.7 µm pore-size type GF/F filters (Millipore). After drying (overnight at 50°C), the GF/F filters were kept at room temperature until further processing. For nanoSIMS analysis, biomass samples were fixed in 4% formaldehyde for 2 h at room temperature, washed and stored in 4% formaldehyde at 4°C until further processing.

Third, the Isis enrichment culture was incubated with ^{14}C-labeled methane (8.6 MBq), ^{13}C-labeled bicarbonate (50 atom percent ^{13}C), ^{34}S-labeled sulfate (50 atom percent ^{34}S), ^{35}S-labeled sulfate (26 MBq) and 50 µM sulfide in Hungate tubes at room temperature for up to 144 hours. At 0 and 24 hours subsamples (0.3 ml) were taken for total sulfide measurements using Cline (Cline, 1969). Two parallel subsamples (0.5 ml) were taken after 1, 3, 6, 11 and 24h. Both were directly filtered through a 0.22 µm GTTP filter either into zinc acetate solution (0.9 M) to fix sulfide or into NaOH (0.6 M) to fix bicarbonate.

The filters containing biomass flocks were subsequently washed with artificial seawater and 20 ml of 1 M HCL solution to dissolve precipitated iron sulfides. One biomass filter was used for scintillation counting and the other filter was transferred into 4% formaldehyde solution for nanoSIMS analysis.

Determination of sulfate reduction and methane oxidation rates

For the first set of incubation experiments, radiolabeled reactants and products ($^{35}SO_4^{2-}$ and total reduced inorganic sulfur, respectively) were separated by cold chromium distillation (Kallmeyer *et al.*, 2004).

For the third set of incubation experiments, radiolabeled reactants ($^{14}CH_4$ and $^{35}SO_4^{2-}$) and products ($^{14}CO_2$ and total reduced inorganic sulfur) were separated using a combination of acid and reducing Cr(II) separations. ^{14}C radiolabeled carbonate was released from the NaOH by acidification and bubbling though a series of chemical traps: (a) 7 ml of a 0.1 M, pH 4 citrate buffer; (b) a 5% zinc acetate trap adjusted to pH 7 with HCl, (c) a second zinc acetate trap, (d) a trap containg 7 ml of Carbosorb E (a CO_2-absorber for scintillation counting; Perkin Elmer), and (e) a second Carbosorb trap. The first trap (a) was designed to trap extraneous aerosols and drops from the acid solution, the second and third traps (b and c) were designed to separate the ^{35}S, while ^{14}C as CO_2 were trapped in the final two traps (d and e).

The radioactivity of biomass, total dissolved reduced inorganic sulfur, dissolved inorganic carbon as well as dissolved sulfate was quantified by scintillation counting (scintillation cocktail, LumaSafeTM Plus; scintillation counter, 2900TR LSA, Packard). Sulfate reduction rates were determined following equations as described (Jørgensen and Fenchel, 1974). Methane oxidation rates were calculated as described (Treude *et al.*, 2003). Due to the fact that the biomass from the third set of experiments contained both ^{14}C- and ^{35}S-label, methane carbon assimilation rates and biomass sulphur accumulation rates could not be directly measured. However, the individual contributions of ^{14}C and ^{35}S to the total recorded radioactivity could be determined due to the different half-lives of 5730 years and 87 days, respectively. We recorded daily changes in the radioactivity

of the biomass via regular scintillation counting over a period of ~3 weeks and based on the assumption that the activity of ^{14}C stays constant over the measuring period. We used following equation to calculate the ^{35}S and ^{14}C in the biomass.

$$A_{^{14}C} = TA_t + A_{^{35}S(t=0)} e^{-\lambda t}$$

where TA(t) = total measured activity at any time point, t = time in days, A = activity of ^{35}S or ^{14}C, λ=decay constant for ^{35}S.

For all experiments, the loss of biomass and medium due to subsampling was taken into account for the calculations of methane oxidation and sulfate reduction rates.

Beta-imaging

The two-dimensional distribution of beta radiation on the filters was captured with a real-time radio-imaging system (BioSpace Measures Micro Imager). Counting time was 8 minutes. Activities were integrated by the instrument software (BetaVision) after manually assigning specific region of interest.

Preparation of cryosections

The sample was fixed in an anoxic chamber by addition of 8% formaldehyde in 100 mM phosphate buffer (pH 7.4) in a 1:1 ratio to the sample. The fixation was performed for 2 hours at room temperature. The sample was briefly washed with cold PB and fixed again with fresh 4% formaldehyde in 100 mM PB (pH 7.4). The samples were stored in 2% formaldehyde in 100 mM PB (pH 7.4) at 4ºC until processed further. Biomass flocs were transferred into 2.3 M sucrose and infiltrated overnight at 4 °C on a rotational shaker. Semi-thin cryosections (300-400 nm) were prepared according to Tokuyasu (1973, 1980), transferred on poly-L-lysine-coated coverslips in a 1:1 mixture of 2.3 M sucrose:methylcellulose and dried.

Immunolabeling on cryosections

Immunofluorescent labeling: Immunolabeling with anti-Mcr and anti-Dsr antibodies as markers for ANME and SRB, respectively was performed as described by Milucka et al. (in preparation).

Immunogold labeling: All incubation and washing steps were performed "section-side down" on drops of 300 μl, and 30 μl, respectively. The coverslips with attached sections were washed in PBS to dissolve the sucrose:methylcellulose support. After washing, the sections were incubated with primary (anti-Mcr) and secondary (goat anti-rabbit conjugated to 1.4 nm gold and FITC; Abcam; cat. nb. ab33110) antibodies; each incubation was followed by three washing steps in PBS with 0.01% Tween. Ultimately, the coverslips were washed with water and incubated for 10 min in 2% methylcellulose (in water). The excess methylcellulose was removed by adsorption on a filter paper and the glass slide was dried.

Transmission electron microscopy

The sample (Black Sea mat) was fixed with 4% formaldehyde in phosphate buffer (pH 7.4). Prior to resin embedding the sample was embedded in 2% agarose and cut in small cubes (*ca.* $1mm^3$). The sample was embedded in Epon resin, contrasted by 1% aqueous osmium tetroxide and negatively stained with uranyl acetate using automated microwave tissue processor (Leica). The embedded sample was sectioned into ~ 70 nm sections using ultramicrotome (Leica). The sections were transferred on a formvar-coated copper grid and observed in the electron microscope (JEM 1010; JEOL; Germany).

The same sections were analyzed by electron energy-dispersive X-ray analysis (EDX) using electron microscope (Tecnai G2 F20; FEI/Philips; The Netherlands) equipped with an EDX detector.

Raman spectroscopy

Solid standards, like iron phosphates, were directly measured; liquid standards like polysulfides (in methanol) and methanol were measured in airtight HPLC vials (with small insert) or were sealed into thin glass capillaries.

Small aliquots of living or fixed (with 4% FA in PB solution) Isis culture were placed on clean CaF_2 slides. The samples were either directly analyzed ('fresh' biomass) or fixed ('fixed' biomass). Alternatively, thin (2-3µm) sections of fresh samples prepared with a cryotome were analyzed. For the Raman analysis a confocal LabRAM HR800 system (Horiba, Germany) equipped with a 532.17 nm laser was used. Prior to analysis the system was aligned using a silica Raman reference with a distinct Raman peak at 520 cm^{-1}. Cells were chosen for analysis by their morphology in the live view mode of the Labspec software (Horiba). The laser intensity (filter D0.3, D0.6, D1, D2 and D3) and exposure times (3 – 40 s) varied during spectrum recording due to the different resistance of the different cell types to laser irradiation. The confocal pinhole was set to 300µm unless indicated differently. The Raman spectra were recorded between ~120 and 1800 cm^{-1} with a spectral centre of 1020 cm^{-1}, which covers most biologically significant signature peaks including sulfur. Raman spectra were baseline-corrected and normalized, and exported to a file format readable by Excel (Microsoft).

NanoSIMS Analysis of Single Cells

Image acquisition. The immunogold-labeled thin sections were analyzed between November and December 2009 using a NanoSIMS 50L manufactured by Cameca. To prevent charging, the thin sections were covered with platinum by a sputter-coater prior to analysis. Secondary ion images of $^{12}C^-$, $^{13}C^-$, $^{12}C^{14}N^-$, $^{31}P^-$, $^{32}S^-$, $^{34}S^-$, and $^{197}Au^-$ were recorded for individual cells using 6 electron multipliers. The nanoSIMS analysis was performed on a 15µm x 15µm image field of the thin sections. The thin sections were sputtered with a 0.3–0.8 pA Cs^+ primary ion beam focused into a spot of ~100-nm diameter that was stepped over the sample in a 256 x 256 pixel raster with a counting time of 1 ms per pixel. The same region was re-scanned up to 100 times. The resulting images (i.e. planes) were combined to create the final image.

Image acquisition and data processing. Images and data were processed using the open-source Matlab-based Look@NanoSIMS processing software working under LINUX environment (Polerecky *et al.*, in prep.). The different planes of each image field were re-aligned to correct for any drift of the sample stage during acquisition and subsequently accumulated to obtain the summed mass images. All nanoSIMS images were graphically displayed as average pixel counts per plane in a false-color scale from black (intensity = 0) to red (maximum intensity per pixel adjusted so as to obtain good visual contrast). Isotope-ratio images (e.g., $^{13}C/^{12}C$ ratio) were created by dividing the average pixel counts per plane of a selected secondary ion (e.g., $^{13}C^-$) by the average pixel counts per plane of a selected reference mass (e.g., $^{12}C^-$). Regions of interest around individual cells were defined by using interactive tresholding with $^{31}P^-$, $^{12}C^{14}N^-$ and $^{32}S^-$ as masks. For each region of interest, the $^{32}S/^{12}C$ and the$^{13}C/^{12}C$ ratios were calculated. Additionally, the $^{34}S/^{32}S$ ratio was calculated for the $^{34}SO_4^{2-}$ incubations. The $^{13}C/^{12}C$ ratios of individual bacterial cells were determined for experiments with and without (i.e. control experiments) added labeled substrate. Subsequently, the $^{13}C/^{12}C$ enrichment of individual cells of the two species was calculated by subtracting the average cellular ratios of ANME and SR bacteria in the control experiments from the ratios obtained for individual cells from the labeling experiment.

Biovolume calculation, biomass conversion and cellular activity calculations. The length and width of the microorganisms used for the biovolume calculation was determined from TEM images. The calculations assumed that ANME shape was cylindric and the SR bacteria were elipsoid. For each species a mean (n=10) cell biovolume was calculated. The biovolume-to-biomass conversion used to calculate the cellular methane carbon assimilation rates from their $^{13}C/^{12}C$ enrichment was done using a calibration factor of 6.4 fmol C μm^{-3} (Musat *et al.*, 2008; Ploug *et al.*, 2010).

Analysis of sulfur compounds

Polysulfides were analyzed modified from the method of Kamyshny *et al.* (2006). Briefly, dissolved polysulfides were methylated using methyl triflate in methanol medium to form

methyl polysulfanes that can be separated and quantified using HPLC. Forty ml of anoxic methanol were vigorously stirred in a closed 70 ml serum vial. Two liquids were rapidly injected into the stirred methanol from syringes: 1) 10 ml of biomass and medium followed immediately by 2) 300 µl methyl triflate. Eighty ml of sodium sulfate solution (375 mM) was added to the reaction mixture and transferred to a 250 ml separatory funnel. Subsequently, the solution was extracted with 2 × 1 ml n-dodecane. Elemental cyclosulfur compounds – S_6, S_7 and S_8 – were also extracted into the n-dodecane. The obtained extract was analyzed by a Dionex GP50 Gradient Pump HPLC equipped with a C18 reverse phase column and a Dionex UVD340S Diode Array Detector. Methanol was used as mobile phase and spectrophotometric detection was performed at 220 and 230 nm wavelengths. Detection limits were 600 nM, 400 nM, 300 nM, 120 nM, 100 nM and 60 nM for S_3^{2-}, S_4^{2-}, S_5^{2-}, S_6^{2-}, S_7^{2-} and S_8^{2-}, respectively. A standard series of polysulfides in saturated with respect to elemental sulfur was prepared by dissolving excess elemental sulfur (S_8) in a solution containing ca. 10 mM total dissolved sulfide in a anoxic solution buffered at pH 10 (50 mM phosphate buffer). The resulting yellow polysulfide solution was allowed to stand overnight to equilibrate and then was methylated as described above. Equilibrium concentrations were calculated using the equilibrium constants of Kamyshny *et al.* (2007). The detection limit for total polysulfide zero-valent sulfur (based on resolved peaks of S_4^{2-}, S_5^{2-} and S_6^{2-}) was 3 µM. The average relative standard deviation for the detection of inorganic polysulfide S^0 by the methyl triflate derivatization-based method is 8% (Kamyshny *et al.*, 2009).

Sulfite and thiosulfate in the medium were derivatized at room temperature in the dark with monobromobimane and analyzed by HPLC according to the methods described in Zopfi *et al.*, 2004.

Free energy calculations

The free energy of sulfate-dependent AOM (Eq. 1) at varying sulfate concentrations was calculated using the following equation:

$$\Delta G = \Delta G^{0'} + R\,T\,\ln\{([HS^-][HCO_3^-])/([CH_4][SO_4^{2-}])\}$$

where R = 0.008314 kJ/mol^{-1} K^{-1} , T =293 K, aHCO_3^-=0.02M; aSO_4^{2-}=0.02M; aCH_4=0.001M; aHS^-=0.001M. $\Delta G^{0'}$ of sulfate-dependent AOM (Eq. 1) is -32.9 kJ mol^{-1}. The free energies of sulfate-sulfide comproportionation reactions in Table 1 were calculated using the same approach as above for sulfate-dependent AOM. Conditions are provided in the table. Activities approximating concentrations typically observed in marine environments and in the experiments were used. Concentration of polysulfide was assumed to be in equilibrium with respect to sulfide and sulfur and these concentrations were estimated from Kamyshny *et al.* (2007).The $\Delta G^{0'}_f$ were also taken from Kamyshny *et al.* 2007. $\Delta G^{0'}_f$ for the reaction to form aqueous S_8 was obtained from Kamyshny 2009.

Figure legends

Figure 1. TEM image and micro-Raman spectra of AOM aggregates. A) Average spectrum of 'fresh' ANME-type cells (n=8) measured in buffer with prominent peaks at 149, 214 and 480 cm^{-1} (red) characteristic for S_8. Lacking resolution above 950 $cm^{-1}$is due to buffer compounds, B) Average spectrum of fixed ANME-type cells (n=7) grown without methane for 4 days with prominent peaks at 748, 1130, 1314 and 1586 cm^{-1} (green) characteristic of cytochrome *c*, C) Average spectrum of SRB-type cells (n=3) grown without methane for 4 days with prominent peaks at 549, 569, 960 and 1061 cm^{-1} attributed to $Fe_3(PO_4)_2$(blue). For all signature peaks the published values of the respective reference compounds are indicated in brackets (Pasteris *et al.*, 2001 [S_8], Trofimov *et al.*, 2009 [S_8], Frost *et al.*, 2002 [vivianite], Pätzold *et al.*, 2008 [cytochrome *c*]). In spectra B and C the CaF_2 peak was removed from the spectrum to increase clarity, D) TEM image showing electron dense particles in sulfate reducers (SRB) and E) EDX spectrum of electron-dense particles.

Figure 2. AOM consortium visualized with DAPI staining and with anti-Dsr and anti-Mcr antibodies. Mcr is localized in the larger, irregularly shaped cells (ANME in red) whereas Dsr is found in the rod-shaped bacteria (SRB in green). The antibodies were used at following dilutions: anti-Dsr 1:200, anti-Mcr 1:200. Scale bar = 5µm

Figure 3. Sulfur turnover in the AOM culture. Total reduced sulfate, reduced sulfur in medium, and reduced sulfur in biomass for the AOM enrichment culture with A) small (<50 µM), and B) large (3.5 mM) external sulfide pool.

Figure 4. Linear correlation between ^{35}S-tracer accumulation in biomass and medium for the AOM enrichment culture incubated with a large (3.5 mM) external sulfide pool.

Figure 5. NanoSIMS data for AOM aggregate stained with gold-labeled antibodies against Mcr after 28 days of incubation with $^{13}CH_4$. A) $^{12}C^{14}N$ image showing cells in green/orange, B) Image showing cells enriched in ^{32}S (red) and ^{31}P (green), C) $^{197}Au/^{12}C$ ratio image showing ANME cells targeted by gold-labled antibodies against MCR in green/orange, D) $^{13}C/^{12}C$ ratio image showing $^{13}CH_4$ assimilation by ANME, E) Potential $^{13}CH_4$ assimilation expressed as $^{13}C/^{12}C$ ratio *versus* $^{32}S/^{12}C$ ratio for ANME cells (n = 198).

Figure 6. Methane and sulfur turnover in the AOM culture. A) Total reduced sulfate, reduced sulfur in medium, and reduced sulfur in biomass *versus* anaerobic methane oxidation measured for the AOM enrichment culture, B) $^{34}S/^{32}S$ ratio for ANME and SRB cells (n > 70 for each cell type and time point) incubated with $^{34}SO_4^{2-}$ as determined by nanoSIMS.

Figure 7. Model of anaerobic oxidation of methane with S^0.

Table 1. Gibbs free energy calculations for methane oxidation and sulfur comproportionation. Activities of dissolved compounds used in the calculations were: $aHCO_3^-$=0.02M; aSO_4^{2-}=0.02M; aCH_4=0.001M; aHS^-=0.001M. The activity of solid elemental sulfur was assumed to be 1. Activity of dissolved elemental sulfur ($S_{8(aq)}$) was estimated from Kamyshny (2009).

Reaction	ΔG°, kJ/rxn	ΔG_{rxn}, J/rxn	Notes
$SO_4^{2-} + CH_{4(aq)} \rightarrow HS^- + HCO_3^- + H_2O$	-32.9	-32.9	
$4S^0 + CH_{4(aq)} + 3H_2O \rightarrow 5H^+ + 4HS^- + HCO_3^-$	+207	-64.7	
$SO_4^{2-} + 3HS^- + 5H^+ \rightarrow 4S^0 + 4H_2O$	-240	+30.1	
$2SO_4^{2-} + 6HS^- + 10H^+ \rightarrow S_{8(aq)} + 8H_2O$	-438	+55.8	
$H^+ + SO_4^{2-} + 7HS^- \rightarrow 4S_2^{2-} + 4H_2O$	+21.1	-12.2	nM S_2^{2}
		+55.3	μM S_2^{2-}
$SO_4^{2-} + 4HS^- + 4H^+ \rightarrow S_5^{2-} + 4H_2O$	-186	+7.5	nM S_5^{2-}
		+24.3	μM S_5^{2-}
$SO_4^{2-} + HS^- + H^+ \rightarrow S_2O_3^{2-} + H_2O$	+39.9	+57	nM $S_2O_3^{2-}$

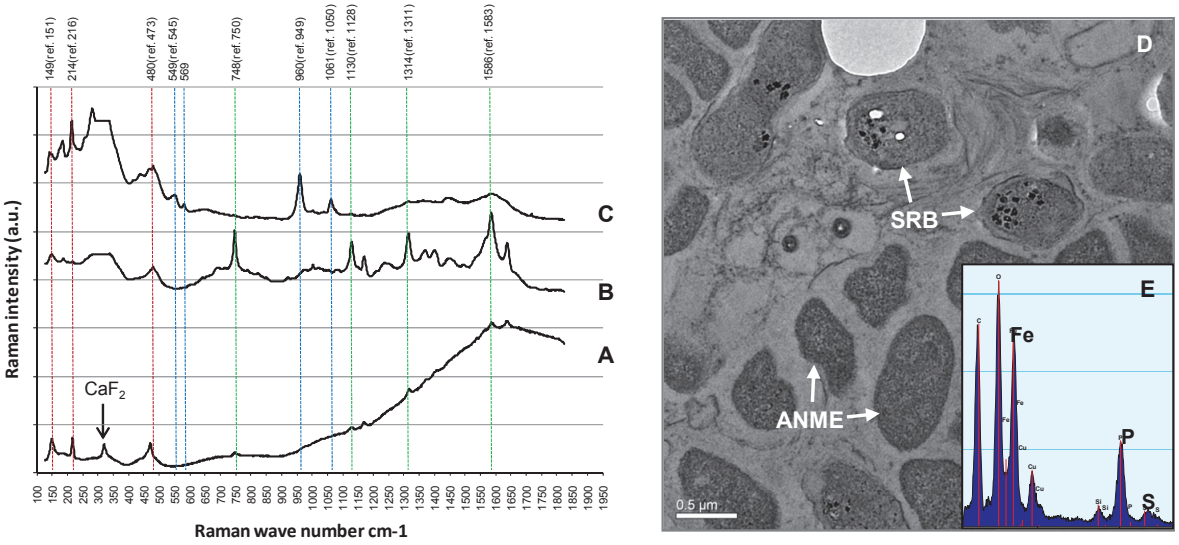

Figure 1

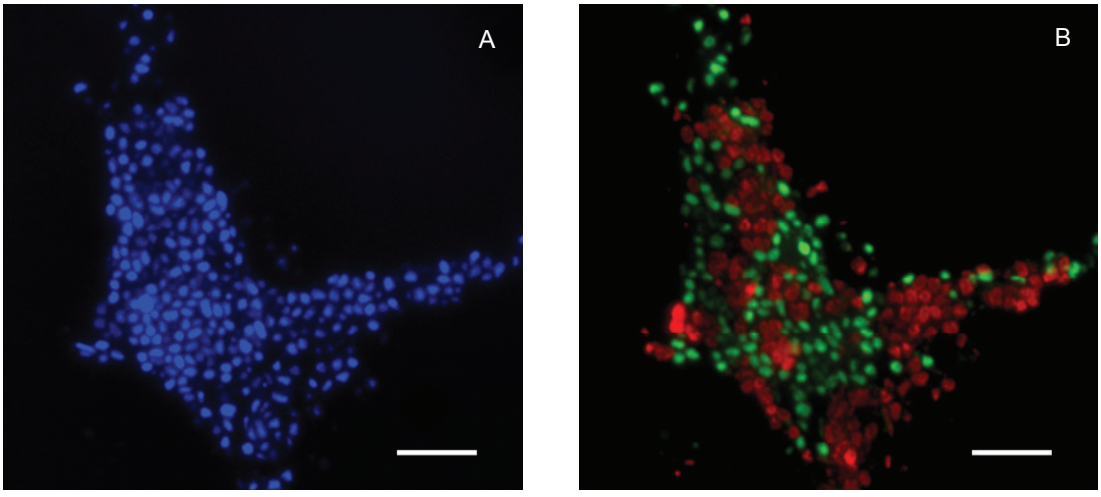

Figure 2

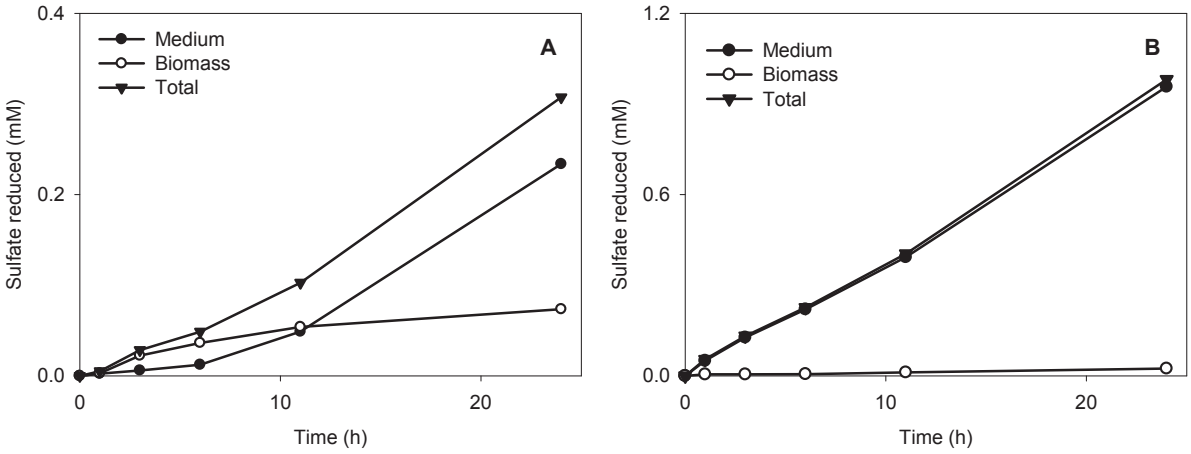

Figure 3

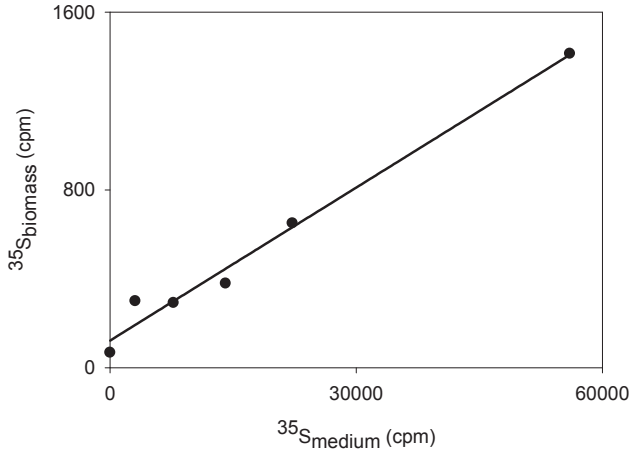

Figure 4

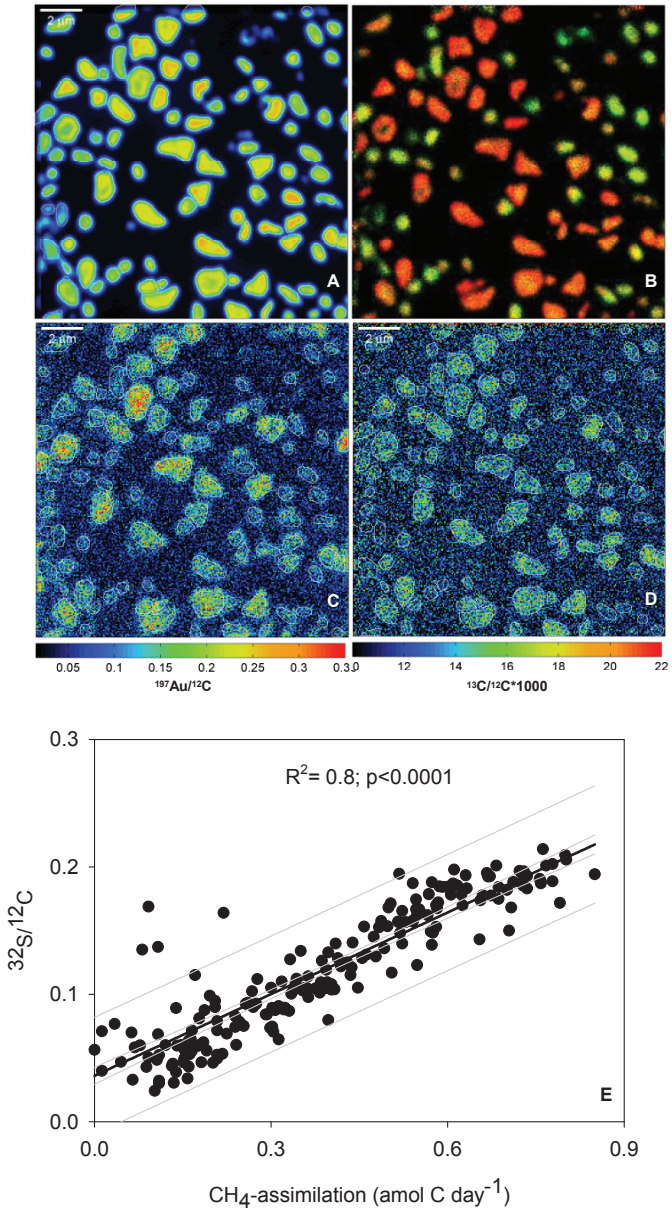
2 µm
A
B
C
D
0.05 0.1 0.15 0.2 0.25 0.3 0.35
197Au/12C
0 12 14 16 18 20 22
13C/12C*1000
R2= 0.8; p<0.0001
32S/12C
0.0 0.1 0.2 0.3
0.0 0.3 0.6 0.9
CH4-assimilation (amol C day-1)
E

Figure 5

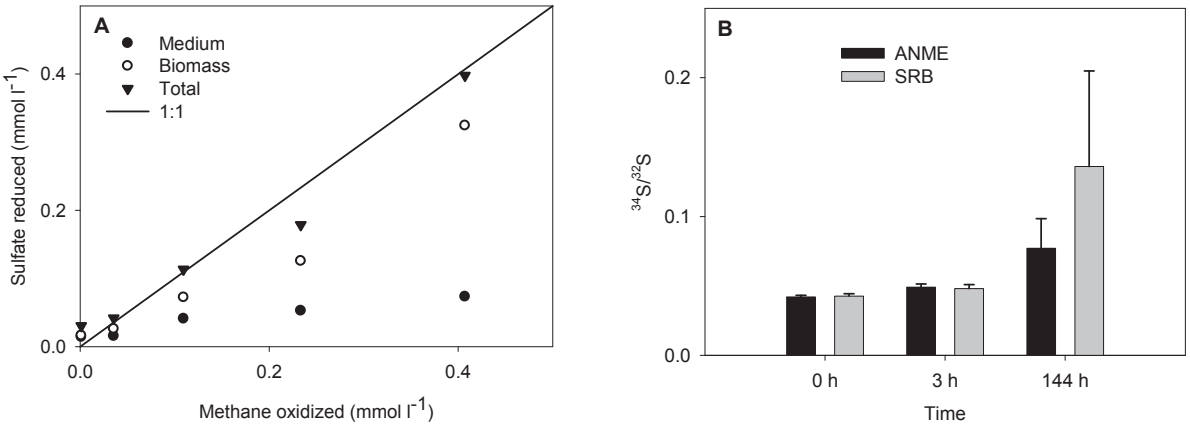

Figure 6

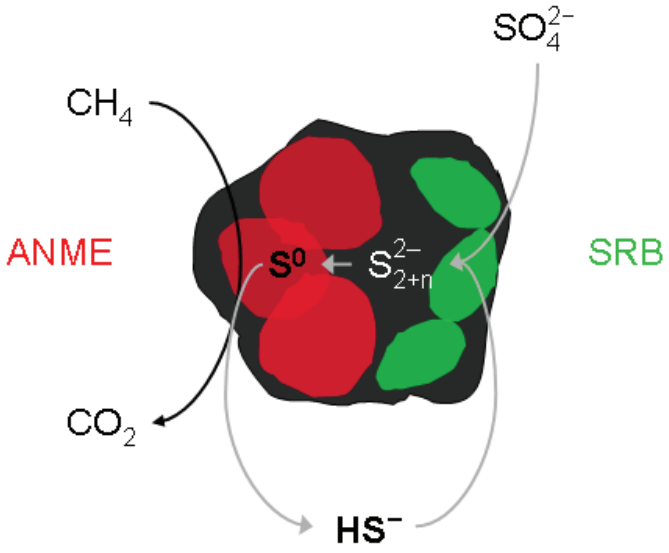

Figure 7

CHAPTER 5

CONCLUSIONS and DISCUSSION

"We often think that when we have completed our study of **one** *we know all about* **two***, because* **two** *is* **one and one***. We forget that we still have to make a study of* **and***."*

Sir Arthur Stanley Eddington (1882–1944)

The studies described in the previous chapters were performed in order to bring insight into the largely unexplored dissimilatory sulfur metabolism coupled to AOM. First, we found and purified enzymes for sulfate reduction (Chapter 2). The gene and protein sequences of the purified enzymes were similar to homologous enzymes from sulfate-reducing *Deltaproteobacteria*. We located these SR enzymes *in situ* with specific antibodies and assigned them to a specific cell type directly in the sample. The SR enzymes were expressed exclusively by the ANME-associated bacteria and not by the ANME themselves (Chapter 3). These results showed for the first time that the bacteria possess an active enzymatic machinery for dissimilatory sulfate reduction and that they are an essential part of active AOM consortia. Our further investigations have focused on how the syntrophy between these two organisms is mediated. We could show that ANME intracellularly accumulate large amounts of zerovalent sulfur (S^0). We propose a model, in which DSS bacteria reduce sulfate to a zerovalent sulfur compound (probably polysulfide) that might be taken up by the ANME and utilized as an electron acceptor for methane oxidation. (Chapter 4). The abovementioned results are discussed in more detail below.

'Environmental biochemistry'

Our proteomic studies on sulfate reducing enzymes are described in Chapters 2 and 3. We chose a protein-based approach to complement the metagenomic studies that were in progress at the time when our study was performed. The *in situ* localization of the proteins was necessary because of the realistic possibility that the

proteins of interest were in the past subjected to horizontal gene transfer. In that case, both gene- (and protein-) derived sequences of these proteins would carry the signature of the donor and not the owner and could be assigned to a wrong organism. Our study started with the assumption that the canonical SR enzymes used by all other known sulfate respiring prokaryotes – ATP sulfurylase, APS reductase and dissimilatory sulfite reductase – are also involved in the AOM-coupled SR. Indeed, we found these proteins to be abundant and active in the crude extract from AOM samples. We could determine their size and subunit composition by SDS-PAGE, their N-terminal amino acid sequence by Edman sequencing and their *in vitro* activity by enzyme assays. A final assignment of the proteins to a particular organism was done with specific antibodies. Although this approach was straightforward some difficulties had to be overcome, the biggest of which was the severe biomass limitation. All AOM enrichment cultures that have been maintained and propagated in our institute in the last 10 years could yield at maximum a few grams of wet weight, which are minute amounts for protein purification. Therefore, we used environmental microbial mat samples obtained from the Black Sea instead of enriched cultures. Reports of protein purifications from environmental samples that have not been subjected to any post-sampling enrichment procedures are rare, which is not surprising when one considers the complexity of the purification process. It is undesirable to start with a sample where the target organism comprises just a small fraction of the overall community and where, correspondingly, the target protein concentration might be very low. Fortunately, in our microbial mat samples the organisms of interest constituted up to ca. 40-50% of all cells present. The mats, however, contained high concentrations of organic extracellular polymeric substances (EPS) that interfered with the column

separation. We could remove these interfering substances by addition of ammonium sulfate. However, the precipitate removed apart from EPS also most of the hydrophobic proteins. The SR proteins were soluble and thus remained in the supernatant.

Our study is one of the few reports on protein purification from environmental samples. The described procedure might help to solve the questions that are unanswerable by genome analysis, such as protein abundance, sub-cellular sequestration, post-translational modifications, oligomerization and intermolecular interactions, in studies of complex environmental samples.

Imaging studies on thin sections

In situ protein detection in microbial cells is mostly done by fluorescently tagging the protein of interest. This method is, however, only established in organisms that are accessible for genetic manipulation. The other method of protein detection – immunolabeling – is not (yet) widespread in environmental microbiology. Immunolabeling has occasionally been used as a method for identification of bacterial species based on their extracellular antigens but immunodetection of intracellular proteins has only been reported in a few 'pet' microorganisms with cell walls susceptible to routine permeabilization agents. Permeabilization is indisputably the limiting factor for high-throughput immunofluorescence analysis in mixed samples of microorganisms (i.e. environmental samples). The extreme species diversity of microorganisms leads to a large heterogeneity in their cell wall composition and thus differences in their resistance or susceptibility to permeabilization agents. In our case, the samples contained mainly archaea with a thick polysaccharide S-layer and gram-negative bacteria. In order to achieve uncompromised target protein accessibility in both organisms we cryo-sectioned the sample into semi-thin (200-400 nm, i.e. less than cell diameter)

sections. The sections were transferred to a support glass slide, labeled with antibodies and imaged in a fluorescent microscope. The preparation was fast (2 days) and the sample was not subjected to drying nor incubated in any organic solvents in order to preserve potential storage compounds. Even with conventional epifluorescence microscopy the images of the sections were sharper than confocal images of whole cells because the reduced thickness of the sections decreased the depth of focus. Unlike electron microscopy, imaging with fluorescent microscope allows examination of large number of cells at once, which is necessary in microbiology for statistical analyses. The sections were (with appropriate adjustments e.g. thickness, coating, embedding) also successfully analyzed with transmission electron microscopy, atomic force microscopy, microRaman spectroscopy and secondary ion mass spectrometry. This flexibility allows for correlative imaging combining any of the above-mentioned approaches and opens new possibilities for microbial ecologists, especially the ones working with samples like mats, aggregates, biofilms and sludge where even imaging with confocal microscope often does not allow single cell discrimination.

Functional identification of microorganisms

Massive high-throughput sequencing of different microbial communities has tremendously increased the number of newly indentified phyla, while the number of cultivated organisms has only moderately increased during the same time. This has resulted in a situation where whole clusters of phylotypes do not contain any cultured representatives and are only present as bare 16S rDNA sequences. Hence it is difficult to deduce the metabolic properties of microorganisms in the environment from their phylogeny and methods for high-throughput functional identification of organisms are desperately needed. This functional identification could come

from metagenomic approaches (ideally automated) that would link abundant 16S rDNA sequences with (at least some) key metabolic genes or *in situ* detection of functional genes or mRNA. Although these methods are currently still at an early stage of development, they are the first steps in the direction of a (cheap) large scale functional identification of microorganisms.

The immunodetection approach introduced above could, in principle, serve the same purpose but, due to currently high antibody prices and cell permeabilization problems, is unlikely to be routinely used for classification of microorganisms in the near future. Still, in a defined system like ours the antibody-based identification of organisms as members of certain microbial 'metabolic groups' might greatly enhance our understanding of the nature of their interactions. Nonetheless, the activity of microorganisms should ideally not be deduced from the presence or abundance of functional genes, proteins or their phylogenetic identity but should be measured. Therefore, culturing efforts should be improved and combined with single cell methods such as nanoSIMS, and microRaman, or other high resolution spectroscopic methods to unequivocally determine the metabolic activity of microorganism.

AOM-associated sulfur chemistry

Relatively early in the history of AOM research it has been speculated that reduced sulfur compounds might play a role in AOM. The numerous attempts to clarify their involvement have only yielded inconclusive results. The physiological experiments were based on additions of different sulfur compounds (e.g. elemental sulfur, inorganic polysulfides, methanethiol) to active AOM enrichments. The aim was to see whether such additions stimulate sulfide production. Generally, no increase of sulfide production was observed (Basen, Deusner; unpublished results). Now we report that very likely zerovalent sulfur (possibly in the form of polysulfides)

is formed and turned over during AOM (Chapter 4). What could be the reason for these discrepancies? First of all, it is not trivial to determine sulfur speciation in an anoxic, sulfide-rich, biological system. Sulfur exists in 8 oxidation states (+6 to -2), including a large palette of zerovalent sulfur compounds. The speciation and abundance of these compounds is strongly affected by temperature, pH and concentration of other sulfur species. Isotope labeling experiments are complicated by the fact that added or excreted S^0 and HS^- rapidly equilibrate with the external polysulfide pool in solution through abiotic isotope exchange. It is, therefore, difficult to assign all sulfur transformations in microbial cultures to biotic processes because abiotic reactions also cause significant changes in sulfur speciation. The reduced sulfur compounds rapidly oxidize when exposed to oxygen, which complicates chemical analysis. The best methods for determining sulfur speciation in anoxic systems would be non-invasive imaging like XANES or Raman spectroscopy for which samples do not need to be exposed to air.

Apart from the complex sulfur chemistry, there are several other considerations that might explain the lack of response of the cultures to sulfur additions. In these experiments, only small amounts of polysulfide (μM) were added based on the assumption that S^0 is present in rate-limiting (< μM) amounts. This assumption was disproven by our measurements that show that the AOM biomass – in particular the ANME biomass – contains several mM of S^0. The addition of small amounts of S^0 (low μM per day) might, therefore, have had little or no effect on the measured sulfide production rates. Moreover, sulfide production was measured according to Cline, which cannot distinguish between polysulfide (added) and sulfide (formed).

The idea of adding the intermediate to stimulate or inhibit the ANME or the SRB, respectively, might not bring the expected result when considering the slow growth of the organisms. It might take up to 70 years to obtain a pure culture of an organism with a doubling time of 6 months. Moreover, if methane activation is the rate-limiting step, the additions of an acceptor (i.e. sulfur) would not increase the overall reaction rate.

We have designed experiments in which stable and radioactive isotopes were added to an active culture and with extraction and imaging techniques we have tracked the flow of the label at different time points. The measurements were facilitated by using 'pool trapping' experiments. In these types of experiments, the anticipated isotope-labeled product is 'trapped' upon formation in a large unlabeled pool of the same compound. The pool of unlabeled molecules 'buffers' further transformations of the labeled product (biotic or abiotic) allowing determinations of rate measurements for intermediates with a fast turnover. Similar isotope experiments could also be used to determine phosphorus and/or iron cycling in the AOM cultures.

PERSPECTIVES

The results obtained during this study raise some questions that I believe would be interesting to address in the near future.

1. Based on our data we suggest that ANME reduce zerovalent sulfur during methane oxidation. The currently known (bacterial) sulfur and polysulfide reductases are either molybdopterin-containing proteins, sporadically associated with *c*-type cytochromes, or *c*-type cytochromes with intrinsic sulfur reducing activity. For archaea, however, c-type cytochromes are uncommon – only 4 out of 20 sequenced archaeal genomes contain any. It is therefore intriguing that in the ANME genome large amounts of genes encoding *c*-type cytochromes and a molybdopterin oxidoreductase with unknown function were found. The presence of these cytochromes was confirmed by spectrophotometry and Raman spectroscopy.

? Which enzymes are responsible for sulfur reduction in ANME? Might the peculiar multiheme cytochromes and/or the molybdopterin oxidoreductase play a role in this process?

2. An alternative hypothesis suggests that the cytochromes in ANME might be involved in extracellular (pure) electron transfer through nanowires. The proposed mechanism is analogous to the one observed in iron-reducing *Geobacter* species. In these organisms conclusive evidence for involvement of cytochromes was obtained from transmission electron microscopy studies, immunolabeling and genetic knock-outs.

? Could we convincingly prove or disprove the theory of nanowires-mediated electron transfer in AOM by cytochrome immunolocalization with high resolution STED microscopy and/or with TEM?

3. The concentration of sulfur in ANME cells (up to 6% cell dry weight) is similar to *Beggiatoa*, which are speculated to play a role in sulfur cycling in marine sediments.

? Does the excessive sulfur storage in ANME have an effect on sulfur biogeochemistry?

4. Transmission electron microscopy, microRaman spectroscopy and nanoSIMS analyses have shown a high iron and phosphorus content of the ANME-associated bacteria. These elements are stored as amorphous particles which suggests that they might be later recruited for metabolic use. Because the respiratory metabolism of sulfate reducing bacteria depends on phosphorylation reactions (ATP+sulfate→APS) it might require intense phosphorus cycling.

? What is the role of these particles in the SRB? Do the iron/phosphorus particles represent transient phosphorus storage for sulfate reduction? If so, do other sulfate reducing bacteria contain such particles as well?

5. Phosphorus mobilization by the AOM organisms has not been previously recognized and, correspondingly, the phosphorus cycling in AOM zones has not been a subject of thorough investigations. Now that we have evidence for phosphorus storage by the SR bacteria in the SMTZ it would be interesting to investigate its possible implications for phosphorus and iron biogeochemistry.

? What would be the effect of the release of iron phosphates from SR bacteria (e.g. upon depletion of a methane source and a subsequent cell death)? Could it explain the peculiar presence of phosphorites in ancient AOM zones?

REFERENCES

1. **Akagi, J.M. & Campbell, L.L. (1962).** Studies on thermophilic sulfate-reducing bacteria III. Adenosine triphosphate-sulfurylase of *Clostridium nigrificans* and *Desulfovibrio desulfuricans*. *Journal of Bacteriology* **84**, 1194-1201.

2. **Aldrich, H.C., Beimborn, D.B., Bokranz, M. & Schönheit, P. (1987).** Immunocytochemical localization of methyl coenzyme-M reductase in *Methanobacterium thermoautotrophicum*. *Archives in Microbiology* **147**, 190-194.

3. **Alperin, M. J. & Hoehler, T. M. (2009a).** Anaerobic methane oxidation by archaea/sulfate-reducing bacteria aggregates: 1. Thermodynamic and physical constraints. *American Journal of Science* **309**, 869-957.

4. **Alperin, M. J. & Hoehler, T. M. (2009b).** Anaerobic methane oxidation by archaea/sulfate-reducing bacteria aggregates: 2. Isotopic constraints. *American Journal of Science* **309**, 958-984.

5. **Alperin M. & Hoehler T. (2010).** The ongoing mystery of sea-floor methane. *Science* **329**, 288-289.

6. **Amann, R.I., Krumholz, L. & Stahl, D.A. (1990).** Fluorescent-oligonucleotide probing of whole cells for determinative, phylogenetic, and environmental studies in microbiology. *Journal of Bacteriology* **172**, 762−770.

7. **Amann, R.I., Ludwig, W. & Schleifer, K.H. (1995).** Phylogenetic identification and *in situ* detection of individual microbial cells without cultivation. *Microbiological Reviews* **59**, 143−169.

8. **Arendsen, A.F., Verhagen, M.F.J.M., Wolbert, R.B.G., Pierik, A.J., Stams, A.J.M., Jetten, M.S.M. & Hagen, W.R. (1993).** The dissimilatory sulfite reductase

from *Desulfosarcina variabilis* is a desulforubidin containing uncoupled metalated sirohemes and S = $^{9}/_{2}$ iron-sulfur clusters. *Biochemistry* **32**, 10323−10330.

9. Barnes, R. O. & Goldberg, E. D. (1976). Methane production and consumption in anoxic marine sediments. *Geology* **4**, 297-300.

10. Beal, E. J., House, C. H. & Orphan, V. J. (2009). Manganese- and iron-dependent marine methane oxidation. *Science* **325**, 184-187.

11. Baliga, B.S., Jagannathan, V. & Vartak, H.G. (1961). Purification and properties of sulfurylase from *Desulfovibrio desulfuricans*. *Journal of Scientific & Industrial Research* **20C**: 33-40.

12. Basen, M., Krüger, M., Milucka, J. & other authors (in revision). Bacterial enzymes for dissimilatory sulfate reduction in a marine microbial mat (Black Sea) mediating anaerobic oxidation of methane. *Environmental Microbiology*

13. Biddle, J. F., Lipp, J. S., Lever, M. A. & other authors (2006). Heterotrophic Archaea dominate sedimentary subsurface ecosystems off Peru. *Proceedings of the National Academy of Sciences of the United States of America* **103**, 3846-3851.

14. Bleicher, K. & Winter, J. (1994). Formate production and utilization by methanogens and by sewage-sludge consortia - interference with the concept of interspecies formate transfer. *Applied Microbiology and Biotechnology* **40,** 910-915.

15. Blumenberg, M., Seifert, R., Reitner, J., Pape, T. & Michaelis, W. (2004). Membrane lipid patterns typify distinct anaerobic methanotrophic consortia. *Proceedings of the National Academy of Sciences of the United States of America* **101**, 11111−11116.

16. Bradford, M.M. (1976). Rapid and sensitive method for quantitation of microgram quantities of protein utilizing principle of protein-dye binding. *Analytical Biochemistry* **72**, 248−254.

17. Boetius, A., Ravenschlag, K., Schubert, C. J. & other authors (2000). A marine microbial consortium apparently mediating anaerobic oxidation of methane. *Nature* **407**, 623-626.

18. Chistoserdova, L., Vorholt, J.A. & Lidstrom, M.E. (2005). A genomic view of methane oxidation by aerobic bacteria and anaerobic archaea. *Genome Biology* **6**, 208.

19. Cline, J.D. (1969). Spectrophotometric determination of hydrogen sulfide in natural waters. *Limnology and Oceanography* **14**, 454−458.

20. Cord-Ruwisch, R. (1985). A quick method for the determination of dissolved and precipitated sulfides in cultures of sulfate-reducing bacteria. *Journal of Microbiological Methods* **4**, 33−36.

21. Dahl, C., Speich, N. & Trüper, H.G. (1994a). Enzymology and molecular biology of sulfate reduction in extremely thermophilic archaeon *Archaeoglobus fulgidus*. *Methods in Enzymology* **243**, 331−349.

22. Dahl, C. & Trüper, H.G. (1994b). Enzymes of dissimilatory sulfide oxidation in phototrophic bacteria. *Methods in Enzymology* **243**, 400−421.

23. Dahl, C., Rakhely, G., Pott-Sperling, A. S. & other authors (1999). Genes involved in hydrogen and sulfur metabolism in phototrophic sulfur bacteria. *FEMS Microbiology Letters* **180**, 317-324.

24. Dahl, C. & Trüper, H.G. (2001). Sulfite reductase and APS reductase from *Archaeoglobus fulgidus*. *Methods in Enzymology.* **331**, 427−441.

25. Daims, H., Brühl, A., Amann, R. & Schleifer, K.H. (1999). The domain-specific probe EUB338 is insufficient for the detection of all bacteria: development and evaluation of a more comprehensive probe set. *Systematic and Applied Microbiology* **22**, 434−444.

26. Dekas, A. E., Poretsky, R. S. & Orphan, V. J. (2009). Deep-sea archaea fix and share nitrogen in methane-consuming microbial consortia. *Science* **326**, 422-426.

27. Devol A. H. & Ahmed S. I. (1981). Are high rates of sulphate reduction associated with anaerobic oxidation of methane? *Nature* **291**, 407-408.

28. Dickens, G. R. (2003). Rethinking the global carbon cycle with a large, dynamic and microbially mediated gas hydrate capacitor. *Earth and Planetary Science Letters* **213**, 169-183.

29. Eisen, J. A., Nelson, K. E., Paulsen, I. T. & other authors (2002). The complete genome sequence of *Chlorobium tepidum* TLS, a photosynthetic, anaerobic, green-sulfur bacterium. *Proceedings of the National Academy of Sciences of the United States of America* **99 (14)**, 9509-9514.

30. Ellermann, J., Rospert, S., Thauer, R.K., Bokranz, M., Klein, A., Voges, M. & Berkessel, A. (1989). Methyl-coenzyme-M reductase from *Methanobacterium thermoautotrophicum* (strain Marburg) - purity, activity and novel inhibitors. *European Journal of Biochemistry* **184**, 63-68.

31. Ettwig, K. F., Shima, S., van de Pas-Schoonen, K. T., Kahnt, J., Medema, M. H., op den Camp, H. J. M., Jetten, M. S. M. & Strous, M. (2008). Denitrifying

bacteria anaerobically oxidize methane in the absence of archaea. *Environmental Microbiology* **10**, 3164-3173.

32. Ettwig, K. F., Butler, M. K., Le Paslier, D. & other authors (2010). Nitrite-driven anaerobic methane oxidation by oxygenic bacteria. *Nature* **464**, 543-548.

33. Friedrich, M.W. (2002). Phylogenetic analysis reveals multiple lateral transfers of adenosine-5'-phosphosulfate reductase genes among sulfate-reducing microorganisms. *Journal of Bacteriology* **184**, 278−289.

34. Fauque G., Herve D. & Le Gall J. (1979). Structure-function relationship in hemoproteins: the role of cytochrome c3 in the reduction of colloidal sulfur by sulfate-reducing bacteria. *Archives in Microbiology* **121**, 261-264.

35. Fossing H. & Jorgensen B. B. (1990). Isotope exchange reactions with radiolabeled sulfur compounds in anoxic seawater. *Biogeochemistry* **9**, 223-245.

36. Fritz, G., Buchert, T., Huber, H., Stetter, K.O. & Kroneck, P.M.H. (2000). Adenylylsulfate reductases from archaea and bacteria are 1 : 1 alpha beta-heterodimeric iron-sulfur flavoenzymes - high similarity of molecular properties emphasizes their central role in sulfur metabolism. *FEBS Letters* **473,** 63−66.

37. Fritz, G., Roth, A., Schiffer, A. & other authors (2002). Structure of adenylylsulfate reductase from the hyperthermophilic *Archaeoglobus fulgidus* at 1.6 Á resolution. *Proceedings of the National Academy of Sciences of the United States of America* **99 (4)**. 1836−1841.

38. Frost R. L., Martens W. N., Williams P., & Kloprogge J. T. (2002). Raman and infrared spectroscopic study of the vivianite-group phosphates vivianite, baricite and bobierrite. *Mineralogical Magazine* **66**, 1063-1073.

39. Gorby, Y. A., Yanina, S., McLean, J. S. & other authors (2006). Electrically conductive bacterial nanowires produced by *Shewanella oneidensis* strain MR-1 and other microorganisms. *Proceedings of the National Academy of Sciences of the United States of America* **103**, 11358-11363.

40. Hall, T.A. (1999). BioEdit: a user-friendly biological sequence alignment editor and analysis program for Windows 95/98/NT. *Nucleic Acids Symposium Series* **41**, 95−98.

41. Hallam, S. J., Putnam, N., Preston, C. M., Detter, J. C., Rokhsar, D., Richardson, P. M. & DeLong, E. F. (2004). Reverse methanogenesis: testing the hypothesis with environmental genomics. *Science* **305**, 1457-1462.

42. Hallam, S.J., Girguis, P.R., Preston, C.M., Richardson, P.M. & DeLong, E.F. (2003). Identification of methyl coenzyme M reductase A (McrA) genes associated with methane-oxidizing archaea. *Applied and Environmental Microbiology* **69**, 5483-5491.

43. Heller, C., Hoppert, M. & Reitner, J. (2008). Immunological localization of coenzyme M reductase in anaerobic methane-oxidizing archaea of ANME 1 and ANME 2 type. *Geomicrobiology Journal* **25**, 149−156.

44. Hinrichs, K. U., Hayes, J. M., Sylva, S. P., Brewer, P. G. & DeLong, E. F. (1999). Methane-consuming archaebacteria in marine sediments. *Nature* **398**, 802-805.

45. Hinrichs, K. U., Summons, R. E., Orphan, V., Sylva, S. P. & Hayes, J. M. (2000). Molecular and isotopic analysis of anaerobic methane-oxidizing communities in marine sediments. *Organic Geochemistry* **31**, 1685-1701.

46. Hinrichs, K. U. & Boetius, A. (2002). The anaerobic oxidation of methane: new insights in microbial ecology and biogeochemistry. In *Ocean Margin Systems*, pp. 457–477. G. Wefer, B. D., D. Hebbeln, B. B. Jørgensen, M. Schlüter and T. C. E. van Weering (eds.). Berlin: Springer-Verlag.

47. Hoehler, T.M., Alperin, M.J., Albert, D.B. & Martens, C.S. (1994). Field and laboratory studies of methane oxidation in an anoxic marine sediment - evidence for a methanogen-sulfate reducer consortium. *Global Biogeochemical Cycles* **8,** 451−463.

48. Hoehler, T. M., Alperin, M. J., Albert, D. B. & Martens, C. S. (2001). Apparent minimum free energy requirements for methanogenic Archaea and sulfate-reducing bacteria in an anoxic marine sediment. *FEMS Microbiology Ecology* **38**, 33-41.

49. Hoppert, M. & Mayer, F. (1999). Principles of macromolecular organization and cell function in bacteria and archaea. *Cell Biochemistry and Biophysics* **31**, 247-284.

50. House, C. H., Schopf, J. W., McKeegan, K. D., Coath, C. D., Harrison, T. M. & Stetter, K. O. (2000). Carbon isotopic composition of individual Precambrian microfossils. *Geology* **28**, 707-710.

51. House, C. H., Orphan, V. J., Turk, K. A., Thomas, B., Pernthaler, A., Vrentas, J. M. & Joye, S. B. (2009). Extensive carbon isotopic heterogeneity among methane seep microbiota. *Environmental Microbiology* **11**, 2207-2215.

52. Jankielewicz A., Schmitz R. A., Klimmek O., & Kröger A. (1994). Polysulfide reductase and formate dehydrogenase from Wolinella succinogenes contain molybdopterin guanine dinucleotide. *Archives in Microbiology* **162**, 238-242

53. Johnson, E. & Mukhopadhyay, B. (2008). A novel coenzyme F_{420}-dependent sulfite reductase and a small sulfite reductase in methanogenic archaea. In *Microbial Sulfur Metabolism*, pp. 202-216. Edited by C. Dahl and C. G. Friedrich: Springer

54. Johnson, E. F. & Mukhopadhyay, B. (2005). A new type of sulfite reductase, a novel coenzyme F_{420}-dependent enzyme, from the methanarchaeon *Methanocaldococcus jannaschii*. *Journal of Biological Chemistry* **280**, 38776-38786.

55. Jørgensen B. B. & Fenchel T. (1974). Sulfur cycle of a marine sediment model system. *Marine Biology* **24**, 189-201.

56. Kallmeyer J., Ferdelman T.G., Weber A., Fossing H.. & Jørgensen B.B. (2004). Evaluation of a cold chromium distillation procedure for recovering very small amounts of radiolabeled sulfide related to sulfate reduction measurements. *Limnology and Oceanography: Methods* **2**, 171-180.

57. Kamyshny A., Ekeltchik I., Gun J. & Lev O. (2006). Method for the determination of inorganic polysulfide distribution in aquatic systems. *Analytical Chemistry* **78**, 2631-2639.

58. Kamyshny Jr., A., Gun, J., Rizkov, D., Voitsekovski, T. & Lev, O. (2007). Equilibrium distribution of polysulfide ions in aqueous solutions at different temperatures by rapid single phase derivatisation. *Environmental Science and Technology* **41**, 6633 - 6644.

59. Kamyshny Jr., A. (2009). Solubility of cyclooctasulfur in pure water and sea water at different temperatures. *Geochimica et Cosmochimica Acta* **73**, 6022-6028.

60. Kappler, O., Janssen, P. H., Kreft, J. U. & Schink, B. (1997). Effects of alternative methyl group acceptors on the growth energetics of the O-demethylating anaerobe *Holophaga foetida*. *Microbiology-UK* **143**, 1105-1114.

61. Kiene R.P., Oremland R.S., Catena A., Miller L.G. & Capone D.G. (1986). Metabolism of reduced methylated sulfur compounds in anaerobic sediments and by a pure culture of an estuarine methanogen. *Applied and Environmental Microbiology* **52**,1037–1045.

62. Klein, M., Friedrich, M., Roger, A. J. & other authors (2001). Multiple lateral transfers of dissimilatory sulfite reductase genes between major lineages of sulfate-reducing prokaryotes. *Journal of Bacteriology* **183**, 6028-6035.

63. Klimes, A., Franks, A. E., Glaven, R. H., Tran, H., Barrett, C. L., Qiu, Y., Zengler, K. & Lovley, D. R. (2010). Production of pilus-like filaments in *Geobacter sulfurreducens* in the absence of the type IV pilin protein PilA. *FEMS Microbiology Letters* **310**, 62-68.

64. Knittel, K., Boetius, A., Lemke, A. & other authors (2003). Activity, distribution, and diversity of sulfate reducers and other bacteria in sediments above gas hydrate (Cascadia margin, Oregon). *Geomicrobiology Journal* **20**, 269−294.

65. Knittel, K., Lösekann, T., Boetius, A., Kort, R. & Amann, R. (2005). Diversity and distribution of methanotrophic archaea at cold seeps. *Applied and Environmental Microbiology* **71**, 467-479.

66. Knittel, K. & Boetius, A. (2009). Anaerobic oxidation of methane: progress with an unknown process. *Annual Reviews of Microbiology* **63**, 311-334.

67. Kobayashi, K., Morisawa, Y., Ishituka, T. & Ishimoto, M. (1975). Biochemical studies on sulfate-reducing bacteria. 14. Enzyme levels of

adenylylsulfate reductase, inorganic pyrophosphatase, sulfite reductase, hydrogenase, and adenosine-triphosphatase in cells grown on sulfate, sulfite, and thiosulfate. *Journal of Biochemistry* **78**, 1079−1085.

68. Krämer, M. & Cypionka, H. (1989). Sulfate formation via ATP sulfurylase in thiosulfate-disproportionating and sulfite-disproportionating bacteria. *Archives in Microbiology* **151**, 232−237.

69. Krüger, M., Meyerdierks, A., Glöckner, F. O. & other authors (2003). A conspicuous nickel protein in microbial mats that oxidize methane anaerobically. *Nature* **426**, 878-881.

70. Krüger, M., Blumenberg, M., Kasten, S. & other authors (2008). A novel, multi-layered methanotrophic microbial mat system growing on the sediment of the Black Sea. *Environmental Microbiology* **10**, 1934−1947.

71. Laemmli, U.K. (1970). Cleavage of structural proteins during assembly of head of bacteriophage T4. *Nature* **227**, 680-685.

72. LeGall, J. & Fauque, G. (1988). Dissimilatory reduction of sulfur compounds. In *Biology of anaerobic microorganisms*, pp. 587−639. Zehnder, A.J.B. (ed.). New York: John Wiley & Sons.

73. Lösekann, T., Knittel, K., Nadalig, T., Fuchs, B., Niemann, H., Boetius, A. & Amann, R. (2007). Diversity and abundance of aerobic and anaerobic methane oxidizers at the Haakon Mosby mud volcano, Barents Sea. *Applied and Environmental Microbiology* **73**, 3348−3362.

74. Mander, G. J., Duin, E. C., Linder, D., Stetter, K. O. & Hedderich, R. (2002). Purification and characterization of a membrane-bound enzyme complex from the sulfate-reducing archaeon *Archaeoglobus fulgidus* related to heterodisulfide

reductase from methanogenic archaea. *European Journal of Biochemistry* **269**, 1895-1904.

75. Mander, G. J., Pierik, A. J., Huber, H. & Hedderich, R. (2004). Two distinct heterodisulfide reductase-like enzymes in the sulfate-reducing archaeon *Archaeoglobus profundus*. *European Journal of Biochemistry* **271**, 1106-1116.

76. Martens, C. S. & Berner, R. A. (1977). Interstitial water chemistry of anoxic Long Island Sound sediments: 1. Dissolved gases. *Limnology and Oceanography* **22**, 10-25.

77. Manz, W., Eisenbrecher, M., Neu, T.R. & Szewzyk, U. (1998). Abundance and spatial organization of gram-negative sulfate-reducing bacteria in activated sludge investigated by in situ probing with specific 16S rRNA targeted oligonucleotides. *FEMS Microbiology Ecology* **25**, 43−61.

78. Meulepas, R.J.W., Jagersma, C.G., Gieteling, J., Buisman, C.J.N., Stams, A.J.M. & Lens, P.N.L. (2009). Enrichment of anaerobic methanotrophs in sulfate-reducing membrane bioreactors. *Biotechnology and Bioengineering* **104**, 458−470.

79. Meulepas, R. J. W., Jagersma, C. G., Khadem, A. F., Stams, A. J. M. & Lens, P. N. L. (2010). Effect of methanogenic substrates on anaerobic oxidation of methane and sulfate reduction by an anaerobic methanotrophic enrichment. *Applied Microbiology and Biotechnology* **87**, 1499-1506.

80. Meyer, B. & Kuever, J. (2007). Phylogeny of the alpha and beta subunits of the dissimilatory adenosine-5'-phosphosulfate (APS) reductase from sulfate-reducing prokaryotes - origin and evolution of the dissimilatory sulfate-reduction pathway. *Microbiology SGM* **153**, 2026−2044.

81. Meyerdierks, A., Kube, M., Lombardot, T., Knittel, K., Bauer, M., Glöckner, F. O., Reinhardt, R. & Amann, R. (2005). Insights into the genomes of archaea mediating the anaerobic oxidation of methane. *Environmental Microbiology* **7**, 1937-1951.

82. Meyerdierks, A., Kube, M., Kostadinov, I., Teeling, H., Glöckner, F. O., Reinhardt, R. & Amann, R. (2010). Metagenome and mRNA expression analyses of anaerobic methanotrophic archaea of the ANME-1 group. *Environmental Microbiology* **12**, 422-439.

83. Michaelis, W., Seifert, R., Nauhaus, K. & other authors (2002). Microbial reefs in the Black Sea fueled by anaerobic oxidation of methane. *Science* **297**, 1013-1015.

84. Moran, J. J., Beal, E. J., Vrentas, J. M., Orphan, V. J., Freeman, K. H. & House, C. H. (2008). Methyl sulfides as intermediates in the anaerobic oxidation of methane. *Environmental Microbiology* **10**, 162-173.

85. Musat N., Halm H., Winterholler B. and other authors (2008). Single-cell view on the ecophysiology of anaerobic phototrophic bacteria. *Proceedings of the National Academy of Sciences of the United States of America* **105 (46)**, 17861-17866.

86. Nauhaus, K., Boetius, A., Krüger, M. & Widdel, F. (2002). *In vitro* demonstration of anaerobic oxidation of methane coupled to sulphate reduction in sediment from a marine gas hydrate area. *Environmental Microbiology* **4**, 296-305.

87. Nauhaus, K., Albrecht, M., Elvert, M., Boetius, A. & Widdel, F. (2007). *In vitro* cell growth of marine archaeal-bacterial consortia during anaerobic oxidation of methane with sulfate. *Environmental Microbiology* **9**, 187-196.

88. Niemann, H., Lösekann, T., de Beer, D. & other authors (2006). Novel microbial communities of the Haakon Mosby mud volcano and their role as a methane sink. *Nature* **443**, 854-858.

89. Odom, J.M. & Peck, H.D. (1981). Localization of dehydrogenases, reductases, and electron-transfer components in the sulfate-reducing bacterium *Desulfovibrio gigas*. *Journal of Bacteriology* **147**, 161-169.

90. Orphan, V. J., House, C. H., Hinrichs, K. U., McKeegan, K. D. & DeLong, E. F. (2001a). Methane-consuming archaea revealed by directly coupled isotopic and phylogenetic analysis. *Science* **293**, 484-487.

91. Orphan, V.J., Hinrichs, K.U., Ussler, W. & other authors (2001b). Comparative analysis of methane-oxidizing archaea and sulfate-reducing bacteria in anoxic marine sediments. *Applied and Environmental Microbiology* **67**, 1922−1934.

92. Orphan, V.J., House, C.H., Hinrichs, K.U., McKeegan, K.D. & DeLong, E.F. (2002a). Direct phylogenetic and isotopic evidence for multiple groups of archaea involved in the anaerobic oxidation of methane. *Geochimica et Cosmochimica Acta* **66**, A571-A571.

93. Orphan, V. J., House, C. H., Hinrichs, K. U., McKeegan, K. D. & DeLong, E. F. (2002b). Multiple archaeal groups mediate methane oxidation in anoxic cold seep sediments. *Proceedings of the National Academy of Sciences of the United States of America* **99 (11)**, 7663-7668.

94. Orphan, V. J., Turk, K. A., Green, A. M. & House, C. H. (2009). Patterns of ^{15}N assimilation and growth of methanotrophic ANME-2 archaea and sulfate-reducing bacteria within structured syntrophic consortia revealed by FISH-SIMS. *Environmental Microbiology* **11**, 1777-1791.

95. Ossmer, R., Mund, T., Hartzell, P.L., Konheiser, U., Kohring, G.W., Klein, A. & other authors (1986). Immunocytochemical localization of component C of the methylreductase system in *Methanococcus voltae* and *Methanobacterium thermoautotrophicum*. *Proceedings of the National Academy of Sciences of the United States of America* **83**, 5789-5792.

96. Pancost, R. D., Damste, J. S. S., de Lint, S., van der Maarel, M. J. E. C., Gottschal, J. C. & Party, M. S. S. (2000). Biomarker evidence for widespread anaerobic methane oxidation in Mediterranean sediments by a consortium of methanogenic archaea and bacteria. *Applied and Environmental Microbiology* **66**,

97. Parshina S.N., Sipma J., Meint Henstra A., & Stams A.J.M. (2010). Carbon monoxide as an electron donor for the biological reduction of sulphate. *International Journal of Microbiology*, 1126-1132.

98. Pasteris J. D., Freeman J. J., Goffredi S. K. & Buck K. R. (2001). Raman spectroscopic and laser scanning confocal microscopic analysis of sulfur in living sulfur-precipitating marine bacteria. *Chemical Geology* **180**, 3-18.

99. Pätzold R., Keuntje M., Theophile K., Müller J., Mielcarek E., Ngezahayo A. & Anders-von Ahlften A. (2008). In situ mapping of nitrifiers and anammox bacteria in microbial aggregates by means of confocal resonance Raman microscopy. *Journal of Microbiological Methods* **3**, 241-248.

100. Pernthaler, A., Dekas, A. E., Brown, C. T., Goffredi, S. K., Embaye, T. & Orphan, V. J. (2008). Diverse syntrophic partnerships from deep sea methane vents revealed by direct cell capture and metagenomics. *Proceedings of the National Academy of Sciences of the United States of America* **105**, 7052-7057.

101. Pimenov, N.V., Rusanov, I.I., Poglazova, M.N., Mityushina, L.L., Sorokin, D.Y., Khmelenina, V.N. & Trotsenko, Y.A. (1997). Bacterial mats on coral-like structures at methane seeps in the Black Sea. *Microbiologiya* **66**, 354−360.

102. Platen, H. & Schink, B. (1987). Methanogenic degradation of acetone by an enrichment culture. *Archives of Microbiology* **149**, 136-141.

103. Ploug H., Musat N., Adam B. & other authors (2010). Carbon and nitrogen fluxes associated with the cyanobacterium *Aphanizomenon sp*. in the Baltic Sea. *ISME journal* **4,** 1215-1223.

104. Polerecky L., Adam B., Musat N., Milucka J., Vagner T. & Kuypers M. M. M. (2012). Look@NanoSIMS – a tool for the analysis of NanoSIMS data in environmental microbiology. *Environmental Microbiology* **DOI: 10.1111/j.1462-2920.2011.02681.x**

105. Prange A., Chauvistré R., Modrow H., Hormes J., Trüper H. G. & Dahl C. (2002). Quantitative speciation of sulfur in bacterial sulfur globules: X-ray absorption spectroscopy reveals at least three different species of sulfur. *Microbiology* **148**, 267-276.

106. Rabus, R., Hansen, T.A. & Widdel, F. (2006). Dissimilatory sulfate- and sulfur-reducing prokaryotes. In *The Prokaryotes − A handbook on the biology of bacteria*, pp. 659−768. Dworkin, M., Falkow, S., Rosenberg, E., Schleifer, K.H., and Stackebrandt, E. (eds). New York: Springer.

107. Raghoebarsing, A. A., Pol, A., van de Pas-Schoonen, K. T. & other authors (2006). A microbial consortium couples anaerobic methane oxidation to denitrification. *Nature* **440**, 918-921.

108. Reeburgh, W. S. (1976). Methane consumption in Cariaco Trench waters and sediments. *Earth and Planetary Science Letters* **28**, 337-344.

109. Reeburgh, W. S. (2007). Oceanic methane biogeochemistry. *Chemical Reviews* **107**, 486-513.

110. Reguera, G., McCarthy, K. D., Mehta, T., Nicoll, J. S., Tuominen, M. T. & Lovley, D. R. (2005). Extracellular electron transfer via microbial nanowires. *Nature* **435**, 1098-1101.

111. Reitner, J., Peckmann, J., Blumenberg, M., Michaelis, W., Reimer, A. & Thiel, V. (2005a). Concretionary methane-seep carbonates and associated microbial communities in Black Sea sediments. *Palaeogeography Palaeoclimatology Palaeoecology* **227**, 18-30.

112. Reitner, J., Peckmann, J., Reimer, A., Schumann, G. & Thiel, V. (2005b). Methane-derived carbonate build-ups and associated microbial communities at cold seeps on the lower Crimean shelf (Black Sea). *Facies* **51**, 71-84.

113. Renosto, F., Martin, R.L., Borrell, J.L., Nelson, D.C. & Segel, I.H. (1991). ATP sulfurylase from trophosome tissue of *Riftia pachyptila* (hydrothermal vent tube worm). *Archives of Biochemistry and Biophysics* **290**, 66−78.

114. Rossi, M., Pollock, W. B. R., Reij, M. W., Keon, R. G., Fu, R. D. & Voordouw, G. (1993). The *hmc* operon of *Desulfovibrio vulgaris* subsp vulgaris Hildenborough encodes a potential transmembrane redox protein complex. *Journal of Bacteriology* **175**, 4699-4711.

115. Scheller, S., Goenrich, M., Boecher, R., Thauer, R. K. & Jaun, B. (2010). The key nickel enzyme of methanogenesis catalyses the anaerobic oxidation of methane. *Nature* **465**, 606-608.

116. Schreiber, L., Holler, T., Knittel, K., Meyerdierks, A. & Amann, R. (2010). Identification of the dominant sulfate-reducing bacterial partner of anaerobic methanotrophs of the ANME-2 clade. *Environmental Microbiology* **12**, 2327−2340.

117. Shima S. & Thauer R. K. (2005). Methyl-coenzyme M reductase and the anaerobic oxidation of methane in methanotrophic Archaea. *Current Opinion in Microbiology* **6**, 643-648.

118. Sirevag, R., Buchanan, B. B., Berry, J. A. & Troughton, J. H. (1977). Mechanisms of CO_2 fixation in bacterial photosynthesis studied by carbon isotope fractionation technique. *Archives of Microbiology* **112**, 35-38.

119. Skyring, G.W., Trudinger P. A. & Shaw, W.H. (1972). Electophoretic characterization of ATP-sulfate adenylyltransferase (ATP-sulfurylase) using acrylamide gels. *Analytical Biochemistry* **48**, 259-265.

120. Sørensen, K.B., Finster, K. & Ramsing, N.B. (2001). Thermodynamic and kinetic requirements in anaerobic methane oxidizing consortia exclude hydrogen, acetate, and methanol as possible electron shuttles. *Microbial Ecology* **42**, 1-10.

121. Sperling, D., Kappler, U., Wynen, A., Dahl, C. & Trüper, H.G. (1998). Dissimilatory ATP sulfurylase from the hyperthermophilic sulfate reducer *Archaeoglobus fulgidus* belongs to the group of homo-oligomeric ATP sulfurylases. *FEMS Microbiology Letters* **162**, 257−264.

122. Sprott, G. D. & Beveridge, T. J. (1993). Microscopy. In *Methanogenesis: ecology, physiology, biochemistry & genetics*, pp. 81-128. Edited by J. G. Ferry: Chapman & Hall.

123. Stetter, K.O. (1988). *Archaeoglobus fulgidus* gen. nov., sp. nov.: a new taxon of extremely thermophilic archaebacteria. *Systematic and Applied Microbiology* **10**, 172−173.

124. Steudel R. (2002). Organic polysulfanes R_2S_n (n > 2). *Chemical Reviews* **102**, 3905-3945.

125. Thauer, R. K., Jungermann, K. & Decker, K. (1977). Energy conservation in chemotrophic anaerobic bacteria. *Bacteriological Reviews* **41**, 100-180.

126. Thauer, R. K. & Shima, S. (2008). Methane as fuel for anaerobic microorganisms. *Incredible Anaerobes: From Physiology to Genomics to Fuels* **1125**, 158-170.

127. Thauer, R.K. (1998). Biochemistry of methanogenesis: a tribute to Marjory Stephenson. *Microbiology-SGM* **144**: 2377−2406.

128. Treude T., Boetius A., Knittel K., Wallmann K. & Jørgensen B.B. (2003). Anaerobic oxidation of methane above gas hydrates at Hydrate Ridge, NE Pacific. *Ocean Marine Ecology – Progress Series* **264**, 1-14.

129. Treude, T., Knittel, K., Blumenberg, M., Seifert, R. & Boetius, A. (2005). Subsurface microbial methanotrophic mats in the Black Sea. *Applied and Environmental Microbiology* **71**, 6375−6378.

130. Treude, T., Orphan, V., Knittel, K., Gieseke, A., House, C.H. & Boetius, A. (2007). Consumption of methane and CO_2 by methanotrophic microbial mats from gas seeps of the anoxic Black Sea. *Applied and Environmental Microbiology* **73**, 3770−3770.

131. Trofimov B. A., Sinegovskaya L. M. & Gusarova N. K. (2009). Vibrations of the S−S bond in elemental sulfur and organic polysulfides: a structural guide. *Journal of Sulfur Chemistry* **5**, 518-554.

132. Valente, F. M. A., Saraiva, L. M., LeGall, J., Xavier, A. V., Teixeira, M. & Pereira, I. A. C. (2001). A membrane-bound cytochrome c(3): A type II cytochrome c(3) from *Desulfovibrio vulgaris* Hildenborough. *Chembiochem* **2**, 895-905.

133. Valentine, D.L., Blanton, D.C. & Reeburgh, W.S. (2000). Hydrogen production by methanogens under low-hydrogen conditions. *Archives in Microbiology* **174**, 415−421.

134. Valentine D. L. & Reeburgh W. S. (2000). New perspectives on anaerobic methane oxidation. *Environmental Microbiology* **2**,477–84.

135. Wagner, M., Roger, A.J., Flax, J.L., Brusseau, G.A. & Stahl, D.A. (1998). Phylogeny of dissimilatory sulfite reductases supports an early origin of sulfate respiration. *Journal of Bacteriology* **180**, 2975−2982.

136. Wallner, G., Amann, R. & Beisker, W. (1993). Optimizing fluorescent *in situ* hybridization with rRNA-targeted oligonucleotide probes for flow cytometric identification of microorganisms. *Cytometry* **14**, 136−143.

137. Warikoo, V., McInerney, M. J., Robinson, J. A. & Suflita, J. M. (1996). Interspecies acetate transfer influences the extent of anaerobic benzoate degradation by syntrophic consortia. *Applied and Environmental Microbiology* **62**, 26-32.

138. Wegener, G., Niemann, H., Elvert, M., Hinrichs, K. U. & Boetius, A. (2008). Assimilation of methane and inorganic carbon by microbial communities mediating the anaerobic oxidation of methane. *Environmental Microbiology* **10**, 2287-2298.

139. Widdel, F., Musat, F., Knittel, K. & Galushko, A. (2007). Anaerobic degradation of hydrocarbons with sulphate as electron acceptor. In *Sulphate-Reducing Bacteria: Environmental and Engineered Systems*, pp. 265-303. L. L. Barton & W. A. Hamilton (eds.). Cambridge University Press.

140. Widdel, F. & Bak, F. (1992). Gram-negative mesophilic sulfate-reducing bacteria. In *The Prokaryotes*, pp. 3352−3378. Balows, A.T., H.G.; Dworkin, M., Harder, W.; and Schleifer, K.-H. (eds.). New York: Springer.

141. Zehnder, A.J.B., & Brock, T.D. (1979). Methane formation and methane oxidation by methanogenic bacteria. *Journal of Bacteriology* **137,** 420−432.

142. Zopfi J., Ferdelman T.G. & Fossing H. (2004). Distribution and fate of sulfur intermediates – sulfite, thiosulfate, and elemental sulfur – in marine sediments. In *Sulfur Biogeochemistry – Past and Present*, pp. 97-116. Amend J., Edwards K.J., and Lyons T.J. (eds.). Geological Society of America Special Paper 379.

LIST of PUBLICATIONS

Manuscript 1.

Bacterial enzymes for dissimilatory sulfate reduction in a marine microbial mat (Black Sea) mediating anaerobic oxidation of methane *(in revision)*

Mirko Basen, Martin Krüger, Jana Milucka, Jan Kuever, Olav Grundmann, Anke Meyerdierks, Friedrich Widdel, and Seigo Shima

Manuscript 2.

Immunological detection of enzymes for sulfate reduction in bacterial cells of anaerobic methane-oxidizing microbial consortia *(in preparation)*

Jana Milucka, Friedrich Widdel, Seigo Shima

Manuscript 3.

Sulfur cycling between the archaea and bacteria is involved in anaerobic oxidation of methane *(in preparation)*

Jana Milucka, Tim Ferdelman, Gabriele Klockgether, Lubos Polerecky, Tomas Vagner, Michael Formolo, Gunter Wegener, Markus Schmid, Michael Wagner, Friedrich Widdel, Marcel Kuypers

Manuscript 4.

Look@NanoSIMS – a tool for the analysis of NanoSIMS data in environmental microbiology *(in preparation)*

Lubos Polerecky, Birgit Adam, Niculina Musat, Jana Milucka, Tomas Vagner, Marcel M.M. Kuypers

Manuscript 5.

Vacuolar respiration of nitrate coupled to energy conservation in *Beggiatoa* sp. *(in revision)*

Martin Beutler, Susanne Borgwardt, Frank Schreiber, Jana Milucka, Jörg Brock, Marc Mussman, Heide Schulz-Vogt, Dirk DeBeer

ACKNOWLEDGMENTS

Let me use this last page of my thesis to express my thanks to the many people whose support and help has brought me through the last years.

… Mr. Widdel, it was very nice of you to entrust me my AOM project. I appreciate your belief in me and my decisions. I very much enjoyed our inventive sessions with AOM schemes and planning experiments.

… Rudi, thank you for your guidance and your assistance with the last steps of my PhD as my ‘substitute’ supervisor.

… Marc, thank you for your time and effort spent by reviewing my thesis and for the nice discussions.

… Professor Stick and Tim, thank you for being members of my defence committee.

… Seigo and professor Thauer, thank you and your ‘Marburg’ group for the pleasant and prolific days that I spent working with you.

… Anke and Jens, thank you for your time and for your valued contributions during our thesis committee meetings.

… Tim and Marcel – your enthusiasm came at the right time during my work. I consider the time we spent together in discussions about AOM as most precious. Thank you for your encouragement and the support during late night-early morning sampling hours. Thank you for your introduction to the world of chemistry and its bio- and geo- prefixes. Most of all, thank you for letting me feel the satisfaction when data start making sense.

… Thomas, Mirko and Christian, I profited a lot from your experiences and advice during the past few years.

… thanks to the whole microbio department for the pleasant times.

… I am very indebted to Marga and Thomas from the MPI in Munich for the pleasant atmosphere, friendliness and great deal of help that made me enjoy my every stay despite being most of the time closed in the dry, dark and silent microtome chamber.

… Karsten from the Fraunhofer institute, thank you for the great help with electron microscopy and for the cheerful discussions about bacteria.

… Verena, Julia and Anne, you have been such fantastic officemates! Whether it was discussion about introns or outlet stores, I loved them all.

… my two doctorate Musketeers – Laura and Caro, thanks for your friendship and care, for filling my days and nights (and hungry stomach when necessary). There should have been more ‘Sardinias’ and more ‘Corsicas’… Sylvain and Roy, I have nearly forgotten you two…! (Bazinga!)

… to my friends and flatmates, and their smaller or larger families - Manuel and Sibyl, Sergio and Agnieszka and Clelia

… my ‘Slovakian horde’ who made me feel home upon my arrival to Bremen and during the whole time since then, thank you for our jazz Tuesdays and our Sunday Sportwelt visits. Thank you, Lubos, for the friendship, and the motivating and encouraging discussions.

… thank you, ‘MPI Munte badminton squad’

… and ultimately, big big thanks to my incredibly tolerant and undeservedly neglected friends from the old days: Mikey, Matka, Lenuska, Anjelik, Betus, Zorka, Janka (a Robo a Eliska), Lenka, Vendy, Jarmilka, Rastik, Michal a Karel.

Ale hlavne:

… mojej najsamlepsej rodine. Za tu vzdy spravnu davku povzbudenia a strachovania a za tu trochu cynicizmu, co vratila moj zadok zase pekne spat na zem. Ako tazko by sa mi tu darilo bez vas!

and most of all

to Marcel - for being a fantastic Y.